Petroleum Science 21 (2024) 4067–4099

Contents lists available at ScienceDirect

Petroleum Science

journal homepage: www.keaipublishing.com/en/journals/petroleum-science

Review Paper

Impacts of microbial interactions on underground hydrogen storage in porous media: A comprehensive review of experimental, numerical, and field studies

Lin Wu [a, b], Zheng-Meng Hou [a, c, d, *], Zhi-Feng Luo [b], Yan-Li Fang [a, b, **], Liang-Chao Huang [a, d], Xu-Ning Wu [a, b], Qian-Jun Chen [a], Qi-Chen Wang [a, d]

[a] Institute of Subsurface Energy Systems, Clausthal University of Technology, Clausthal-Zellerfeld, 38678, Germany
[b] National Key Laboratory of Oil and Gas Reservoir Geology and Exploitation, Southwest Petroleum University, Chengdu, 610500, Sichuan, China
[c] Sino-German Energy Research Center, Sichuan University, Chengdu, 610065, Sichuan, China
[d] Sino-German Research Institute of Carbon Neutralization and Green Development, Zhengzhou University, Zhengzhou, 450000, Henan, China

ARTICLE INFO

Article history:
Received 2 July 2024
Received in revised form
31 July 2024
Accepted 31 August 2024
Available online 3 September 2024
Handling Editor: Baojun Bai
Edited by Yan-Hua Sun

Keywords:
Microbial interaction
Porous medium
Underground bio-methanation
Underground hydrogen storage (UHS)
Storage efficiency
Storage safety

ABSTRACT

Amidst the rapid development of renewable energy, the intermittency and instability of energy supply pose severe challenges and impose higher requirements on energy storage systems. Among the various energy storage technologies, the coupled approach of power-to-hydrogen (H_2) and underground H_2 storage (UHS) offers advantages such as extended storage duration and large-scale capacity, making it highly promising for future development. However, during UHS, particularly in porous media, microbial metabolic processes such as methanogenesis, acetogenesis, and sulfate reduction may lead to H_2 consumption and the production of byproducts. These microbial activities can impact the efficiency and safety of UHS both positively and negatively. Therefore, this paper provides a comprehensive review of experimental, numerical, and field studies on microbial interactions in UHS within porous media, aiming to capture research progress and elucidate microbial effects. It begins by outlining the primary types of UHS and the key microbial metabolic processes involved. Subsequently, the paper introduces the experimental approaches for investigating gas–water–rock–microbe interactions and interfacial properties, the models and simulators used in numerical studies, and the procedures implemented in field trials. Furthermore, it analyzes and discusses microbial interactions and their positive and negative impacts on UHS in porous media, focusing on aspects such as H_2 consumption, H_2 flow, and storage safety. Based on these insights, recommendations for site selection, engineering operations, and on-site monitoring of UHS, as well as potential future research directions, are provided.

1. Introduction

The industrial revolution brought unprecedented economic growth, technological advancement, and improved living standards. However, it was accompanied by the extensive use of carbon-intensive fossil fuels, such as coal and oil, leading to a sharp increase in carbon dioxide (CO_2) emissions (Paraschiv and Paraschiv, 2020). According to data from the International Energy Agency (IEA), global energy-related carbon emissions increased by 1.1% in 2023, reaching a historic high of 37.4 Gt (IEA, 2024). Significant CO_2 emissions contribute to the greenhouse effect, resulting in frequent extreme weather events, rising sea levels, and severe impacts on biodiversity and human life. To combat global warming, numerous countries have signed the Paris Agreement on Climate Change (Schleussner et al., 2016). This agreement aims to limit the increase in the global average temperature to below 2 °C above pre-industrial levels while pursuing efforts to limit the temperature rise to 1.5 °C. Additionally, 198 countries have committed to achieving carbon neutrality between 2030 and 2070 through various measures (Chen et al., 2022). These measures primarily focus on replacing traditional carbon-intensive fossil

* Corresponding author. at: Agricolastraße 10, Clausthal-Zellerfeld, 38678, Germany.
** Corresponding author. at: Agricolastraße 10, Clausthal-Zellerfeld, 38678, Germany.
E-mail addresses: hou@tu-clausthal.de (Z.-M. Hou), yanli.fang@tu-clausthal.de (Y.-L. Fang).

https://doi.org/10.1016/j.petsci.2024.08.015

Nomenclature

Abbreviations	
ACE	Acetogenesis
AP	Ambient pressure
CCCUS	Carbon capture, circular utilization, and sequestration
CCR	Confined core reactor
DSGR	Depleted sandstone gas reservoir
DSHR	Depleted sandstone hydrocarbon reservoir
EPS	Extracellular polymeric substances
FDM	Finite difference method
FEM	Finite element method
FT	Fracture toughness
FVM	Finite volume method
GWRM	Gas–water–rock–microbe
HP	High-pressure
HT	High-temperature
IC	Ionic composition
IEA	International Energy Agency
GC	Gas composition
MC	Mineral composition
MCC	Microbial community composition
MER	Methane evolution rate
MET	Methanogenesis
MTS	*M. thermolithotrophicus* solution
NA	Not available
RSR	Reservoir simulation reactor
RT	Room temperature
SR	Sulfate reduction
SRB	Sulfate-reducing bacteria
UBM	Underground bio-methanation
UCS	Unconfined compressive strength
UHS	Underground H_2 storage
USC	Underground sun conversion
USS	Underground sun storage
VFAC	Volatile fatty acid concentration
WSR	Wellbore simulation reactor
Symbols	
ad	Number of adsorbed microbes, L^{-1}
c	Mole fraction
c_{mi}	Molality of each reactant, mol/L
C_A	Concentration of electron acceptor, mol/L
C_D	Concentration of electron donor mol/L
C_s	Brine salinity, g/L
$C_{s,c}$	Characteristic salinity, g/L
C_X	Concentration of biomass, L^{-1}
d	Decay coefficient, s^{-1}
d_p	Pore diameter, m
D	Cell diffusion coefficient, m^2/s
E_a	Reaction activation energy, J/mol
f_d	Thermodynamic drive, J/mol
f_e	Dimensionless flow efficiency coefficient
F	Frequency factor
J	Dispersion/diffusion flux, mol/(m^2·s)
k_a	Rate of attachment per microbe, s^{-1}
k_d	Rate of detachment per microbe, s^{-1}
k_p	Absolute permeability, m^2
k_{p0}	Absolute permeability of a clean reservoir, m^2
K_A	Half-saturation constant of electron acceptor, mol/L
K_D	Half-saturation constant of electron donor, mol/L
n	Population size of microbes, m^{-3}
n_a	Number of attached microbes, m^{-3}
n_d	Number of detached microbes, m^{-3}
n_c	Quantity of microbes required to induce maximal bio-clogging effect, m^{-3}
N	Biomass of microbes, g/L
pH	pH value of brine
q	Source or sink term related to microbial consumption, mol/(m^3·s)
r_s	Consumption rate of substrate, mol/(L·s)
R	Gas constant, J/(mol·K)
R_r	Resistance factor
S	Saturation
t	Time, s
t_e	Characteristic time of eating, s
t_E	Time when the exponential growth is reached, s
t_L	End time of lag phase, s
T	Temperature, K

(*continued*)

v	Convective flux, m/s
Y	Yield coefficient, g/mol
Greek symbols	
μ_{dec}	Specific decay rate, s^{-1}
μ_{gr}	Specific growth rate, s^{-1}
μ_{max}	Maximum specific growth rate, s^{-1}
μ_{opt}	Specific growth rate of microbes under optimal conditions, s^{-1}
φ	Pore fraction occupied by microbes
ψ_i	Influencing coefficient
ϕ	Porosity
ϕ_0	Porosity of a clean reservoir
ϕ_b	Biofilm volume fraction
χ	Average stoichiometric number
λ	Lag coefficient
ς_i	Reaction order
ρ	Molar density, mol/m^3
Superscripts or subscripts	
g	Gas phase
i	Index
k	Chemical composition
min	Minimum value
max	Maximum value
opt	Optimum value
w	Water phase

fuels with clean renewable energy, enhancing the energy efficiency of existing technologies, and deploying carbon-negative technologies (Liu et al., 2017; Wang et al., 2021; Hou et al., 2023d; Wu et al., 2023b).

While renewable energy is embraced by countries for its low to zero carbon emissions, it also presents some challenges. The most notable one is the intermittency and instability of energy supply (Wiel et al., 2019), driven by the significant impact of weather and geographical location on specific renewable energy sources like wind, solar, and hydro power. Additionally, situations of renewable power curtailment may occur (Denholm and Mai, 2019). For example, in China between 2011 and 2015, around 100 billion kWh of wind power remained unused, an amount equivalent to the combined annual output of China's two large hydroelectric power stations: the Three Gorges Dam and the Gezhouba Dam (Cui et al., 2020). In 2016, on a nationwide scale, an average of 17% of installed wind power generation was curtailed, with curtailment rates reaching as high as 43% in provinces abundant in wind power such as Gansu, and 38% in Xinjiang. Beyond China, the issue of renewable energy curtailment is also prevalent in countries like the USA, Germany, and the UK (Shen et al., 2024).

In this context, energy storage plays a pivotal role in ensuring a stable energy supply and mitigating the curtailment of renewable energy (Denholm and Mai, 2019). Common energy storage methods encompass electrochemical storage (e.g., lithium batteries, supercapacitors, and flow batteries), thermal energy storage, compressed air energy storage, flywheel energy storage, pumped hydro storage, and hydrogen (H_2)-based chemical storage (Amirante et al., 2017; Rahman et al., 2020; Chen et al., 2023; Hou et al., 2024). Among these, H_2-based chemical storage involves utilizing surplus energy to electrolyze water, yielding H_2 gas, which can either be directly stored or converted into methane (CH_4), methanol, ammonia, and other substances for storage or utilization (Glenk and Reichelstein, 2019; Blanco et al., 2020). Notably, the integration of power-to-H_2 and underground H_2 storage (UHS) in depleted hydrocarbon reservoirs, aquifers, salt caves, etc., offers attributes of prolonged storage duration and extensive storage capacity (Zivar et al., 2021; Xie et al., 2023), as depicted in Fig. 1. Consequently, this approach garners substantial attention and showcases significant prospects for further advancement.

However, the process of directly storing H_2 underground,

especially in porous media such as depleted hydrocarbon reservoirs and aquifers, faces several challenges (Dopffel et al., 2021; Heinemann et al., 2021). For instance, H_2, being a favorable electron donor, can undergo chemical reactions with formation water, rock minerals, and microbes, resulting in H_2 consumption. A notable example is the town gas storage, converted from an aquifer, in Lobodice, Czech Republic. Over a period of seven months, there was a 17% loss of H_2, while CH_4 content increased by 18%, primarily due to the catalytic activity of hydrogenotrophic methanogens (Šmigáň et al., 1990). To turn the adverse bio-methanation reaction into a beneficial factor for underground energy storage in porous media, the concept of underground bio-methanation (UBM) of H_2 and CO_2, utilizing methanogens as biocatalysts, was proposed (Panfilov, 2010; Strobel et al., 2020; Xiong et al., 2023). This approach can enrich the energy potential of stored gas. It is also considered a broad form of UHS method and represents an innovative integration of power-to-CH_4 and underground CH_4 storage. Furthermore, UBM facilitates carbon circular utilization and geological sequestration, making it a novel carbon-negative technology (Hou et al., 2023b).

Apart from the influence of methanogens, other microbes such as sulfate-reducing bacteria (SRB) and acetogens can also contribute to H_2 consumption, potentially resulting in various adverse effects such as the production of toxic hydrogen sulfide (H_2S) gas, blockages, and corrosion of metal equipment (Dopffel et al., 2021). However, the metabolic activities of these microbes may also improve reservoir wetting properties, which is beneficial for the storage and withdrawal of H_2 (Liu et al., 2023b). Therefore, microbial metabolism can have both positive and negative impacts on UHS in porous media, and the catalytic role of methanogens in emerging UBM technology is even indispensable (Strobel et al., 2020). A thorough understanding of microbial interactions and their impacts on UHS in porous media is crucial for guiding the implementation of UHS, helping to mitigate safety risks and enhance storage performance.

To date, numerous review papers have been published involving microbial metabolism in UHS. However, most only briefly touch on microbial activities and the associated potential risks (Heinemann et al., 2021; Zivar et al., 2021; Muhammed et al., 2022; Liu et al., 2023a; Wang et al., 2023; Zeng et al., 2023; Fernandez et al., 2024). Additionally, some papers have integrated discussions of microbial-related aspects into their reviews of numerical modeling and field projects for UHS (Muhammed et al., 2022; Du et al., 2024; Saeed and Jadhawar, 2024). Recently, several review papers have specifically focused on microbial activities in UHS. For example, Strobel et al. (2020) introduced the concept of UBM along with several relevant field projects. Thaysen et al. (2021) highlighted potential H_2-consuming microbial reactions and the effects of environmental conditions on microbial activity. Xiong et al. (2023) detailed the biogeochemical mechanisms occurring in UBM within depleted hydrocarbon reservoirs. Dopffel et al. (2021, 2024) concentrated on both the microbiology and the potential side effects and risks associated with UHS in porous media and salt caverns. Bhadariya et al. (2024) reviewed microbial detection methods and strategies for managing microbial activities in UHS.

It's evident that previous reviews have lacked an extensive analysis of microbial-related research, leading to an incomplete understanding of microbial interactions and their impacts on UHS in porous media. This paper aims to address this gap by following the review procedure presented in Fig. 2. The primary contributions of this paper can be summarized as follows:

- It presents the first comprehensive review of experimental, numerical, and field studies on microbial interactions in UHS within porous media, providing essential insights into research progress in this area.
- It systematically elaborates on microbial interactions in UHS, facilitating a thorough comprehension of both their positive and negative impacts on UHS in porous media.
- The recommendations presented in this paper offer valuable guidance for future research and field implementations of UHS in porous media.

The remaining sections are organized as follows: Section 2 and Section 3 briefly introduce the principal types of UHS and the main microbial metabolism processes involved, respectively. In Section 4, various experimental approaches for studying gas–water–rock–microbe (GWRM) interactions and interfacial properties are introduced. Additionally, this section also outlines the models and simulators employed in numerical modelling, as well as the procedures implemented in field tests. Section 5 reviews and discusses important research findings that specifically address microbial interactions and their impacts on H_2 consumption, H_2 flow, and storage safety. Section 6 offers detailed recommendations for site selection, engineering operation, and on-site monitoring in UHS. Finally, Section 7 summarizes the main conclusions and provides an outlook on future research directions.

2. Primary types of UHS

In addition to surplus renewable energy electrolysis, H_2 can also be obtained through high temperature electrolysis in nuclear power plants, coal-to-H_2 processes, industrial by-product H_2, and other sources. It can then be stored in depleted hydrocarbon reservoirs, saline aquifers, and salt caverns (Zivar et al., 2021), as illustrated in Fig. 3. Subsequently, the stored H_2 can serve as a power generation source or as fuel. Considering the initial energy production form, the final energy consumption form, and methods of energy conversion, Panfilov (2016) primarily categorizes underground H_2 storage into four types. The relevant introductions are provided below.

Underground storage of pure H_2: Pure H_2 primarily derives from chemical electrolysis utilizing surplus renewable electricity or high temperature electrolysis conducted in nuclear power plants (Panfilov, 2016). Salt caverns are considered the most ideal underground storage sites for pure H_2 due to their excellent sealing

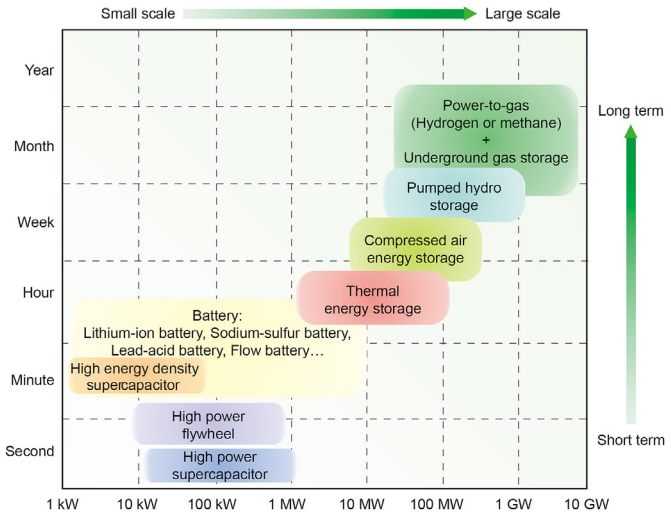

Fig. 1. Comparison of key energy storage technologies (Adapted with permission from Wu et al., 2024. Copyright, 2024; Elsevier).

properties, minimal presence of indigenous impurity gases, and lower risks of contamination from external gases. Recently, investigation has also begun into the feasibility of storing pure H_2 in depleted gas reservoirs (RAG, 2024). The best application for extracted pure H_2 lies in fuel cell vehicles, given the stringent purity requirements imposed by fuel cells. For instance, standards such as ISO 14687:2019 and SAE J2719-202003 specify a purity level of 99.97%, while GB/T 3634.2–2011 sets slightly higher standards at 99.99% (Du et al., 2021).

Underground storage of H_2-natural gas mixtures: A small amount of pure H_2 produced by electrolysis is stored in underground natural gas storage sites. This method of H_2 storage is mainly used for transportation via natural gas pipelines. The resulting mixture of H_2 and natural gas can be used directly or processed to extract pure H_2 (Panfilov, 2016). The maximum allowable H_2 concentration in natural gas, without significantly impacting the energy potential of the mixed gas or the integrity of the transportation pipelines, varies by country. For example, in the UK, the allowable limit is 0.1%, while in the Netherlands, up to 12% is permitted (Quarton and Samsatli, 2018). Recently, the consideration and testing of blending H_2 up to 20% in natural gas have also been underway (Jia et al., 2023).

Underground storage of H_2-rich town gas or syngas: These two types of gases are primarily produced by coal gasification. The mixture containing H_2 (50%–60%), CO, and CH_4 is called town gas, while the mixture containing H_2 (20%–40%) and CO is called syngas (Panfilov, 2016). The CO in the mixture is also an energy carrier, and the content of CO_2 depends on the production technology. Storage of town gas was the first experience with injecting H_2-rich gas into the subsurface. Poland, France, the Czech Republic, Germany, and the USA have all conducted underground storage of town gas for balancing seasonal fluctuations since the last century (Strobel et al.,

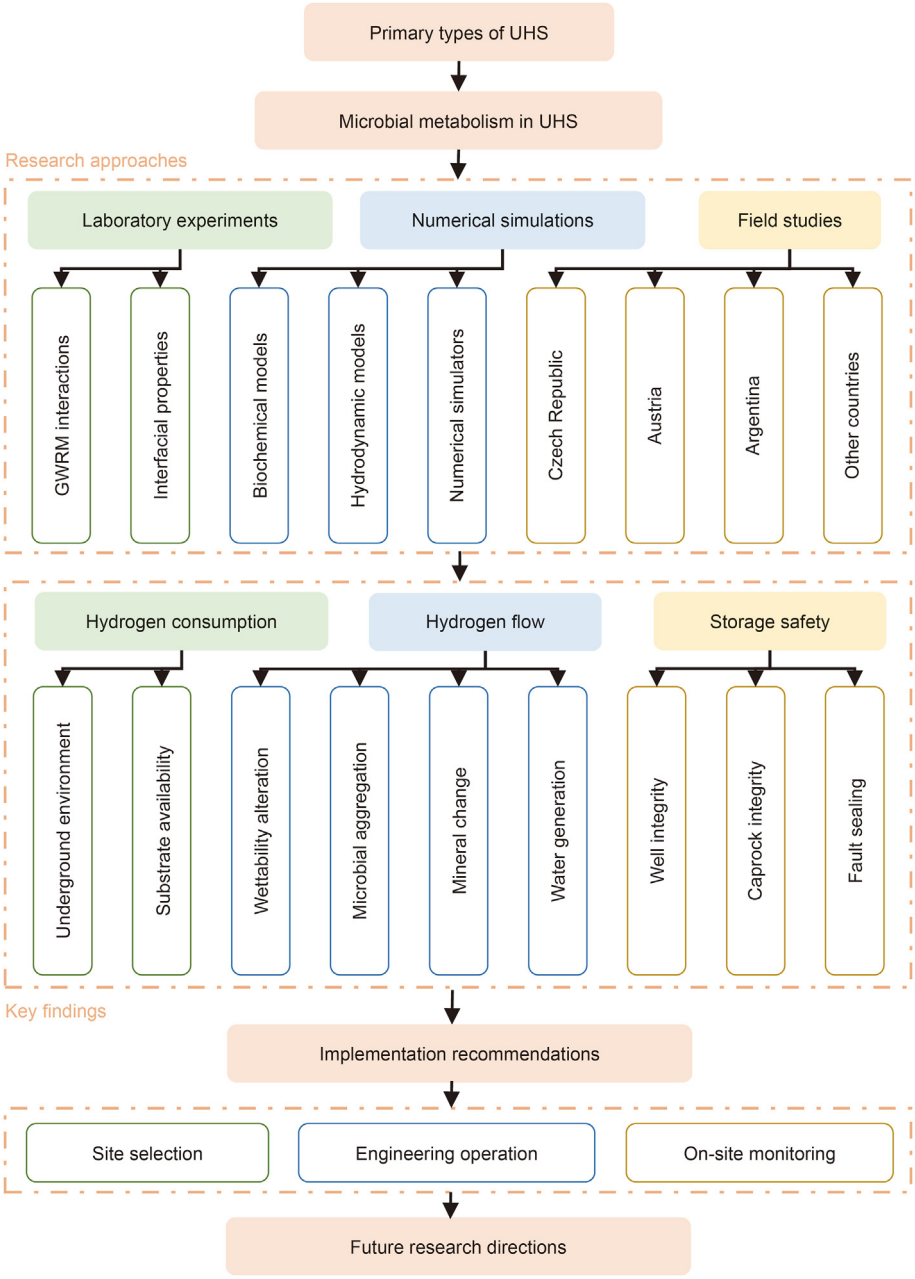

Fig. 2. Review procedure for investigating microbial interactions and their impacts on UHS in porous media.

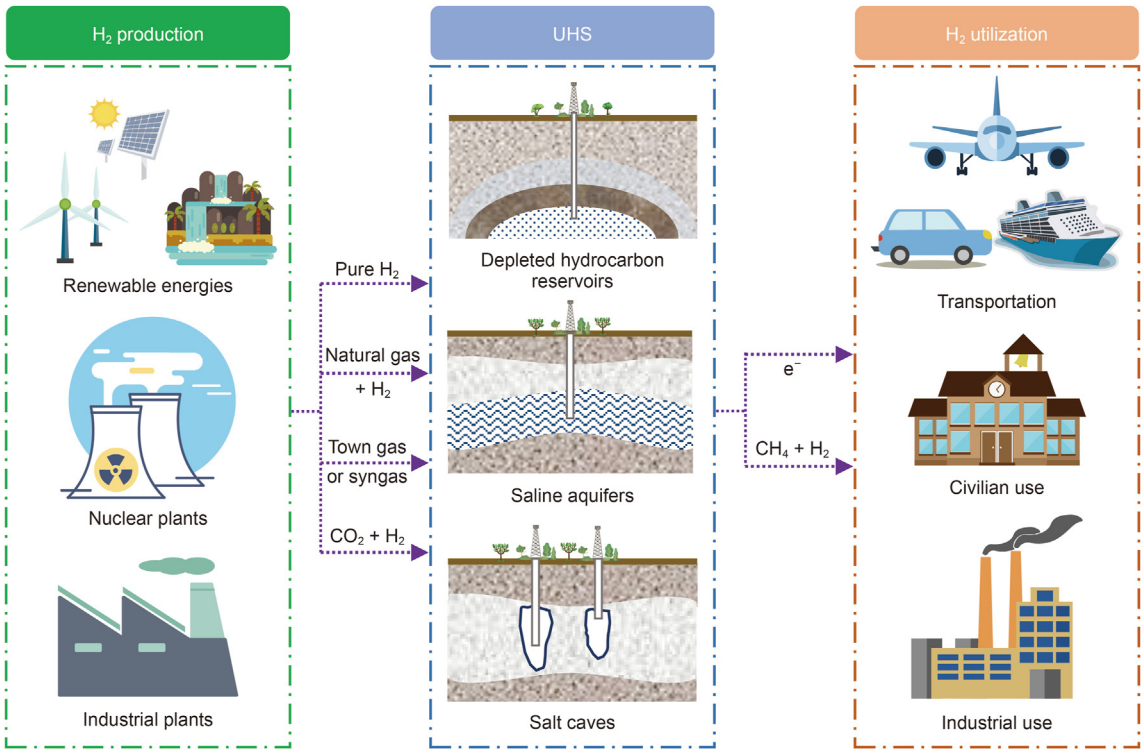

Fig. 3. Schematic of H_2 production, UHS, and H_2 utilization.

2020). The extracted mixed gas is primarily used for power generation through thermo-mechanical conversion in gas turbines or as fuel without any conversion for lighting and heating in areas lacking natural gas (Panfilov, 2016).

Underground bio-methanation (UBM) of H_2: It was first proposed by Panfilov (2010) and involves using hydrogenotrophic methanogens as biocatalysts to synthesize CH_4 from H_2 and CO_2, thereby enhancing the energy potential of the stored gas. Due to its ability to achieve circular utilization and geological sequestration of CO_2, this technology has been termed carbon capture, circular utilization, and sequestration (CCCUS) by Hou et al. (2023b) and Wu et al. (2023c). This type of H_2 storage is particularly well-suited for depleted hydrocarbon reservoirs and aquifers, as their porous nature, relatively low salinity, and abundant water availability are more conducive to the survival of methanogens. Since the proportion of injected CO_2 can be optimized, the resulting synthetic natural gas contains a lower proportion of CO_2. This allows the extracted gas to be directly injected into the natural gas grid and subsequently used as fuel (Panfilov, 2016). Compared to surface industrial processes that require high temperatures and costly precious metal catalysts, UBM is more economically feasible (Hou et al., 2023a).

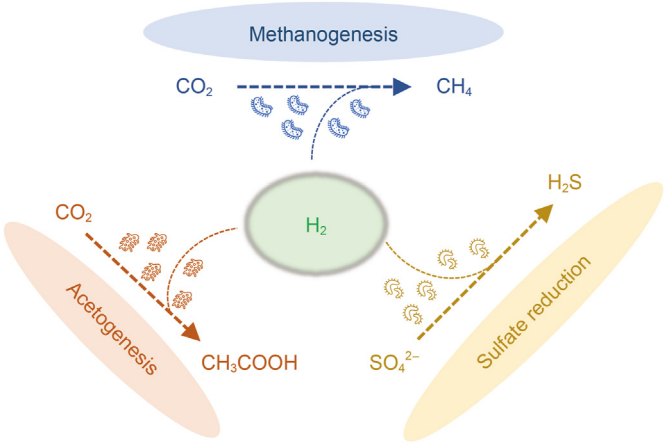

Fig. 4. Three main microbial metabolic processes in UHS.

3. Microbial metabolism in UHS

Various microbes, such as archaea and bacteria, are widely present underground (Buriánková et al., 2022; Schwab et al., 2022; Bassani et al., 2023), primarily in the form of biofilms or in a free state. When large amounts of H_2 are injected underground, some microbes can utilize H_2 as an electron donor for their metabolism (microbial H_2 oxidation), leading to the consumption of the injected H_2. Thaysen et al. (2021) summarized 13 types of biotic H_2-consuming processes and ranked their likelihood based on the H_2 threshold of the reactions and the standard free energy change. Among these processes, methanogenesis, acetogenesis, and sulfate reduction are most relevant for UHS (Fig. 4). The reaction equations and the associated changes in Gibbs free energy are detailed in Table 1. A brief introduction to these three microbial metabolic processes is provided below.

Methanogenesis: The process of synthesizing CH_4 using H_2 and CO_2, known as the Sabatier reaction (Leonzio, 2016), serving as the cornerstone of UBM technology. Surface reactions typically demand precious metal catalysts like Ni, Co, Rh, and Ru, operating at high temperatures, thereby restricting their large-scale commercial viability (Stangeland et al., 2017). However, in underground environments, particularly in zones with extremely low redox potential where other beneficial electron acceptors such as oxygen, nitrates, and sulfates are scarce or absent, hydrogenotrophic methanogens become active, facilitating methanogenesis (Molíková et al., 2022). This metabolic process releases a substantial amount of heat, which may explain the notable temperature rise observed at the Ketzin

Table 1
Reaction equations and changes in Gibbs free energy for three main microbial metabolic processes in UHS (Dopffel et al., 2021; Thaysen et al., 2021).

Metabolism	Reaction equation	Change in Gibbs free energy, kJ/mol
Methanogenesis	$H_2 + 1/4\ HCO_3^- + 1/4\ H^+ \rightarrow 1/4\ CH_4 + 3/4\ H_2O$	−33.9
Acetogenesis	$H_2 + 1/2\ HCO_3^- + 1/4\ H^+ \rightarrow 1/4\ CH_3COO^- + H_2O$	−26.1
Sulfate reduction	$H_2 + 1/4\ SO_4^{2-} + 1/4\ H^+ \rightarrow 1/4\ HS^- + H_2O$	−38.0

Table 2
Optimum and critical ranges of environmental conditions for microbial metabolism in UHS (Modified after Heinemann et al., 2021; Zeng et al., 2023).

Microbial type	Temperature, °C		pH			Salinity, g/L	
	Optimum	Maximum	Optimum	Minimum	Maximum	Optimum	Maximum
Methanogens	30–40	122	6.0–7.5	4.5	9.0	< 60	200
Acetogens	20–30	72	6.0–7.5	3.6	10.7	< 40	300
SRB	20–30	113	6.0–7.5	0.8	11.5	< 100	240

gas storage in Germany (Strobel et al., 2020). Three primary groups of methanogens are commonly identified: *Methanobacteriales*, *Methanococcales*, and *Methanomicrobiales* (Panfilov, 2016; Muhammed et al., 2022). These hydrogenotrophic methanogens play a pivotal role in the conversion process by supplying indispensable functional groups such as coenzymes and reductases. A prototypical reaction pathway is depicted by the Wolfe cycle (Xiong et al., 2023).

Acetogenesis: This process involves synthesizing acetate using H_2 and CO_2. Common acetogens include *Clostridium thermoautotrophicum*, *Clostridium aceticum*, *Butyribacterium methylotrophicum*, *Sporomusa sphaeroides*, *Acetobacterium woodii*, and others (Panfilov, 2016; Muhammed et al., 2022). Because methanogens and acetogens metabolize almost identical substrates, there may be strong competition between them, depending on environmental conditions and microbial populations (Bauer, 2023). It is worth noting that under different thermodynamic conditions, the produced acetate may revert back to the initial states of H_2 and CO_2 (Konegger et al., 2023), and the generated acetate may also directly serve as a carbon source necessary for the growth of certain biomass, such as sulfate-reducing bacteria (SRB) (Panfilov, 2016).

Sulfate reduction: SRB employ sulfate ions and H_2 to produce water and H_2S, the latter of which is both toxic and highly corrosive to metals and concrete. This metabolic process also leads to the loss of stored energy. Prominent SRB encompass *Desulfobacter vibrioformis*, *Desulfobacterium cetonicum*, *Desulfotomaculum kuznetsovii*, *Desulfacinum infernum*, among others (Zhang et al., 2022; Bauer, 2023). SRB are naturally present in gas and oil reservoirs, particularly prevalent when kerogens abundant in sulfur serve as the predominant constituents for crude oil and natural gas formation. Furthermore, this phenomenon may transpire within hydrocarbon reservoirs wherein incompatible water is introduced during flooding, attributed to the existence of sulfate (Cavallaro et al., 2005; Muhammed et al., 2022).

The activities of methanogens, acetogens, and SRB are highly sensitive to reservoir environments, influenced by factors such as temperature, salinity, and pH. Thaysen et al. (2021) conducted a comprehensive review of the impact of reservoir environments on these three types of microbes. Despite considerable variations in microbial sensitivity to environmental conditions, preliminary estimations of optimal ranges and critical thresholds for each microbial type have been possible (Heinemann et al., 2021; Zeng et al., 2023), as outlined in Table 2. Precisely determining these parameter ranges is crucial for site selection, facilitating the mitigation of energy losses from microbial metabolism and enhancing the conversion efficiency in UBM technology.

4. Research approaches

This section introduces various experimental approaches for studying GWRM interactions and interfacial properties, such as wettability. Additionally, it outlines the biochemical and hydrodynamic models, as well as the simulators used in numerical modelling. Finally, the procedures implemented in field tests are described. The key findings from these studies are primarily presented and discussed in Section 5.

4.1. Laboratory experiments

4.1.1. Overview of laboratory experiments

Numerous studies have delved into GWRM interactions, predominantly concentrating on alterations in gas composition, hydrochemical properties, microbial community composition, and mineral composition resulting from microbial metabolism (Table 3), aimed at evaluating H_2 consumption or analyzing underlying mechanisms. Notably, these studies typically involve gas, water, and microbes. However, the consideration of rock influence and the size of rock samples primarily hinge on the bioreactors employed. Furthermore, the temperature and pressure conditions that the bioreactor can withstand dictate the extent to which reservoir conditions can be replicated. Additionally, some studies have investigated the impact of microbial activity on interfacial properties. The primary emphasis has been on wettability, with little attention given to interfacial tension and capillary forces.

4.1.2. GWRM interactions

Šmigáň et al. (1990) first carried out microbial experiments with formation water from the town gas storage in Lobodice, Czech Republic, aimed at investigating the causes behind the significant changes observed in gas composition. In their experiments, the modified Hungate technique was utilized (Bryant, 1972). Due to the small volume of culture tubes, solid-phase materials could only be represented by rock powder. Aftab et al. (2023, 2024), and Al-Yaseri et al. (2024) utilized 50 mL culture tubes to incubate SRB under room temperature conditions before measuring parameters such as contact angle and interfacial tension. The solid-phase material in their experiments consisted of small-volume rock bars (2 cm × 2 cm × 0.5 cm). The use of culture tubes limits the scope of experiments to relatively simple setups. Additionally, due to the rudimentary nature of the culture tubes and the necessity to ensure sealing conditions, dynamic monitoring of parameters is nearly impractical.

Using various types of bottles as bioreactors is also quite common in previous studies. For example, Dohrmann and Kruger

Table 3
Comprehensive comparison of experimental studies on microbial interactions in UHS within porous media.

Research	Focus	Storage scenario	Solid	Fluid	Gas	Microbe	P & T conditions	Bioreactor	Key parameters
Šmigáň et al. (1990)	Conversion of H_2 and CO_2 into CH_4 by methanogens	Aquifers	Powdered rocks	Formation water	80% H_2 + 20% CO_2	Autochthonous microbes	1.5 bar, 37–60 °C	Culture tube	GC
Bauer (2017)	Microbial processes in H_2-loaded reservoirs	Depleted gas reservoirs	Drill cores	Reservoir water	4%–10% H_2 + 0.3% –2.5% CO_2 + CH_4	Autochthonous microbes	45 bar, 45 °C	HP reactor	IC, GC, MC, MCC, pH, etc.
Haddad et al. (2022)	GWRM interactions	Deep aquifers	Rock cuttings, core samples	Formation water	1% CO_2 + CH_4; 10% H_2 + CH_4	Autochthonous microbes	85.8–95 bar, 47 °C	HP reactor	IC, GC, MC, MCC, etc.
Aftab et al. (2023)	Wettability under realistic geo-conditions	Sandstone reservoirs	Quartz bars	Nutrient medium, brine	H_2	SRB	Incubation: RT; Measurement: 0 –270 bar, 50 °C	Culture tube	pH, contact angle, IC, etc.
Ali et al. (2023)	Microbiotic effects on rock wettability	Sandstone reservoirs	Quartz slides	Seawater	H_2	Cyanobacteria	Incubation: RT; Measurement: 3–130 bar, 25 –50 °C	Incubation flask	Contact angle
Bauer (2023)	Potential of methanogenic conversion using H_2 and CO_2 under in-situ conditions	Depleted gas reservoirs	Drill cores, sintered ceramic plates, 1-m-long rock cores	Reservoir water	10%–40% H_2 + 2.5% –10% CO_2 + CH_4/He	Autochthonous microbes, methanogens	20–45 bar, 40 °C	Reservoir simulation reactor, mini reactor, confined core reactor	IC, GC, MC, MCC, VFAC, etc.
Dohrmann and Kruger (2023)	Microbial H_2 consumption at near in-situ conditions	Natural gas fields	NA	Native formation fluid, adapted fluid	10% H_2 + N_2; 1% –2% CO_2 + 0.4% –1.5% H_2 + N_2	Autochthonous microbes	AP and 100 bar, 30 –60 °C	Serum bottle, HP reactor	GC, MCC, etc.
Dopffel et al. (2023)	Microbial H_2 consumption at hypersaline conditions	Hypersaline reservoirs, salt caverns	NA	Nutrient medium, original cavern brine	10%–100% H_2 + 5% –20% CO_2 + N_2	Halophilic cultures, autochthonous microbes	30–37 °C	Sterile bottle	GC, pressure, cell number, pH, etc.
Konegger et al. (2023)	Effect of operational modes on UBM	Depleted gas reservoirs	One-meter-long rock cores	Reservoir water	10%–80% H_2 + 0.5% –20% CO_2 + Ar	Autochthonous microbes	5–20 bar, 40 °C	Wellbore simulation reactor, confined core reactor	IC, GC, MC, MCC, VFAC, etc.
Liu et al. (2023b)	Microbial H_2 consumption and wettability alteration	Sandstone reservoirs	Silicon micromodel	Growth medium	H_2	Halophilic SRB	35 bar, 37 °C	Microfluidic pore network	Gas saturation, contact angle, etc.
Rooney and Li (2023)	Wellbore cement alteration by H_2-triggered bio-geochemical reactions	Depleted reservoirs	Wellbore cement core, shale	Synthetic formation brine	90% H_2/N_2 + 5% CO_2	Microbes in synthetic formation brine.	100 bar, 60 °C	HP and HT reactor	GC, MC, etc.
Schwab et al. (2023)	Microbial activities at hypersaline conditions	Hypersaline reservoirs, salt caverns	NA	Nutrient medium	80% H_2 + 20% CO_2	Halophilic enrichment cultures	2 bar, 30 °C	Serum bottle	IC, GC, MCC, acetate/lactate concentrations, etc.
Strobel et al. (2023b)	Microbial growth in two-phase saturated porous media	Porous sandstone reservoirs	Glass-silicon-glass micromodel	Culture medium	80% H_2 + 20% CO_2	Methanogenic archaea	1.1–1.75 bar, 37 –63 °C	Glass-silicon-glass micromodel	Cell number
Vítězová et al. (2023)	Biomethane production from H_2 and CO_2	Depleted reservoirs	Rock samples	Growth medium, formation water	80% H_2 + 20% CO_2	Autochthonous microbes	3–4 bar, 48 °C	Serum bottle, fermenter	GC, MCC, etc.
Aftab et al. (2024)	Microbial effect on interfacial properties	Porous reservoirs	Basalt rock bars	Medium solution	H_2	SRB	Incubation: RT; Measurement: 25–50 °C, 0–4000 psi	Culture tube/bottle	Contact angle, capillary pressure, and interfacial tension

(*continued on next page*)

Table 3 (*continued*)

Research	Focus	Storage scenario	Solid	Fluid	Gas	Microbe	P & T conditions	Bioreactor	Key parameters
Al-Yaseri et al. (2024)	Microbial effects on the capillary pressure	Depleted hydrocarbon reservoirs	Core samples	Medium solution	H_2	SRB	Incubation: RT; Measurement: up to 2500 psi	Culture tube	Capillary pressure, interfacial tension, etc.
Boon et al. (2024)	Microbial induced wettability alteration	Sandstone reservoirs	Sandstone rock slabs, pure quartz slabs	Living brine	H_2	SRB	3 bar, 37 °C	HP and HT titanium cell	Static contact angle, bubble volume, pH, etc.
Khajooie et al. (2024)	Microbial activity in water-filled pore space	Porous reservoirs	Sand particles, rock fragments	Nutrient medium	80% H_2+ 20% CO_2	Methanogenic archaea	2 bar, 50–60 °C	Glass bottle, serum bottle, infusion bottle	GC, pressure, etc.
Mura et al. (2024)	GWRM interactions	Deep aquifers	Crushed rocks, rock core	Formation water	2%–10% H_2 + CH_4	Autochthonous microbes	85–95 bar, 35 –47 °C	HP reactor	IC, GC, MC, MCC, pH, etc.
Vasile et al. (2024a)	Microbial risk assessment under in-situ conditions	Depleted gas reservoirs	Core rocks	Formation water	10% H_2+ 90% CH_4; 99% H_2 + 1% CO_2	Autochthonous microbes	150 bar, 50 °C	HP and HT reactor	GC, cell density, VFAC, pH, pressure, etc.

Notes: AP-Ambient pressure; GC-Gas composition; HP-High-pressure; HT-High-temperature; IC-Ionic composition; MC-Mineral composition; MCC-Microbial community composition; RT-Room temperature; SRB-Sulfate-reducing bacteria; VFAC-Volatile fatty acid concentration.

(2023) employed different sizes of serum bottles to investigate the consumption of H_2 by autochthonous microbes in formation water from natural gas fields under anaerobic conditions without the addition of nutrients, aiming to analyze the effects of reactor size and liquid volume. Additionally, the impact of heat shock was explored by dynamically adjusting the experimental temperature (30 → 60 → 30 °C). Dopffel et al. (2023) utilized sterile bottles to investigate H_2 consumption by salt-tolerant SRB *Desulfohalobium retbaense* and salt-tolerant methanogen *Methanocalculus halotolerans* under different H_2 partial pressures. The results are compared with those of autochthonous microbes in brine obtained from salt caverns in Northern Germany, both with and without the addition of nutrients. Schwab et al. (2023) analyzed the effects of salinity levels (2.5–4.4 mol/L) and different carbon source combinations on methanogenesis, SR, and acetogenesis by using serum bottles as bioreactors, aiming to simulate microbial H_2 consumption in high-salinity environments. Vítězová et al. (2023) studied the methanation of H_2 and CO_2 by autochthonous microbes in the formation water from the Tvrdonice gas storage in the Czech Republic, using serum bottles as bioreactors. To ensure an adequate supply of gaseous substrates for the microbes, the headspace was replenished with an H_2/CO_2 mixture (4:1) after each measurement of pressure and gas composition.

In the aforementioned studies, no rock samples were added to the bottles, so the influence of rocks was not considered. Khajooie et al. (2024) initially analyzed the impact of rock pore space on H_2 consumption using six sealed glass bottles (Fig. 5). Among these, three bottles contained rock specimens saturated with *M. Thermolithotrophicus* solution (MTS), while the remaining three contained only MTS, with amounts equivalent to the pore volume of the rock samples. Additionally, they investigated the effects of different rock types and rock particle sizes on microbial activity. Since these bottles have larger volumes compared to the culture tubes used previously, they can, to some extent, accommodate pressure sensors and be connected to devices such as mass spectrometers for dynamic analysis of pressure and gas composition (Fig. 5). However, similar to culture tubes, experiments using bottles can only be conducted under low pressure, with the previous highest pressure being 3 bar (Vítězová et al., 2023).

To better replicate the reservoir's temperature and pressure conditions, some high-pressure and high-temperature bioreactors have been developed and employed. Their temperature and pressure capacities, along with the corresponding volumes, are illustrated in Fig. 6. In the Underground Sun Storage (USS) project led by RAG Austria AG, ten high-pressure reservoir simulation reactors (RSRs) were deployed (Bauer, 2017). A sequence of operations involving CH_4 injection, CH_4 extraction, and injection of a mixed gas containing 4%–10% H_2 and 0.3%–2.5% CO_2, was performed to simulate underground storage of H_2 and natural gas mixtures. In the following Underground Sun Conversion (USC) project (Bauer, 2023), cyclic injection experiments with 10%–40% H_2 and 2.5%–10% CO_2 were conducted using RSRs, exploring the viability of using native microbes in the formation water for converting H_2 and CO_2 into CH_4. Furthermore, three confined core reactors (CCRs) each capable of accommodating 1-m-long rock cores were also deployed, enhancing the simulation of in-situ conditions by facilitating the forcing of gas through these cores. In the subsequent USC–Flex Store project (Konegger et al., 2023), wellbore simulation reactors (WSRs) with smaller capacities were employed. The adjustments in total pressure and the ratio of injected gases (H_2 to CO_2), combined with analyses of dominant microbes and physicochemical characteristics, aimed to elucidate potential and existing microbial pathways and to identify optimal operational strategies for UBM technology.

Haddad et al. (2022) and Mura et al. (2024) simulated H_2 losses

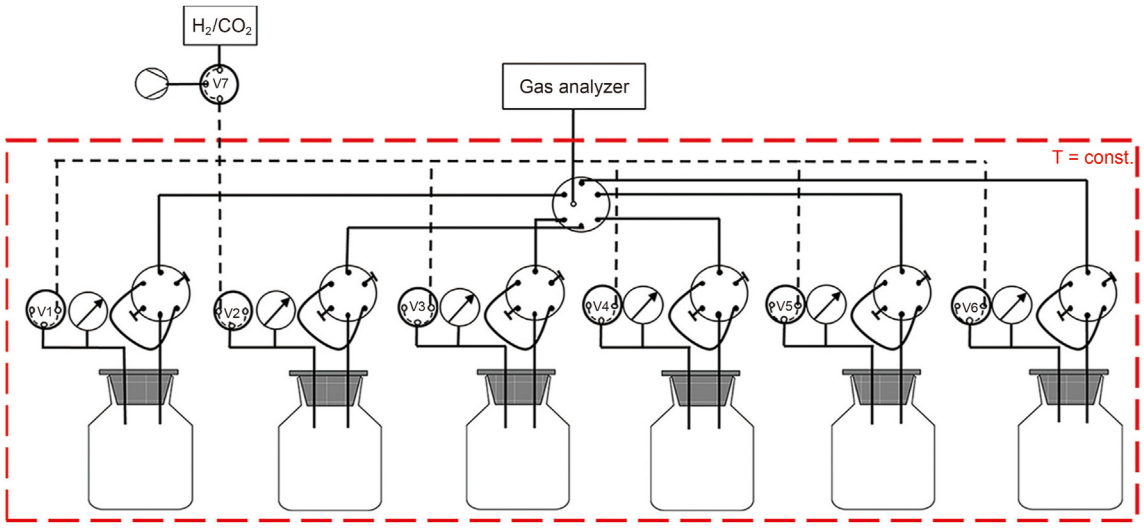

Fig. 5. Schematic of the experimental setup for analyzing pore effects on H_2 consumption (Adapted with permission from Khajooie et al., 2024. Copyright, 2023; Hydrogen Energy Publications LLC).

induced by autochthonous microbes in three aquifers in the Paris Basin, France, using high-pressure reactors as shown in Fig. 7. The experiment process was divided into two stages. In the first stage, a gas composition of 99% CH_4 + 1% CO_2 was used to simulate the gas phase of the stored natural gas. This was followed by the injection of H_2, reaching a maximum concentration of 10%. Dohrmann and Kruger (2023) utilized high-pressure reactors to explore the potential H_2 consumption by autochthonous microbes in the reservoir fluid of the Schneeren Gas Field, under pressure and temperature conditions close to in-situ conditions. After H_2 consumption, reinjection was conducted to simulate the periodic pressure fluctuations experienced during H_2 storage and to explore their effects on microbial activity. Vasile et al. (2024a) used innovative high-pressure, high-temperature, multi-sensing bioreactors (Bio-Xplorer) to simulate the conditions of two depleted gas reservoirs in Italy and investigate associated microbial risks. Cylindrical rock samples obtained through deep coring, along with formation water, were inserted into the bioreactors and subjected to the desired conditions of temperature, pressure, and H_2 mixture. Additionally, Rooney and Li (2023) focused on the impact of biogeochemical reactions on the wellbore cement ring in UHS. The experiments involved immersing wellbore cement cores and shale in synthetic formation brine. Generally, the aforementioned high-pressure bioreactors are equipped with pressure and temperature sensors and allow for dynamic sampling of gases and liquids, enabling

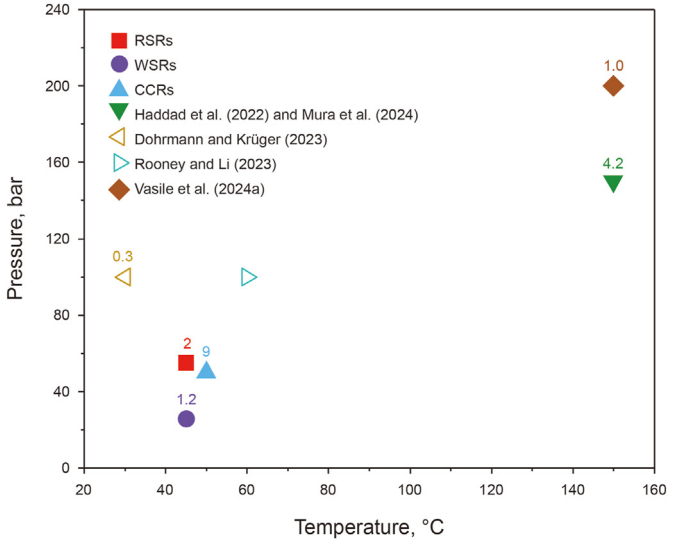

Fig. 6. Maximum temperature and pressure thresholds for high-pressure bioreactors (Data from Bauer, 2017; Haddad et al., 2022; Bauer, 2023; Dohrmann and Kruger, 2023; Konegger et al., 2023; Rooney and Li, 2023; Mura et al., 2024; Vasile et al., 2024a). Labels indicate the corresponding volumes in liters. Hollow symbols denote unknown upper limits; the values associated with these symbols represent the maximum values employed in the experiments.

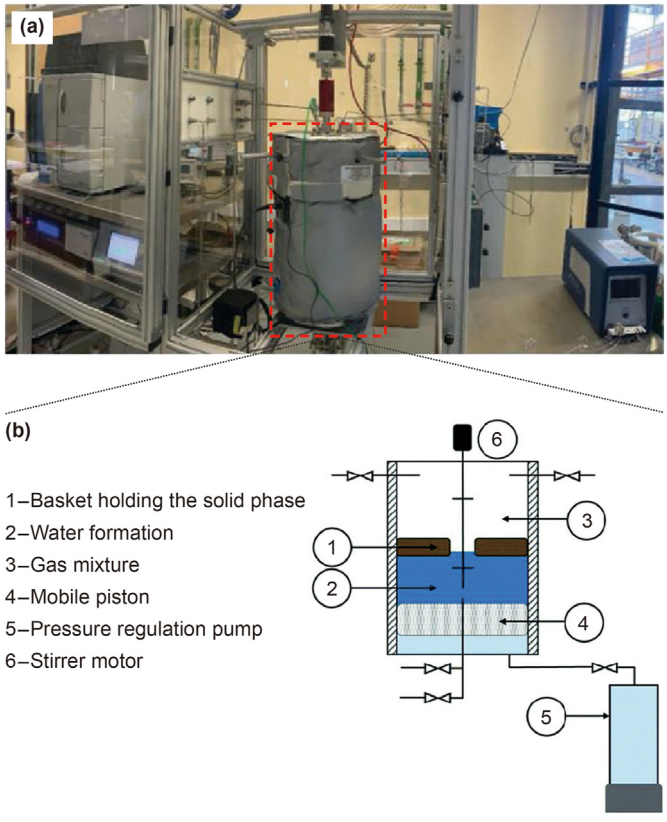

Fig. 7. Photography (**a**) and schematic (**b**) of the high-pressure bioreactor used by Haddad et al. (2022) (Adapted under the terms of the license CC BY-NC 3.0).

comprehensive dynamic analysis of various key parameters.

Apart from CCRs, other mentioned reactors including tubes, bottles, and high-pressure reactors are limited to analyzing batch-type GWRM interactions, without considering spatial fluid flow. In contrast, microfluidic pore networks provide a valuable approach for dynamic analysis (Liu et al., 2023b; Strobel et al., 2023b). When paired with microscopic examination, this method enables direct observation of various phenomena, such as microbial-induced clogging, temporal and spatial variations in fluid saturation caused by microbial processes, and changes in wettability.

4.1.3. Interfacial properties

The wettability alteration caused by GWRM interactions is typically evaluated through measurements of contact angles before and after microbial activity. In a study by Ali et al. (2023), the cyanobacteria *Geitlerinema* sp. was cultured in synthetic seawater under room temperature and ambient pressure conditions. This study examined the impact of initial rock wettability using strongly water-wet quartz samples and strongly oil-wet quartz samples coated with a layer of stearic acid. Post-culturing, the quartz samples were dried, and the advancing and receding angles were measured using a brine droplet method on an inclined plate within a cell designed for high-pressure and high-temperature conditions. This approach of cultivating microbes at room temperature and subsequently assessing contact angles under elevated temperatures and pressures was similarly adopted by Aftab et al. (2023, 2024), and Al-Yaseri et al. (2024). Their research explored wettability changes across various rock types, utilizing the sessile drop technique to measure the contact angles.

In a study by Boon et al. (2024), both microbial cultivation and contact angle measurements occurred under uniform temperature conditions using the experimental setups depicted in Fig. 8 (a), employing the captive-bubble cell method. This investigation also explored the impact of surface roughness by utilizing both rough sandstone and smooth pure quartz samples. However, due to the strong heterogeneity of underground rocks, the aforementioned measurement methods may struggle to accurately reflect this characteristic. Additionally, fluid flow in porous rocks can lead to complex dynamic changes in the wettability contact angle. Consequently, the contact angle measured by these methods may deviate from the actual conditions underground. Contrastingly, the microfluidic pore network-based method utilized by Liu et al. (2023b), illustrated in Fig. 8(b1) and (b2), achieved a more realistic representation of actual porous conditions in UHS. By following steps including pore space cleaning, pressurization to operating pressure (35 bar), bacterial inoculation, H_2 drainage, and microfluidic system closure, the key stages of H_2 injection and well shutdown in UHS were effectively simulated. The contact angles in the porous medium before and after microbial activity were directly measured through microscopic observation.

Other methods for measuring contact angles, such as the Wilhelmy plate method and the capillary rise method, are prevalent across various fields. However, due to their lack of specificity without microbial influence, they are not included in the scope of this review. Capillary pressure and interfacial tension have received minimal study and, for the reasons mentioned previously, are excluded from this review. Detailed discussions are available in Aslannezhad et al. (2023).

4.2. Numerical simulations

4.2.1. Overview of numerical simulations

As shown in Table 4, prior numerical simulations have typically concentrated on either bio-geochemical or bio-hydrodynamic aspects (Fig. 9), largely due to the complexities involved in simultaneously integrating biochemistry, geochemistry, and hydrodynamics. PHREEQC was primarily employed for the former, analyzing intricate GWRM interactions and the resultant H_2 losses. For bio-hydrodynamic studies, simulators such as CMG, Eclipse, and DuMu^X were used, focusing predominantly on the effects of microbes on the injection and extraction of H_2 under various operating modes and parameters. In the following subsections, the key models and simulators are introduced. Since the geochemical models used show no difference with or without microbial metabolism, the relevant models are omitted. Detailed information can be found in Refs. (Xu, 2008; Parkhurst and Appelo, 2013; Steefel et al., 2015; Addassi et al., 2021; Lu et al., 2022; Saeed and Jadhawar, 2024).

4.2.2. Biochemical models

The microbial life cycle generally flows through four key phases: the lag phase, exponential phase, stationary phase, and decay phase (Muloiwa et al., 2020). During the lag phase, microbes need time to adapt to new environmental conditions, leading to relatively stable population levels. In the exponential phase, the number of microbes rapidly increases, signifying the period of fastest growth. The stationary phase is marked by a delicate balance between microbial reproduction and death, leading to no overall increase in population, typically due to the exhaustion of essential nutrients and the accumulation of toxic by-products. In the decay phase, the depletion of essential nutrients for microbial growth results in a steep decrease in microbial populations. Additionally, in certain instances, an acceleration phase and a deceleration phase may also be included (Hagemann et al., 2016), as shown in Fig. 10. Using precise kinetic models to describe the phases of microbial growth and death is critical for evaluating the impacts of microbial interactions on UHS.

In numerical simulations that explore microbial effects on UHS, the majority have employed a dual Monod model to compute microbial specific growth rates (Eq. (1)), enabling consideration of the influence of two limiting substrates (i.e., electron donor and electron acceptor) on microbial growth (Hagemann et al., 2016; Veshareh et al., 2022; Shojaee et al., 2024b). In the context of sulfate reduction simulations, dissolved H_2 is typically used as the electron donor, with sulfate ions acting as the electron acceptor. In contrast, for methanogenesis and acetogenesis simulations, while dissolved H_2 remains the electron donor, the choice of electron acceptors can vary. For example, Hogeweg et al. (2024) used dissolved CO_2 as the electron acceptor, while Veshareh et al. (2022) included all forms of dissolved inorganic carbon in an oxidation state of +4, such as bicarbonate, CO_2(aq), and $CaHCO_3^+$, as electron acceptors. The specific choice primarily hinges on the simulator's capacity to incorporate the series of chemical reactions of CO_2 in water.

$$\mu_{gr} = \mu_{max} \frac{C_A}{C_A + K_A} \frac{C_D}{C_D + K_D} \tag{1}$$

where μ_{gr} represents the specific growth rate, $s^{-1;}$ while μ_{max} denotes the maximum specific growth rate, s^{-1}; C_A and C_D are the concentrations of electron acceptor and donor, mol/L, respectively, with K_A and K_D being their corresponding half-saturation constants (mol/L) (Shojaee et al., 2024b). At high substrate concentrations, the specific growth rate is largely independent of the substrate levels. Conversely, at low substrate concentrations, the specific growth rate is significantly influenced by them.

Although the dual Monod model is extensively utilized, it initiates microbial growth immediately and transitions directly from the deceleration phase to the decay phase, making it inadequate for accurately predicting the lag and stationary phases (Hagemann et al., 2016). Laboratory experiments indicate that the lag phase

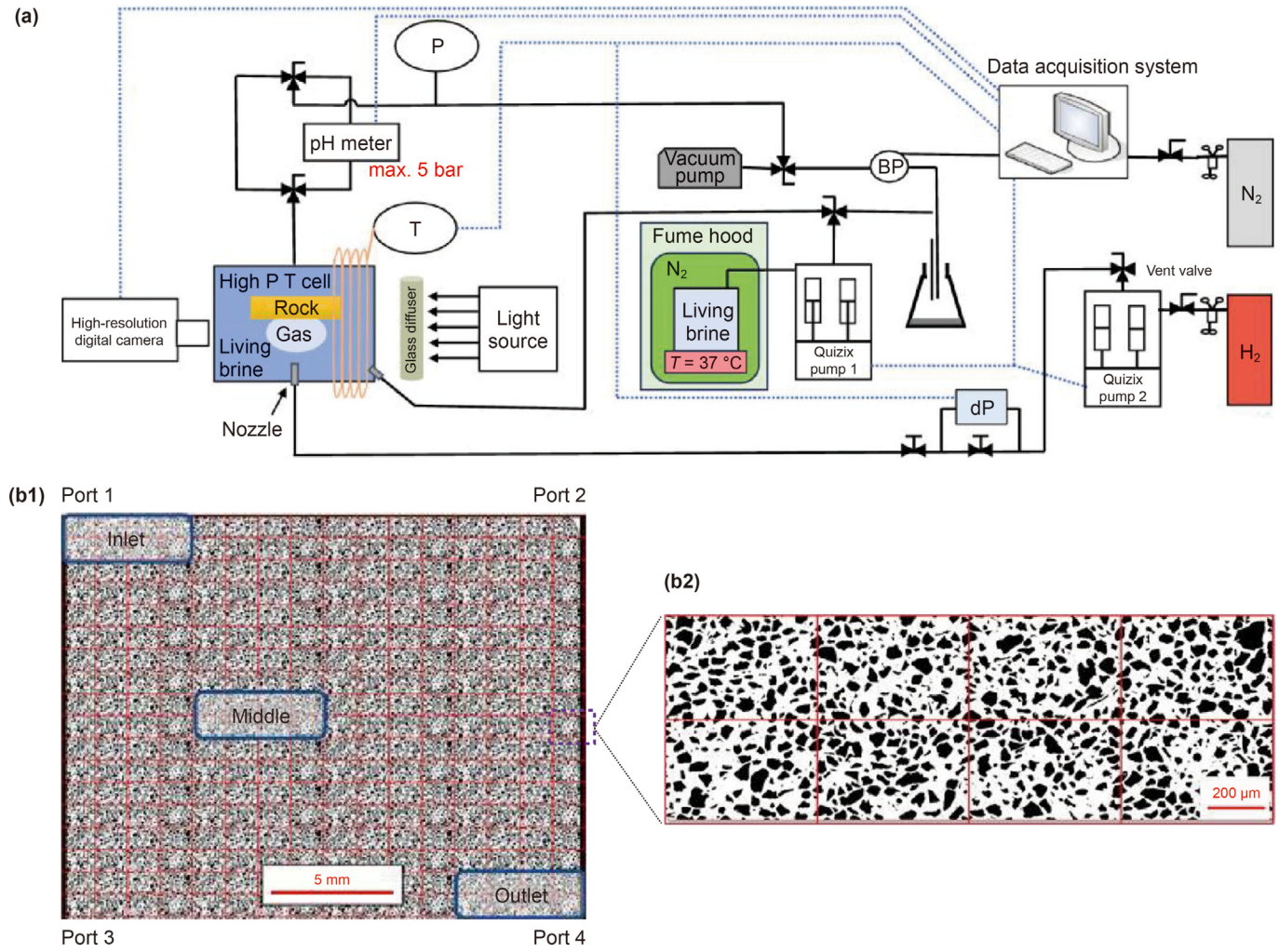

Fig. 8. Experimental setups for evaluating wettability under microbial influence. (**a**) Captive-bubble method in a high-pressure and high-temperature cell (Adapted under the terms of the license CC BY 4.0 from Boon et al., 2024); (**b1**, **b2**) Microfluidic pore network-based method (Adapted under the terms of the license CC BY 4.0 from Liu et al., 2023b).

may be completely absent or extend for several weeks. Consequently, Panfilov (2010) introduced enhancements to this model by representing the maximum specific growth rate as a function of the characteristic time of eating and the maximum population size, as illustrated in Eq. (2). A significant challenge in applying this model is the difficulty in obtaining accurate parameters.

$$\mu_{\max} = \frac{1}{t_e} \frac{n}{1 + n^2/n_{\max}^2} \tag{2}$$

where t_e denotes the characteristic time of eating, s; n represents the population size of microbes, m^{-3}; and $n_{\max}$ is the maximum population size of microbes, m^{-3}. Additionally, the lag phase can also be considered by multiplying the maximum specific growth rate by the lag coefficient λ, represented as a piece-wise function (Wood et al., 1995; Strobel et al., 2023a).

$$\lambda = \begin{cases} 0, & \text{if } t < t_L \\ \dfrac{t - t_L}{t_E - t_L}, & \text{if } t_L \le t \le t_E \\ 1, & \text{if } t > t_E \end{cases} \tag{3}$$

where t represents the time starting from the initial contact of the substrates with the liquid, s; t_L is the end time of lag phase, s; t_E is the time when the exponential growth is reached, s.

In some simulations that account for geochemical reactions, such as those conducted using PHREEQC software, the impact of environmental conditions on microbial growth is also considered (Veshareh et al., 2022; Shojaee et al., 2024b). In these simulations, the maximum specific growth rate is not a constant value but varies with changes in environmental conditions by applying influencing coefficients. Influencing factors can include temperature, salinity, pH, microbial concentration, and more. Therefore, the maximum specific growth rate can be presented in the following general formulation (Rosso et al., 1995; Peleg, 2021; Jin, 2023):

$$\mu_{\max} = \mu_{\text{opt}} \prod \psi_i \tag{4}$$

where μ_{opt} represents the specific growth rate of microbes under optimal conditions, s^{-1}; and ψ_i is the influencing coefficient of each factor. Table 5 summarizes the general calculation models for various influencing factors and their applications in simulations investigating microbial interactions in UHS. In these simulations, the values of key parameters, which are combined values of the same type of microbes, may deviate from the actual situations. Hogeweg et al. (2022a) enhanced the accuracy of the simulation results by directly fitting the specific growth rate curve obtained

Table 4
Comprehensive comparison of numerical simulations of microbial interactions in UHS within porous media.

Research	Focus	Storage scenario	Physio-chemical process	Spatial dimension	Microbial metabolism	Microbial growth limit	Simulator
Panfilov (2010)	Analysis of in-situ self-organization and CH_4 generation in UHS	Porous reservoirs	Bio-hydrodynamics	1D, 2D	MET	Substrate	NA
Ebigbo et al. (2013)	Investigation of the mechanisms underlying the conversion of H_2 to CH_4	Porous reservoirs	Bio-hydrodynamics	Pore-scale 3D	MET, ACE, acetotrophic methanogenesis	Substrate	NA
Hagemann et al. (2016)	Impact of H_2 on the hydrodynamic and biochemical behavior	Depleted gas reservoirs	Bio-hydrodynamics	2D	MET, ACE, SR, Iron reduction	Substrate	DuMu^X
Panfilov et al. (2016)	Analysis of self-organization and shock waves in UBM and UHS	Porous reservoirs	Bio-hydrodynamics	1D	MET	Substrate	NA
Pfeiffer et al. (2016)	Demonstrating the potential applications of the coupled simulator	Depleted gas reservoirs	Bio-hydrodynamics	2D	MET	Substrate	OpenGeoSys−Eclipse
Hemme and van Berk (2018)	Identification of potential risks in UHS	Depleted gas reservoirs	Bio-geochemistry	1D	MET, SR	Substrate	PHREEQC
Eddaoui et al. (2021)	Impact of pore clogging on UHS	Aquifers	Bio-hydrodynamics	3D	MET	Substrate	DuMu^X
Nikolaev et al. (2021)	Examining the effects of operational parameters on UBM	Depleted gas reservoirs	Bio-hydrodynamics	3D	MET	Substrate	DuMu^X
Ali et al. (2022)	Evaluation of H_2 loss due to methanogenesis	Depleted gas reservoirs	Bio-hydrodynamics	3D	MET	Substrate	Eclipse-E300
Hogeweg et al. (2022a)	Examining the viability of freshwater injection to facilitate UBM	High-saline gas reservoirs	Bio-hydrodynamics	2D	MET	Substrate, salinity	DuMu^X
Hogeweg et al. (2022b)	Evaluating the impact of methanogenesis on UHS performance	Depleted gas reservoirs	Bio-hydrodynamics	3D	MET	Substrate	DuMu^X
Minougou (2022)	Assessing microbial effects on H_2 consumption	Depleted gas reservoirs	Bio-hydrodynamics	3D	MET	Substrate	DuMu^X
Veshareh et al. (2022)	Assessment of bio-geochemical effects on UHS	Depleted hydrocarbon chalk reservoirs	Bio-geochemistry	0D	MET, ACE, SR	Substrate, pH	PHREEQC
Bauer (2023)	Predicting CH_4 production in UBM	Depleted gas reservoirs	Bio-hydrodynamics	2D	MET	Substrate	STAR-CCM+
Elgendy et al. (2023)	Implementing bio-geochemical reactions in CMG	Depleted gas reservoirs	Bio-geochemistry	0D	MET	Substrate	CMG GEM
Maniglio et al. (2023)	Assessing the impact of biotic reactions on UHS	Depleted gas reservoirs	Bio-hydrodynamics	3D	MET, SR	Substrate	CMG STARS
Rosman et al. (2023)	Evaluating the impact of H_2S generation on UHS	Depleted gas reservoirs	Bio-hydrodynamics	3D	SR	Substrate	Eclipse E300
Strobel et al. (2023b)	Analyzing the microbial dynamics in porous media at the pore scale	Porous reservoirs	Bio-hydrodynamics	2D	MET	Substrate	NA
Tremosa et al. (2023)	Assessing H_2 reactivity in UHS	Aquifers	Bio-geochemistry	0D	MET, ACE, SR	Substrate, thermodynamic potential	PHREEQC
Wu et al. (2023a)	Evaluating the efficiency of UBM	Depleted gas reservoirs	Bio-geochemistry	0D	MET	Substrate, pH, temperature, salinity	PHREEQC
Gao et al. (2024)	Quantitative analysis of microbial impact on H_2 storage	Aquifers	Bio-geochemistry, Bio-hydrodynamics, Geomechanics	2D	Iron reduction	Substrate	NA
Hamdi et al. (2024)	Salinity effects on H_2S generation in UHS	Depleted gas reservoirs	Bio-hydrodynamics	3D	SR	Substrate	Eclipse E300
Hogeweg et al. (2024)		Depleted gas reservoirs		3D	MET, SR	Substrate	DuMu^X

			Bio-geochemistry, Bio-hydrodynamics				
	Assessing H_2 loss due to bio-geochemical reactions in UHS			1D	MET	Substrate	MRST
Safari et al. (2024)	Investigating the performance of UBM	Depleted gas reservoirs	Bio-hydrodynamics				
Shojaee et al. (2024b)	Analysis of the interactions between microbial activity and geochemical reactions	Seawater-rich formations	Bio-geochemistry	0D	MET, ACE, SR	Substrate, pH, temperature	PHREEQC
Song et al. (2024)	Evaluating microbial H_2 consumption in UHS	Depleted reservoirs	Bio-hydrodynamics	Pore-scale 3D	MET	Substrate	NA
Vasile et al. (2024b)	Assessing microbial risk in UHS	Depleted gas reservoirs	Bio-geochemistry	0D, 3D	MET, ACE, SR	Substrate	COMSOL, CMG-GEM, PHREEQC
Wang et al. (2024a)	Analyzing the impacts of bio-methanation on UHS performance	Porous reservoirs	Bio-hydrodynamics	2D	MET	Substrate	CMG GEM

Notes: ACE-Acetogenesis; MET-Methanogenesis; SR-Sulfate reduction. All three of these abbreviated microbial metabolic processes utilize H_2 as an electron donor. The term "0D" indicates a batch reaction.

from experimental data under varying salinity.

Additionally, models such as the Haldane model, the Moser model, and the Tesseir model are commonly used to compute specific growth rates. The characteristics and applications of these various models can be explored in Muloiwa et al. (2020). It is crucial to emphasize that regardless of the specific growth rate calculation model selected, obtaining accurate input parameters is the most critical aspect.

The specific growth rate, in conjunction with the yield coefficient, can be employed to establish the relationship between substrate consumption rate and microbial population size (Shojaee et al., 2024b):

$$r_s = -\frac{\mu_{gr}}{Y}N \tag{5}$$

where r_s represents the consumption rate of substrate, mol/(L·s); Y denotes the yield coefficient, g/mol; and N is the biomass, g/L.

Regarding microbial decay, two methods are commonly employed in previous studies for calculating the specific decay rate μ_{dec}. The first approach utilizes a constant specific decay rate ($\mu_{dec} = d$); thus, the biomass change rate is typically determined using the following formula (Wu et al., 2023a; Shojaee et al., 2024b):

$$r_{bio} = -Yr_s - dN \tag{6}$$

where r_{bio} represents biomass growth rate, g/(L·s); and d denotes the decay coefficient, s^{-1}. The second approach allows the decay rate to vary linearly with microbial population size ($\mu_{dec} = d \cdot n$). This method is frequently used in simulations employing the DuMu^X (Hagemann et al., 2016; Hogeweg et al., 2022b). Detailed information on calculating microbial population changes using this approach can be found in Section 4.2.3.

Recently, in pursuit of greater alignment with engineering scales, some studies have adopted reservoir simulators (e.g., Eclipse and CMG) to simulate microbial interactions in UHS (Table 4). Methods based on the Arrhenius equation are commonly used for the approximate calculation of reaction rates. The general expression is formulated as follows (Maniglio et al., 2023; Wang et al., 2024a):

$$r_s = F \cdot \exp\left(-\frac{E_a}{R}\frac{1}{T}\right)\prod c_{mi}^{\varsigma_i} \tag{7}$$

where F is the frequency factor, with its dimensions determined by the reaction order; E_a stands for the reaction activation energy, J/mol; R denotes the universal gas constant, J/(mol·K); T signifies the reaction temperature, K; c_{mi} stands for the molality of each reactant, mol/L; and ς_i is the reaction order. The specific approximation methods vary slightly among different studies. For instance, Maniglio et al. (2023) assumed the activation energy to be 0 in their simulation, with the remaining parameters fitted using the PHREEQC benchmark. Wang et al. (2024a) further simplified the reaction order of the reactants to 1, where the only parameter requiring determination was F, established through single-cell simulations. Meanwhile, Ali et al. (2022) employed ruthenium metal-based catalyst activation energy for a similar methanation reaction.

4.2.3. Hydrodynamic models

The spatial distribution of substrate gases and microbes is influenced by a multitude of factors, directly impacting microbial metabolism and UHS performance. Hence, it is crucial to consider the effect of hydrodynamics in numerical modeling. Saeed and Jadhawar (2024) reviewed hydrodynamic models relevant to

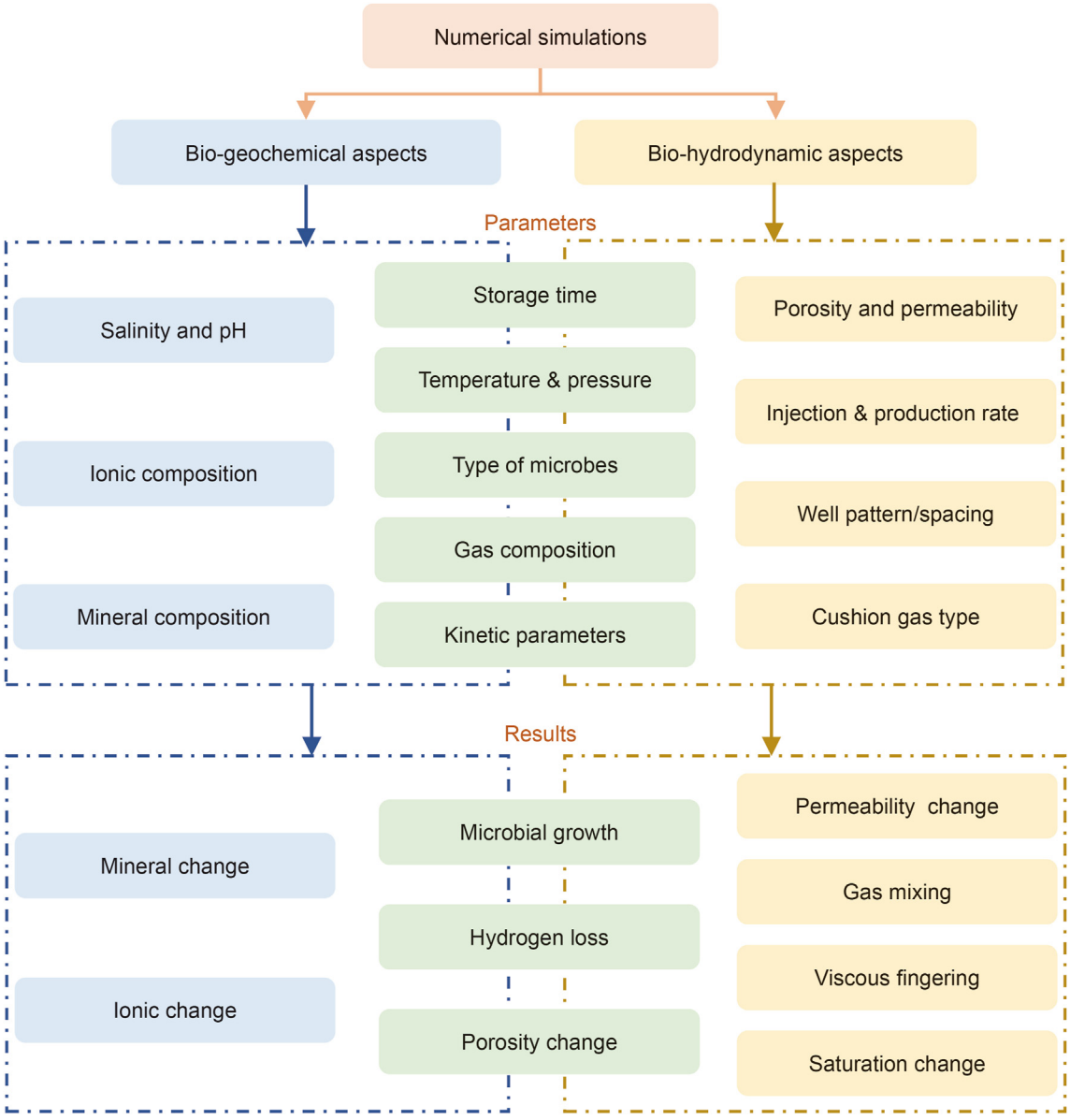

Fig. 9. Overview of key parameters and outcomes discussed from previous numerical simulations.

UHS, encompassing models for calculating fluid properties, rock properties, rock–fluid properties, fluid–fluid properties, etc. However, there was a notable absence in considering microbial effects. Therefore, this subsection focuses on hydrodynamic models under the influence of microbes.

The foremost and pivotal aspect is the conservation equations. At a macroscopic level, porous media and all present fluids can be perceived as continuous and equivalent media. This assumption forms the basis for deriving mass conservation equations for gas and water. One commonly employed mass conservation equation that considers advective and dispersive/diffusive transport is as follows (Hagemann et al., 2016):

$$\phi\frac{\partial\left(\rho_g c_g^k S_g+\rho_w c_w^k S_w\right)}{\partial t}+\nabla\cdot\left(\rho_w c_w^k v_w+J_w^k+\rho_g c_g^k v_g+J_g^k\right)=q^k \tag{8}$$

where ϕ represents porosity; ρ is molar density, mol/m^3; c is mole fraction; S is saturation; v is convective flux, m/s; J is dispersion/diffusion flux, mol/(m^2·s); and q is the source or sink term related to microbial consumption, mol/(m^3·s). The subscripts g and w refer to the gas phase and the water phase, respectively, and the superscript k represents the chemical composition.

The growth and decay of microbes depend on the availability of substrates. Furthermore, microbes can attach to and detach from rocks, and they move through random motion (similar to diffusion) and chemotaxis, making the conservation equations for microbes highly complex. The non-structural mass conservation equation, which considers only microbial growth, decay, and diffusion, is as follows (Hagemann et al., 2016):

$$\frac{\partial n}{\partial t}=S_w\mu_{gr}\,n-\mu_{dec}n+\nabla\cdot(D\nabla n) \tag{9}$$

where D is the cell diffusion coefficient, m^2/s; and μ_{dec} varies linearly with the microbial population size, as detailed in Section 4.2.2. These models were integrated into the DuMu^x, and subsequent studies using DuMu^x has primarily been based on these frameworks with minor changes (Nikolaev et al., 2021; Hogeweg

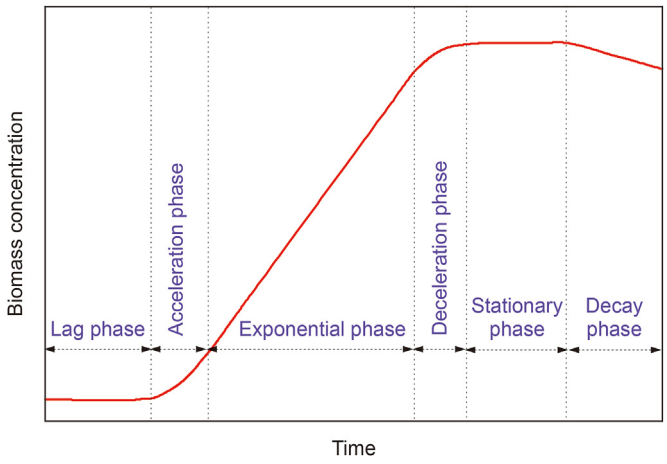

Fig. 10. The six stages of the microbial life cycle (Redrawn under the terms of the license CC BY 4.0 from Hagemann et al., 2016).

et al., 2022b, 2024). In contrast, Eddaoui et al. (2021) proposed a model based on the assumption that the two forms of microbial existence (i.e., biofilm and plankton) are likely to occur within porous geological media, while also taking advection into account. The mass balance equations of attached and detached microbes are as follows:

$$\frac{\partial}{\partial t}(\phi S_w n_a) = \mu_{gr} S_w n_a - \mu_{dec} S_w n_a + k_a S_w n_d - k_d S_w n_a \tag{10}$$

$$\frac{\partial}{\partial t}(\phi S_w n_d) + \nabla \cdot (n_d v_w) - \nabla \cdot (D S_w \nabla n_d) = \mu_{gr} S_w n_d - \mu_{dec} S_w n_d - k_a S_w n_d + k_d S_w n_a \tag{11}$$

where n_a and n_d represent the numbers of attached and detached microbes, m^{-3}, respectively; while k_a and k_d are the rates of attachment and detachment per microbe, s^{-1}. In this model, attachment is influenced by diffusion, geometrical interception, and inertial deviation. The specific calculation methods of relevant parameters can be found in Eddaoui et al. (2021). Similarly, Gao et al. (2024) incorporated microbial adsorption/desorption into their coupled hydrological-mechanical-chemical-biological model. Their treatment of microbial adsorption includes both reversible and irreversible adsorption processes.

In natural porous media with pore sizes comparable to the size of microbes, the presence of microbes can potentially result in complete pore clogging, irrespective of whether the microbes are

Table 5
General models for calculating influencing factors and their application.

Influencing factor	Model	Source	Application
pH	$\psi_{pH} = \left(\frac{(pH - pH_{min})\{1 - \exp[b_1(pH - pH_{max})]\}}{(pH_{opt} - pH_{min})\{1 - \exp[b_1(pH_{opt} - pH_{max})]\}}\right)^2$	Zwietering et al. (1992)	NA
	$\psi_{pH} = \frac{(pH - pH_{min})(pH - pH_{max})}{(pH - pH_{min})(pH - pH_{max}) - (pH - pH_{opt})^2}$	Rosso et al. (1995)	Wu et al. (2023a)
	$\psi_{pH} = \frac{(pH - pH_{min})(pH - pH_{max})}{(pH_{opt} - pH_{min})(pH_{opt} - pH_{max})}$	Wijtzes et al. (2001)	Veshareh et al. (2022)
	$\psi_{pH} = \frac{(pH - pH_{min})(2pH_{opt} - pH_{min} - pH)}{(pH_{opt} - pH_{min})^2}$	Leroi et al. (2012)	NA
	$\psi_{pH} = \begin{cases} -\frac{(pH - pH_{min})(pH + pH_{min} - 2pH_{opt})}{(pH_{opt} - pH_{min})^2}, & pH_{min} < pH < pH_{opt} \\ 1, \quad pH = pH_{opt} \\ -\frac{(pH - pH_{max})(pH + pH_{max} - 2pH_{opt})}{(pH_{opt} - pH_{max})^2}, & pH_{opt} < pH < pH_{max} \end{cases}$	Shojaee et al. (2024b)	Shojaee et al. (2024b)
Temperature	$\psi_T = \frac{(T - T_{max})(T - T_{min})^2}{(T_{opt} - T_{min})[(T_{opt} - T_{min})(T - T_{opt}) - (T_{opt} - T_{max})(T_{opt} + T_{min} - 2T)]}$	Rosso et al. (1995)	NA
	$\psi_T = \begin{cases} -\frac{(T - T_{min})(T + T_{min} - 2T_{opt})}{(T_{opt} - T_{min})^2}, & T_{min} < T < T_{opt} \\ 1, \quad T = T_{opt} \\ -\frac{(T - T_{max})(T + T_{max} - 2T_{opt})}{(T_{opt} - T_{max})^2}, & T_{opt} < T < T_{max} \end{cases}$	Shojaee et al. (2024b)	Shojaee et al. (2024b)
	$\psi_T = \left(\frac{(T - T_{min})\{1 - \exp[b_2(T - T_{max})]\}}{(T_{opt} - T_{min})\{1 - \exp[b_2(T_{opt} - T_{max})]\}}\right)^2$	Zwietering et al. (1992)	NA
Salinity	$\psi_{C_s} = \frac{(C_s - 2C_{s,opt} + C_{s,max})(C_{s,max} - C_s)}{(C_{s,max} - C_{s,opt})^2}$	Leroi et al. (2012)	NA
	$\psi_{C_s} = \exp\left[-\left(\frac{C_s}{C_{s,c}}\right)^{b_3}\right]$	Peleg (2021)	Wu et al. (2023a)
Thermodynamic potential	$\psi_{TP} = 1 - \exp\left(-\frac{f_d}{\chi RT}\right)$	Jin (2023)	Tremosa et al. (2023)
Microbial concentration	$\psi_{C_X} = 1 - \frac{C_X}{C_{X,max}}$	Jin (2023)	NA

Notes: pH is the pH value of the brine; T is the temperature, K; C_s is the salinity of the brine, g/L; $C_{s,c}$ is the characteristic salinity that marks the curve's drop region, g/L; f_d is the thermodynamic drive, J/mol; χ is the average stoichiometric number; R is the gas constant, J/(mol·K); C_X is the concentration of biomass, L^{-1}; and b_1, b_2, and b_3 are regression coefficients. The subscripts min, opt, and max represent the minimum, optimum, and maximum values of each factor for the growth of microbes, respectively.

attached or detached. This phenomenon subsequently impacts the porosity and permeability of the reservoir. Eddaoui et al. (2021) developed a porosity evolution model that considers both the number of detached and attached microbes, formulated as follows:

$$\phi = \phi(n_a, n_d) = \frac{\phi_0}{1 + \left(\frac{n_a + n_d}{n_c}\right)^2} \tag{12}$$

where n_c represents the quantity of microbes required to induce maximal bio-clogging effect, m^{-3}; and ϕ_0 denotes the porosity of a clean reservoir devoid of microbes. The alteration in permeability is determined using the Carman–Kozeny formula:

$$k_p = k_p(n_a, n_d) = \left(\frac{d_p^2}{180}\right) \frac{\phi(n_a, n_d)^3}{(1 - \phi(n_a, n_d))^2} \tag{13}$$

where k_p is the absolute permeability, m^2; and d_p is the pore diameter, m. However, Zhang et al. (1992) believed that microbial clogging effects might not notably alter porosity but could significantly impact permeability. They introduced a dimensionless flow efficiency coefficient for correction, which is mainly determined by the bimodal function of the pore throat diameter:

$$\frac{k_p}{k_{p0}} = f_e \left(\frac{\phi}{\phi_0}\right)^3 = f_e \left(\frac{\phi_0 - \varphi}{\phi_0}\right)^3 \tag{14}$$

where k_{p0} denotes the absolute permeability of a clean reservoir devoid of microbes, m^2; f_e represents the dimensionless flow efficiency coefficient; and φ is the pore fraction occupied by microbes. In the commercial software CMG, other relationships between porosity and permeability based on Carman-Kozeny equation are also suggested (Jeong et al., 2019). Another significant approach to compute permeability evolution involves considering the equilibrium relationship between mobile microbes and adsorbed microbes without initially computing porosity. The model is outlined as follows (Jeong et al., 2019):

$$k_p = 1 + (R_r - 1)\frac{ad}{ad_{max}} \tag{15}$$

where R_r represents the resistance factor; ad_{max} denotes maximum adsorption capacity of microbes, L^{-1}; and ad signifies the number of adsorbed microbes, L^{-1}, typically calculated by the Langmuir isotherm adsorption equation:

$$ad = \frac{\left(c_1^{ad} + c_2^{ad} X_{NaCl}\right) X_a}{1 + c_3^{ad} X_a} \tag{16}$$

where X_{NaCl} represents salinity, g/L; c_1^{ad}, c_2^{ad}, and c_3^{ad} are constants.

In some pore-scale simulations (e.g., Ebigbo et al., 2013; Song et al., 2024), a biofilm volume fraction ϕ_b is often defined to accurately track the interface between the biofilm and the bulk water. By solving the mass balance equation for the biofilm that includes this volume fraction, pore clogging due to microbial growth and its impact on fluid flow can be evaluated more precisely (Peszynska et al., 2016).

The microbial effect on capillary pressure can be evaluated by analyzing alterations in porosity and absolute permeability, utilizing the Leverett scaling relation (Steefel et al., 2015; Eddaoui et al., 2021). However, this method doesn't account for variations in wettability, interfacial tension, etc. While there have been studies on microbial effects on wettability, interfacial tension, relative

Table 6
Comprehensive comparison of potential simulators for analyzing microbial interactions in UHS (modified after Steefel et al., 2015; Hagemann, 2018; Saeed and Jadhawar, 2024).

	DuMu^x	MRST	TOUGHREACT	PHREEQC	PHAST	CMG	Eclipse	OpenGeoSys	COMSOL
Capability									
Main application	Porous flow	Reservoir simulation	Reactive transport	Geochemical simulation	Reactive transport	Reservoir simulation	Reservoir simulation	Multiphysics	Multiphysics
Maximum dimension	3D	3D	3D	1D	3D	3D	3D	3D	3D
Biochemical reaction	Yes	Yes	Yes	Yes	Yes	Limited	Limited	Yes	Limited
Geochemical reaction	Limited	Limited	Yes	Yes	Yes	Limited	Limited	Yes	Limited
Multi-phase flow	Yes	Yes	Yes	No	No	Yes	Yes	Yes	Yes
Multi-component flow	Yes	Yes	Yes	Yes	Yes	Yes	Yes	Yes	Yes
Non-isothermal flow	Yes	Yes	Yes	No	No	Yes	Yes	Yes	Yes
Geomechanical simulation	Yes	Limited	No	No	No	Limited	Limited	Yes	Yes
Numerical scheme									
Spatial discretization	FVM	FVM	FVM	Mixing cell	FDM	FDM	FDM	FEM	FEM
Time discretization	Back Eueler	Implicit/Explicit	Implicit/Explicit	Various	Various	Implicit	Implicit	Various	Implicit
User interaction									
Graphical user interface	No	Yes	No	Yes	Yes	Yes	Yes	Yes	Yes
Programming language	C++	MATLAB	Fortran	C++	Fortran, C, C++	C++	C++	C++	Java
Open source	Yes	Yes	No	Yes	Yes	No	No	Yes	No
Computational requirement	Moderate	Moderate	Moderate to high	Low	Low to moderate	Moderate to high	Moderate to high	Moderate to high	High
Refs.	Flemisch et al. (2011); Hogeweg et al. (2024)	Lie (2019); Lie and Møyner (2021)	Xu (2008)	Parkhurst and Appelo (2013)	Parkhurst et al. (2010)	Okoroafor et al. (2023); Wang et al. (2024a)	Okoroafor et al. (2023); Rosman et al. (2023)	Kolditz et al. (2012)	COMSOL (2021)

Notes: FDM-Finite difference method; FEM-Finite element method; FVM-Finite volume method.

Table 7
Global field studies of microbial interactions in UHS within porous media.

Country	Project/site name	Year	Reservoir properties					Operation mode	Injected gas composition	Gas volume	H_2S in the gas phase	Source
			Type	Depth, m	Temperature, °C	Salinity, g/L	pH					
Czech Republic	Lobodice gas storage	Around 1989	Sandstone aquifer	400–500	20–45	1.75	6.5–7.0	NA	54% H_2 + 12% CO_2 + 9% CO + 22% CH_4	NA	No	Šmigáň et al. (1990); Buzek et al. (1994); Thaysen et al. (2021)
	Tvrdonice gas storage	2020	DSHR	900–1600	48–50	10.21	8.1	Batch	50% H_2 + 12.5% CO_2 + 37.5 % N_2	[a] 392 Sm^3	No	Vítězová et al. (2023)
Austria	USS	2013–2017	DSGR	1023	40	14	6.0–6.5	Batch	10% H_2 + 90% natural gas	[a] 1.22 Mio. Nm^3	No	Bauer (2017)
	USC	2017–2021	DSGR	1023	40	14	6.0–6.5	Batch and cycle	0–20% H_2 + 0–2.5% CO_2 + natural gas	[b] 5 + 0.6 Mio. Nm^3	Maximum: 3.58 mg/Nm^3	Bauer (2023)
	USC-FlexStore	2020–2023	DSGR	1023	40	14	6.0–6.5	Batch and cycle	Batch: 10% H_2 + 0.3%–1.3% CO_2	[b] Batch: 1.32 Mio. Nm^3	Total 0.45 kg	Könegger et al. (2023)
Argentina	Hychico-BRGM	2010–2018	DSGR	815	55	NA	NA	Batch	10% H_2 + 90% natural gas	NA	NA	Pérez et al. (2016); Dupraz et al. (2018)
Other countries	Site selection for UBM and microbial risk assessment in UHS, primarily conducted through indoor experiments involving field rock samples and formation waters											Bültemeier (2023); Mura et al. (2024); Vasile et al. (2024a)

Notes: DSGR-Depleted sandstone gas reservoir; DSHR-Depleted sandstone hydrocarbon reservoir; USC-Underground sun conversion; USS-Underground sun storage.
[a] Total volume of gas injected. [b] Total volume of gas moved.

permeability, and fluid viscosity, and various models have been proposed, their use is primarily confined to scenarios of microbial enhanced oil recovery (Jeong et al., 2019; Niu et al., 2020). Although some relevant experiments have been undertaken in the context of UHS (Section 4.1.3), mathematical models have yet to be developed, necessitating further investigation.

4.2.4. Numerical simulators

As outlined in Table 4, various simulators are currently utilized to investigate microbial interactions in UHS. These tools serve different purposes such as flow simulation in porous media, reservoir simulation, or multi-physics field coupling, each with unique functionalities and characteristics. A comprehensive comparison of these simulators is provided in Table 6.

For investigating the intricate GWRM interaction mechanisms in UHS, simulators capable of handling complex geochemical reactions, such as PHREEQC and TOUGHREACT, are recommended (Vilcáez, 2015; Veshareh et al., 2022). While PHREEQC allows easy definition of various biogeochemical reactions, it is limited in terms of simulation dimensions and cannot model critical processes such as unsaturated flow and heat transfer. A primary limitation of TOUGHREACT is its inability to simulate rock deformation; addressing this shortcoming typically requires coupling with additional software, such as Flac3D (Taron et al., 2009), which significantly increases computational time.

For research focused on microbial influences on H_2 storage performance, including aspects like gas mixing and recovery, fluid flow-focused simulators such as $DuMu^X$ and MRST are advantageous (Hogeweg et al., 2022b; Safari et al., 2024). However, these tools currently handle geochemical reactions to a limited extent, making the incorporation of complex geochemical reactions challenging. When the interaction between H_2 and reservoir hydrocarbons (e.g., residual natural gas) is also of a concern, utilizing reservoir-specific simulators like CMG and Eclipse would is more appropriate (Ali et al., 2022; Rivolta et al., 2024). These simulators can effectively integrate on-site geological and engineering data but currently use the Arrhenius equation to model microbial growth instead of kinetic models specifically tailored for microbes, potentially leading to significant deviations in simulation results.

Therefore, selecting a simulator that aligns with specific research objectives is crucial. To accurately assess microbial impacts on UHS, the development of more precise models and comprehensive simulators is essential.

4.3. Field studies

4.3.1. Overview of field studies

Currently, three countries (i.e., Austria, the Czech Republic, and Argentina) have conducted field tests of UBM (Table 7). Austria leads in the number of field test projects, each of which is relatively large in scale. These tests predominantly utilize depleted sandstone gas reservoirs, which are generally characterized by shallow burial depth, low temperature, and low salinity, conditions favorable for the growth of methanogens. The field tests typically operate in two main modes: batch and cycle. Additionally, several other countries are in the preliminary stages of site selection for UBM (e.g., Germany) or are evaluating the microbial risks associated with using depleted gas reservoirs or aquifers for UHS (e.g., France and Italy). The following subsections primarily introduce the procedures implemented in field trials.

4.3.2. Czech Republic

Lododice gas storage: It is the only aquifer gas storage in the Czech Republic and the first underground gas storage in the country. Around 1989, when town gas was stored, the initial

composition of the injected gas consisted of 54% H_2, 12% CO_2, and 22% CH_4. However, after a storage period of seven months, significant changes were observed in the gas withdrawn: the H_2 content had decreased to 37%, the CO_2 content to 9%, and the CH_4 content had increased to 40% (Šmigáň et al., 1990). To investigate the cause of the significant changes in gas composition, isotopic monitoring was conducted onsite. The $\delta^{13}CCH_4$ value of the injected town gas was measured at −34.5‰, while the $\delta^{13}CCH_4$ value of the gas extracted after storage was −80‰. These isotopic changes, along with findings from laboratory experiments involving formation water with methanogen-like microbes at concentrations of 10^3 to 10^4 cells per mL, decisively indicated that the CH_4 generated during storage was primarily produced via the catalytic action of methanogens (Šmigáň et al., 1990; Buzek et al., 1994).

Tvrdonice gas storage: It was transformed from a depleted system of hydrocarbon reservoirs located in the Czech part of the Vienna basin (Vítězová et al., 2023). The field test primarily aims to assess the potential and applicability of power-to-CH_4. During the test, 392 Sm^3 of mixed gas was injected into the formation through the test well Z-73A, comprising 50% H_2, 12.5% CO_2, and 37.5% N_2 to simulate the composition of town gas previously stored in the Lobodice gas storage. Subsequently, 19 m^3 of formation water collected from the adjacent well HR-41 was injected. This was due to the reservoir conditions of the test well at the time of the test not being conducive to producing sufficient water in a reasonable timeframe. The wellhead injection method is illustrated in Fig. 11. The methanogenesis process and other changes within the reservoir were monitored 6 h after completing the reservoir water injection. The results showed a notable shift in the $\delta^{13}C$ values of CH_4, which increased from initial −53.6‰ to approximately −30‰ over 10 days. Additionally, the population of methanogens peaked at about 43% in the microbial community on the 22nd day post-injection, and the injected H_2 and CO_2 were completely consumed within approximately 40 days (Section 5.1.2.2). These findings demonstrate the feasibility of synthesizing green CH_4 from H_2 and CO_2 underground.

4.3.3. Austria

Currently, Austria has undertaken three field study projects concerning microbial interactions in UHS: USS, USC, and USC-FlexStore (Bauer, 2017, 2023; Konegger et al., 2023; Hellerschmied et al., 2024). Field tests for all three projects were conducted in a small depleted sandstone gas reservoir, specifically the Lehen-002 reservoir in Pilsbach, Upper Austria, with a total capacity of approximately 6 million Nm^3. Similarly, the reservoir underwent on-site monitoring, and regular analysis of gas and formation water was performed.

USS: A pivotal aspect of this project involved assessing the viability of storing renewable energy in the form of H_2 admixture amidst intricate field conditions (Bauer, 2017). The injected gas amounted to 1.22 million Nm^3, comprising roughly 10% H_2 (115,444 Nm^3) and 90% natural gas. Gas injection spanned three months, followed by a four-month shutdown period to monitor changes in reservoir temperature, pressure, gas composition, etc. Subsequently, production recommenced through the injection well LEH-002 for three months, yielding 1.24 million Nm^3 of gas, with the H_2 content declining to 7.6% (94,549 Nm^3) and the CO_2 content decreasing from 0.22% to 0.01%. A minor portion (3%) of H_2 loss was attributed to methanogens. Strobel et al. (2020) roughly estimated the metabolic rate for CH_4 production to be about 1.66×10^{-9} mol/($s \cdot Sm^3$). The project underscored the feasibility of storing 10% H_2 mixed with natural gas for RAG's gas storage facilities.

USC: Similar to the Tvrdonice gas storage project, this initiative endeavors to assess the viability of UBM of CO_2 and H_2, thereby enabling large-scale, long-term energy storage (Bauer, 2023). In the batch experiments, a gas mixture comprising up to 10% H_2 and up to 2.5% CO_2 was injected from the well LEH-002 five times, with an average volume of approximately 0.5 million Nm^3 per injection. Additionally, modified cycle experiments were conducted 11 times due to the limited connectivity between the test wells. In this approach, a gas mixture containing up to 20% H_2 and up to 2.5% CO_2 was initially injected into the new well LESP-001A, which is characterized by high water saturation and robust microbial activity. Subsequently, the gas was transferred to the well LEH-002, resulting in a total movement of over 0.6 million Nm^3 of gas. Several phenomena observed during the field test affirmed the feasibility of UBM. Notably, the produced water showed an enrichment of methanogens, with 89% of the microbial population

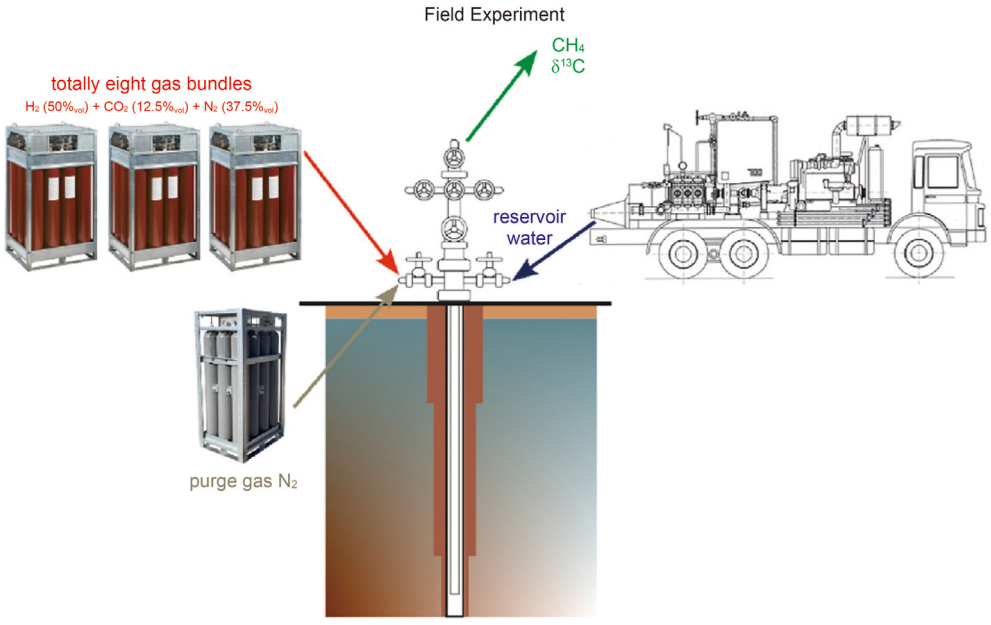

Fig. 11. The wellhead injection method used during the field test at Tvrdonice gas storage (Reprinted under the terms of the license CC BY-NC-ND 4.0 from Vítězová et al., 2023).

identified as belonging to the *Methanobacteriaceae* family, and a significant reduction in CO_2 levels.

USC-FlexStore: The primary focus of this project lies in researching and demonstrating the flexible operational modes of UBM (Konegger et al., 2023). This involves injecting different gas ratios to delineate the boundaries and optimal conditions for UBM. Two batch experiments were conducted in the well LEH-002. In the first experiment, 0.6 million Nm^3 of gas was injected, maintaining a constant 10% H_2 content while varying CO_2 levels between 0.3% and 1.3%. The second experiment injected a total of 0.715 million Nm^3 of gas without additional CO_2 injection. Additionally, the modified cycle experiment was performed 16 times in each well. Gas injected into the well LESP-001A was primarily withdrawn from the well LEH-002, with a certain CO_2 content (up to 2.3%) added before injection to simulate scenarios in future energy systems where CO_2 is consistently available and H_2 is intermittently supplied through storage with fluctuating production. Field test findings indicated the flexibility of CO_2 proportions in the UBM process (Section 5.1.2.2).

Several follow-up projects are underway, building upon the discoveries of the aforementioned initiatives. For instance, the USS2030 project is gearing up to store pure H_2 in an underground natural gas reservoir located in Gampern, Upper Austria (RAG, 2024).

4.3.4. Argentina

In 2010, Hychico in Argentina initiated a project to produce H_2 from wind energy and store it in a depleted gas reservoir. The field test of UHS was divided into three main stages (Pérez et al., 2016; Bellini et al., 2022). Initially, natural gas was injected into well F-160 to reach the original formation pressure, which allowed for the confirmation of reservoir properties and sealing capabilities. Subsequently, a mixture of 10% H_2 and natural gas was injected to achieve a pressure of 10 bar, alongside an analysis of reservoir properties and gas composition in this stage. Finally, natural gas was re-injected to analyze the H_2 sealing at the original reservoir pressure. Throughout the test, the conversion of H_2 to CH_4 was monitored.

Hychico and French Geological Survey (BRGM) then launched a cooperative project focused on UBM (Dupraz et al., 2018; Bellini et al., 2022). This project included biological characterization, both laboratory and field testing, and modeling efforts aimed at identifying the critical factors involved in the production of CH_4 from H_2 and CO_2, and at optimizing this process. However, there have been no subsequent reports on related field tests, and only results from indoor experiments demonstrating favorable conversions are available (Stephant et al., 2018).

4.3.5. Other countries

In addition to the aforementioned projects that have directly conducted field tests, several other projects indirectly related to field studies have been initiated. For instance, DBI Gas & Environmental Technologies Ltd. (DBI GUT) in Germany launched the Bio-UGS project in 2020, which primarily investigates biological conversion of CO_2 and H_2 to CH_4 in porous underground gas storage facilities (Bültemeier, 2023). Despite the absence of field tests to date, the project has produced a catalog of recommendations for conducting such tests, incorporating selection criteria for identifying suitable sites. Furthermore, some studies aim to assess microbial risks in UHS through laboratory experiments utilizing rock samples or formation waters sourced from actual depleted gas reservoirs in Italy and Germany (Dohrmann and Kruger, 2023; Bellini et al., 2024; Vasile et al., 2024a), as well as saline aquifers in France (Mura et al., 2024; Ranchou-Peyruse et al., 2024). Details on these studies are provided in Section 4.1.2.

5. Microbial interactions and their impacts on UHS

This section introduces and discusses the intricate microbial interactions and their positive and negative impacts on UHS in porous media from three perspectives: H_2 consumption, H_2 flow, and storage safety.

5.1. H_2 consumption

Various factors, such as the underground environment and substrate availability, can influence microbial activity in porous media. Consequently, H_2 consumption induced by native microbes in formation water collected on-site can vary markedly during laboratory experiments. These variations may present as

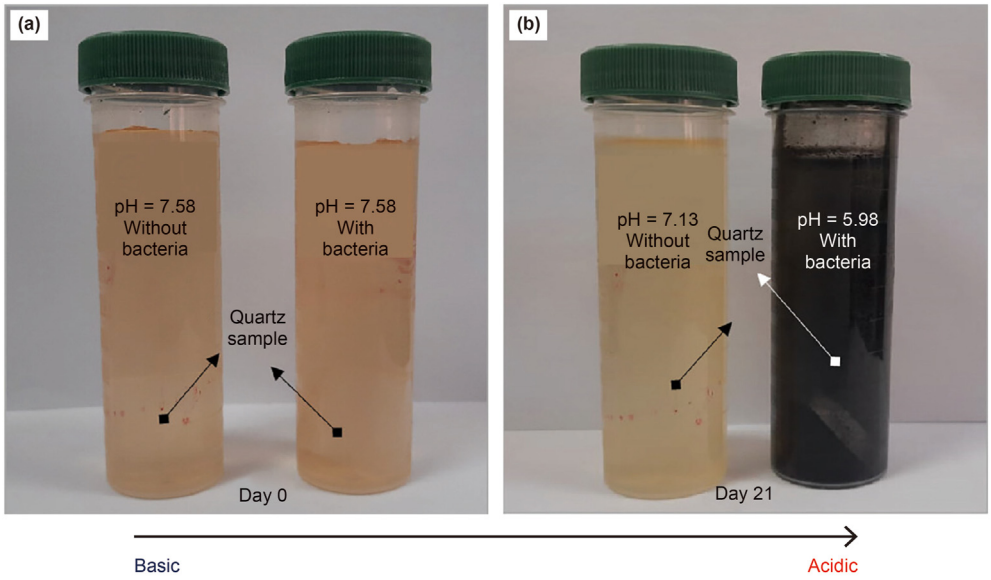

Fig. 12. pH decease induced by the metabolism of SRB (Adapted with permission from Aftab et al., 2023. Copyright, 2023; American Chemical Society). The solution turns dark due to the formation of water-insoluble precipitates, such as FeS.

insignificant H_2 consumption (Vasile et al., 2024a), immediate H_2 consumption without the addition of nutrients (Dohrmann and Kruger, 2023), or successful multi-cycle bio-methanation (Bauer, 2023; Vítězová et al., 2023). Understanding the intricate impact mechanisms of these factors is crucial for improving UHS performance. The details are elaborated below.

5.1.1. Underground environment

The complex GWRM interactions are affected by the initial underground environment, including factors such as pH, salinity, and temperature. These interactions also induce changes in the underground environment, which in turn impact microbial activity and H_2 consumption.

5.1.1.1. pH. The dynamic trend in pH evolution driven by microbial growth primarily depends on the type of microbes involved. Methanogens, for instance, typically consume substantial amounts of H^+ and HCO_3^- (Table 1), leading to an increase in pH. This trend has been widely observed in previous studies (Veshareh et al., 2022; Dopffel et al., 2023; Shojaee et al., 2024b). However, the impact of this pH increase on the final activity of methanogens varies: the pH may rise from near neutrality to strong alkalinity, thereby inhibiting their activity (Shojaee et al., 2024b), or it may transition from acidity to near neutrality, enhancing their activity (Elgendy et al., 2023). Similarly, acetogens also consume H^+ and HCO_3^-. However, a key difference lies in the significant production of acetate, which, upon accumulation, can lead to a decrease in pH, potentially triggering an "acid crash" effect (Ramió-Pujol et al., 2015). In the laboratory experiment of the USC-FlexStore project, conducted under a CO_2 partial pressure of 4 bar, acetate accumulation reached 4.9 g/L, resulting in a pH drop to 5.0 (Konegger et al., 2023). This self-limiting process is beneficial in reducing H_2 consumption in UHS, but may be detrimental to UBM. Nevertheless, numerical simulation results presented by Veshareh et al. (2022) depicted a divergent trend, indicating a significant increase in pH. This discrepancy may be attributed to limitations in the simulation method.

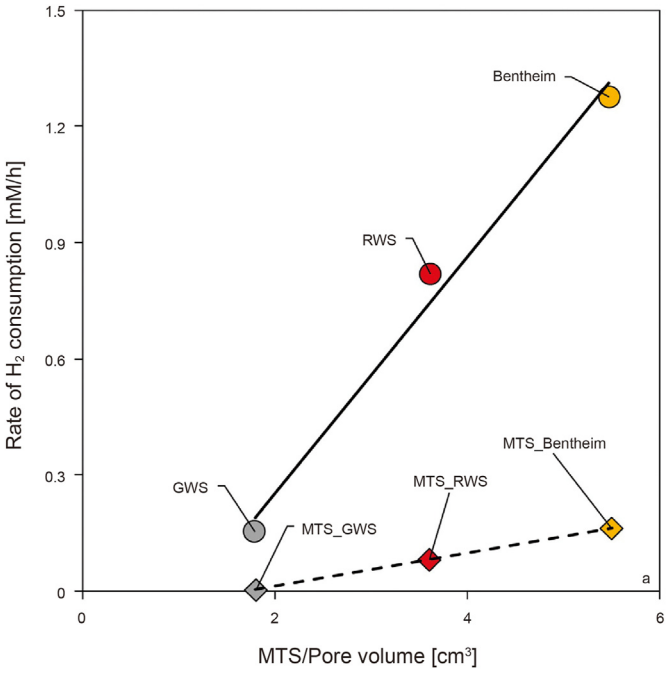

Fig. 14. Effect of pore/MTS volume on H_2 consumption: Comparison of rock samples (circles) saturated with MTS solution and bulk MTS (quadrilaterals) with amounts equivalent to corresponding pore volumes (Adapted with permission from Khajooie et al., 2024. Copyright, 2023; Hydrogen Energy Publications LLC).

The disparity in pH evolution trends is even more pronounced

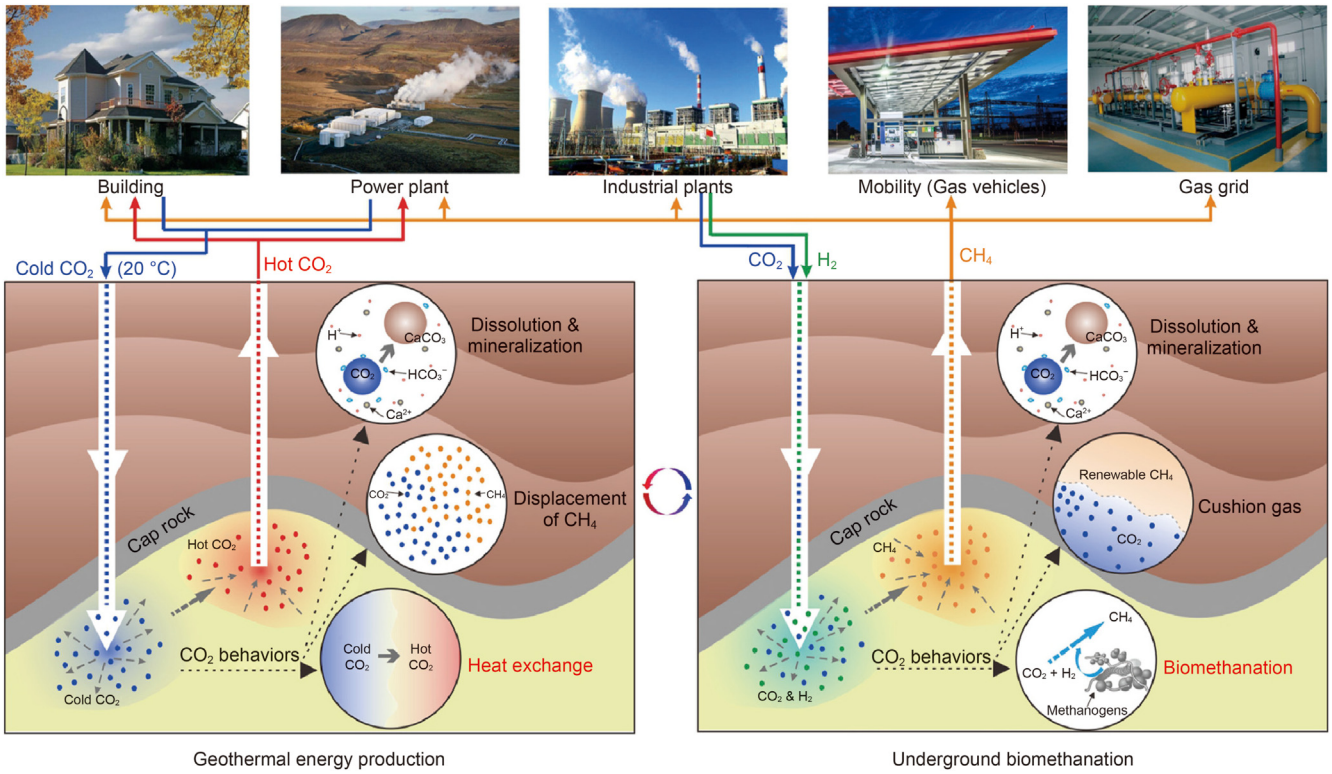

Fig. 13. Schematic of UBM coupled with geothermal energy production (Adapted with permission from Wu et al., 2023c. Copyright, 2023; Elsevier).

for SRB. In the experiments conducted by Aftab et al. (2023) and Boon et al. (2024), where only SRB were utilized, the pH change trends were entirely opposite: in one study, the pH decreased from near neutrality to 5.98 (Fig. 12), whereas in the other, it increased from near neutrality to slightly below 9.0. This variance may stem from the selection of different SRB strains, specifically, *Desulfovibrio marinisediminis* and *Oleidesulfovibrio alaskensis*, respectively. The former employs various organic compounds as carbon sources to produce acetate (Aftab et al., 2023), whereas the latter utilizes acetate as a carbon source (Boon et al., 2024).

Furthermore, microbial metabolism may involve the dynamic generation and consumption of formic acid and other volatile fatty acids. However, the concentrations of these substances are generally lower compared to acetic acid. For example, in the experiments conducted by Konegger et al. (2023), the concentrations of formic acid, butyric acid, and *i*-butyric acid were typically below 50, 500, and 300 mg/L, respectively, while the concentration of acetic acid was generally 5–10 times higher than that of butyric acid. In extreme cases, the concentrations of these substances can be so low that they cannot be detected (Konegger et al., 2023; Vasile et al., 2024a). Consequently, from the perspective of pH change alone, these substances have a less pronounced effect on microbial activity compared to acetic acid.

5.1.1.2. Salinity. Generally, low salinity is more conducive to microbial metabolism (Table 2). At higher salinity levels, microbes consume H_2 more slowly and in smaller amounts (Schwab et al., 2023; Wu et al., 2023a). This is primarily because high salinity exacerbates adverse effects on microbial proteins, enzymes, and cell membranes. Additionally, increased salinity reduces gas solubility in brine, which subsequently decreases the supply of substrate gases (Wu et al., 2023a). Consequently, reservoirs reporting microbial activity in UHS typically exhibit low salinity characteristics (Table 7). Although high salinity can inhibit microbial reproduction and even cause cell death, the presence of sufficient and appropriate nutrients can mitigate these adverse effects to some extent. Schwab et al. (2023) observed that the addition of acetate and methanol enhanced the sulfate reduction rate, achieving complete sulfate consumption after 1445 days, even at high salinity levels of 4.4 mol/L NaCl.

The salinity of brine in UHS undergoes complex changes due to the dynamic concentrations of various ions. Notably, HCO_3^- is consumed by methanogens and acetogens, while SO_4^{2-} is consumed by SRB, leading to a decrease in their concentrations. Changes in the concentrations of other ions are closely related to the precipitation and dissolution of minerals. Aftab et al. (2023) reported significant decreases in the concentrations of metal elements after culturing SRB with quartz bars. Specifically, iron concentrations decreased by about 80%, while calcium and magnesium concentrations each decreased by 40%–50%. This decrease can be attributed to the reaction of sulfide, a metabolite produced by sulfate reduction, with these metal ions (Aftab et al., 2023). The interaction results in the formation of water-insoluble precipitates such as FeS, CaS, and MgS (Fig. 12). Additionally, microbes convert part of the H_2 into water, thereby increasing water content (Hemme and van Berk, 2018; Wu et al., 2023a). Collectively, these processes may lead to a reduction in salinity, which in turn fosters microbial growth and H_2 consumption. Therefore, Wu et al. (2023a) observed a positive feedback mechanism in underground bio-methanation. Although it is certain that increased water content leads to a reduction in salinity, it remains unclear whether this effect is always dominant compared to the potential increase in salinity due to mineral dissolution. Further in-depth analysis and additional case studies are necessary.

5.1.1.3. Temperature. The impact of temperature on microbial activity and H_2 consumption in UHS can be elucidated as follows (Hemme and van Berk, 2018; Veshareh et al., 2022; Wu et al., 2023a; Minougou et al., 2024; Safari et al., 2024). First, temperature fluctuations exert influence on gas dissolution and diffusion. For instance, heightened temperatures tend to decrease the solubility of CO_2 and H_2 in brine, thereby impeding the supply of microbial substrate gases and diminishing H_2 consumption. On the contrary, an increase in temperature speeds up gas diffusion, while also reducing gas solubility and potentially alleviating pH decline. This dual impact could promote microbial growth and enhance H_2 consumption. Additionally, temperature variations impact particle collision, potentially influencing both equilibrium and kinetic reaction rates in geochemistry. Consequently, this modulation may affect H_2 consumption. Moreover, temperature escalation directly suppresses microbial activity by impeding enzyme function, thereby reducing H_2 consumption. This factor may be predominant.

The reservoir temperature undergoes dynamic changes during UHS operations. On one hand, injecting fluids like cold H_2 causes a drop in reservoir temperature, which may gradually recover due to heat conduction during shut-in stages. On the other hand,

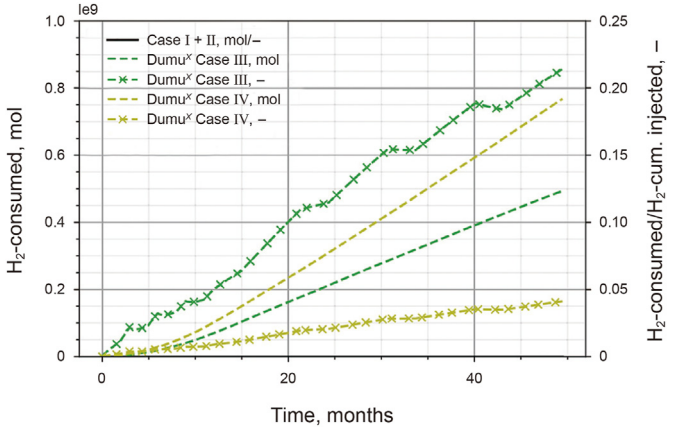

Fig. 15. Absolute and relative quantities of H_2 consumption by methanogens across different gas compositions (10% H_2 in Case III and 80% H_2 in Case IV) (Adapted under the terms of the license CC BY 4.0 from Hogeweg et al., 2022b).

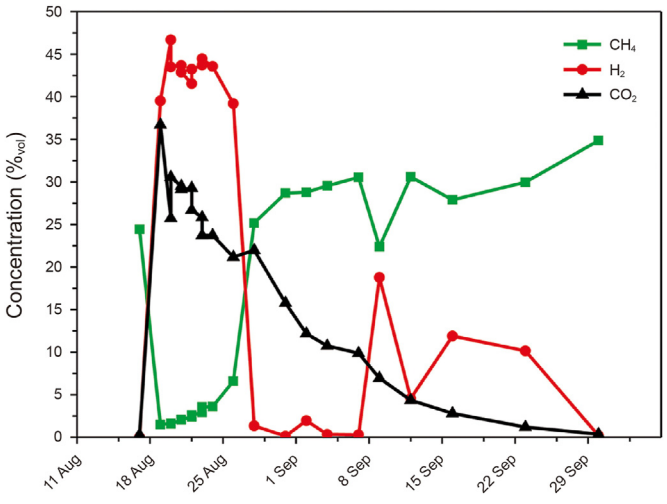

Fig. 16. Evolution of gas composition during the field test at Tvrdonice gas storage. The injected gas volume was 392 Sm^3, consisting of 50% H_2, 12.5% CO_2, and 37.5% N_2 (Reprinted under the terms of the license CC BY-NC-ND 4.0 from Vítězová et al., 2023).

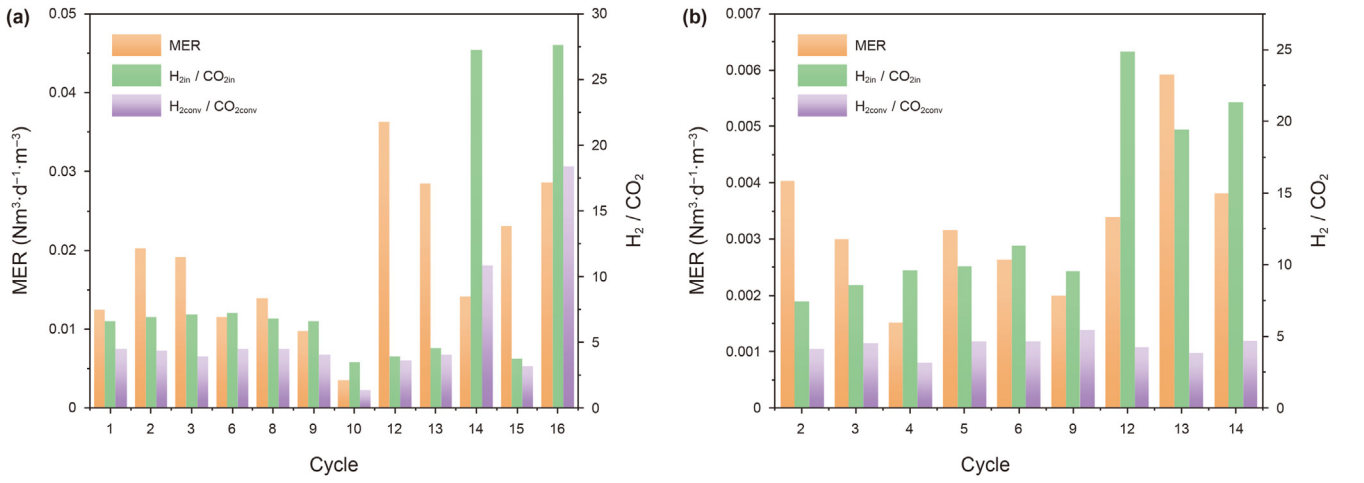

Fig. 17. Effect of injection ratios on conversion processes during the field tests of the USC-FlexStore project: (**a**) well LESP-001A and (**b**) well LEH-002 (Data from Konegger et al., 2023). *Notes*: MER-Methane evolution rate, H_{2in}/CO_{2in}-Ratio of injected H_2 to CO_2, H_{2conv}/CO_{2conv}-Ratio of converted H_2 to CO_2.

microbial processes like methanogenesis generate substantial heat while consuming considerable amounts of H_2, which can lead to an increase in temperature. This mechanism may explain the significant temperature rise observed at the Ketzin gas storage in Germany, where temperatures increased by 30–40 °C between 1964 and 1985 (Strobel et al., 2020). As the metabolism of methanogens increases reservoir temperature, which in turn limits their reproduction, Hou et al. (2023c) and Wu et al. (2023c) proposed an innovative technology to enhance H_2/CO_2 conversion efficiency and economic benefits in UBM. This technology, termed CCCUS, couples UBM with geothermal energy production (Fig. 13). Additionally, Dohrmann and Kruger (2023) conducted experimental analyses on the impact of heat shock on H_2 consumption. Their results indicate that as temperature increases, H_2 consumption decreases, and as temperature decreases, H_2 consumption recovers. These research findings lend support to the necessity and feasibility of the CCCUS technology to a certain extent.

5.1.1.4. Pore characteristics. The effects of pore size and heterogeneity on H_2 consumption are presented here, while the impacts of microbial growth on pores and subsequent H_2 flow will be addressed in Section 5.2.2. Khajooie et al. (2024) reported that microbial activities within intact rocks are 8–10 times higher than in corresponding bulk *M. thermolithotrophicus* solution (MTS) (Fig. 14), due to the presence of pores, which provide favorable conditions for microbial colonization. As the pore volume and surface area increase, the H_2 consumption rate also rises accordingly. However, the size of individual pore volumes significantly affects this relationship. As the surface area increases, the individual pore volumes can become very small, potentially approaching the nominal size of microbes (e.g., the nominal size of *M. thermolithotrophicus* is approximately 1.5 μm). This size limitation can inhibit microbial colonization and restrict microbial reproduction. Additionally, field tests conducted in the USC project indicate that certain areas within the "deep reservoir" exhibit low or no microbial activity due to heterogeneity, leading to low H_2 consumption. This conclusion is supported by the observation that the H_2 and CO_2 contents in the extracted gas show no significant change (Bauer, 2023). Currently, there is limited research on the effect of pore characteristics on H_2 consumption in UHS, necessitating further investigation in this area.

5.1.2. Substrate availability

5.1.2.1. H_2 availability. H_2 serves as an electron donor in microbial metabolism, making its availability crucial. According to Nikolaev et al. (2021) and Hogeweg et al. (2022b), higher concentrations of injected H_2 lead to greater absolute amounts of converted H_2 by methanogens (Fig. 15), although the relationship is not linear. Additionally, the concentrations of CH_4 and H_2 in the produced gas also increase accordingly. However, the relative amount of converted H_2 exhibits an opposite trend, with higher conversion ratios at lower H_2 concentrations. Similarly, Dopffel et al. (2023) reported comparable results, suggesting that the experimental observations might primarily arise from physiological constraints; specifically, high H_2 concentrations may negatively impact H_2 uptake or the function of hydrogenases within the cells. Dohrmann and Kruger (2023) and Vítězová et al. (2023) observed that reactions proceeded more rapidly in smaller reactors. This can be attributed to the increased interference between liquid and gas in smaller scales, leading to a swifter transfer rate of gas to liquid and enhanced accessibility of H_2 to microbes, thus resulting in accelerated reaction rates. Additionally, Liu et al. (2023b) observed that as microbes consumed H_2, the continuity of the gas phase was disrupted, generating isolated bubbles. This, in turn, increased the contact area between H_2 and microbial cells, consequently accelerating the H_2 consumption rate. This observation further underscores the significance of H_2 availability in microbial processes.

5.1.2.2. CO_2 availability. In the processes of methanogenesis and acetogenesis, CO_2 serves as an essential electron acceptor, thereby influencing the consumption of H_2. When the partial pressure of CO_2 is low and the stoichiometric ratio of methanogenesis (4:1) is used for the ratio of H_2 to CO_2, H_2 can be completely consumed and converted into carbon-neutral CH_4 within a few days to several months (Bauer, 2023; Konegger et al., 2023; Vítězová et al., 2023; Wu et al., 2023a). For instance, during the field test at Tvrdonice gas storage, H_2 and CO_2 were completely consumed within approximately forty days in the complex underground environment (Fig. 16). As the partial pressure of CO_2 increases, its solubility also rises, potentially resulting in an almost linear increase in the reaction rate and a corresponding decrease in the time required for complete conversion (Bauer, 2023). However, upon surpassing a certain pressure threshold, the significant decrease in pH may inhibit methanogen activity, thereby potentially reducing reaction rates and H_2 consumption by methanogens, as discussed in Section 5.1.1.1.

In this scenario, given that acetogens thrive better at low pH levels compared to methanogens, CO_2 and H_2 may initially be

converted by acetogens into acetate (Section 5.1.1.1). Subsequently, the accumulated acetate can generate CO_2 and H_2 through metabolic pathways such as syntrophic acetate oxidation, also known as reverse acetogenesis (Bauer, 2023; Konegger et al., 2023). Then, combined with a gas mixture containing less CO_2 and more H_2, CH_4 can also be produced. This is why, during the field test of the USC-FlexStore project, at ultra-high injection ratios ranging from 20 to 28, the methane evolution rates experienced a considerable increase (Fig. 17). Therefore, the accumulation of acetate due to excessively high CO_2 partial pressure does not necessarily signify a complete loss of energy. The synthesis of the intermediate acetate is inevitable and even can be considered a part of the proper implementation of UBM on site (Bauer, 2023; Konegger et al., 2023). However, the pathway involving acetate synthesis first and then CH_4 production will diminish the rate of CH_4 synthesis and prolong the conversion time. Thus, efforts should be made to minimize this pathway during UBM.

Hemme and van Berk (2018) highlighted that a shorter storage period is advantageous for reducing H_2 consumption in each cycle. Nonetheless, since each injection can introduce CO_2, the total H_2 consumption will be higher. Additionally, while reducing the CO_2 content in the injected gas can beneficial for mitigating H_2 consumption by methanogens, it does not completely inhibit H_2 conversion, as carbonate minerals can still supply CO_2 (Hemme and van Berk, 2018; Haddad et al., 2022). However, the slow dissolution process of carbonate minerals results in a correspondingly sluggish H_2 conversion process. Conversely, Shojaee et al. (2024b) presented contrasting and surprising findings. Despite the absence of CO_2 in the injected gas, the rock composition being entirely dolomite still led to the complete consumption of all injected H_2 at a partial pressure of 203 bar by methanogens within 40 months. This notable discrepancy may be attributed to inconsistencies in the kinetic parameters selected during the simulation process.

Cushion gas and residual gas may also serve as sources of CO_2 and influence H_2 consumption. Maniglio et al. (2023) observed that using CO_2 as the cushion gas leads to a notable rise in the H_2 conversion rate compared to injecting gas containing CO_2 (maximum 5%). Additionally, as the injection rate increases, viscous instability may occur, enabling more H_2 to infiltrate the lower cushion gas layer of CO_2 during injection (Wang et al., 2024a). This phenomenon expands the mixing area of H_2 and CO_2, intensifying methanogenesis and consequently augmenting H_2 consumption. Minougou (2022) also reported that the lowest H_2 recovery ratio occurred when CO_2 was employed as the cushion gas primarily due to methanogenesis. In contrast, the impact of CO_2 in the residual gas is relatively minor. Ali et al. (2022) reported that when the residual gas contains 4% CO_2, the methanation reaction consumes only 0.3% H_2. Even when considering gas diffusion, the H_2 consumption remains just 2.5%, despite the presence of a larger mixing zone of H_2 and CO_2.

Furthermore, CO_2 may also be introduced during early

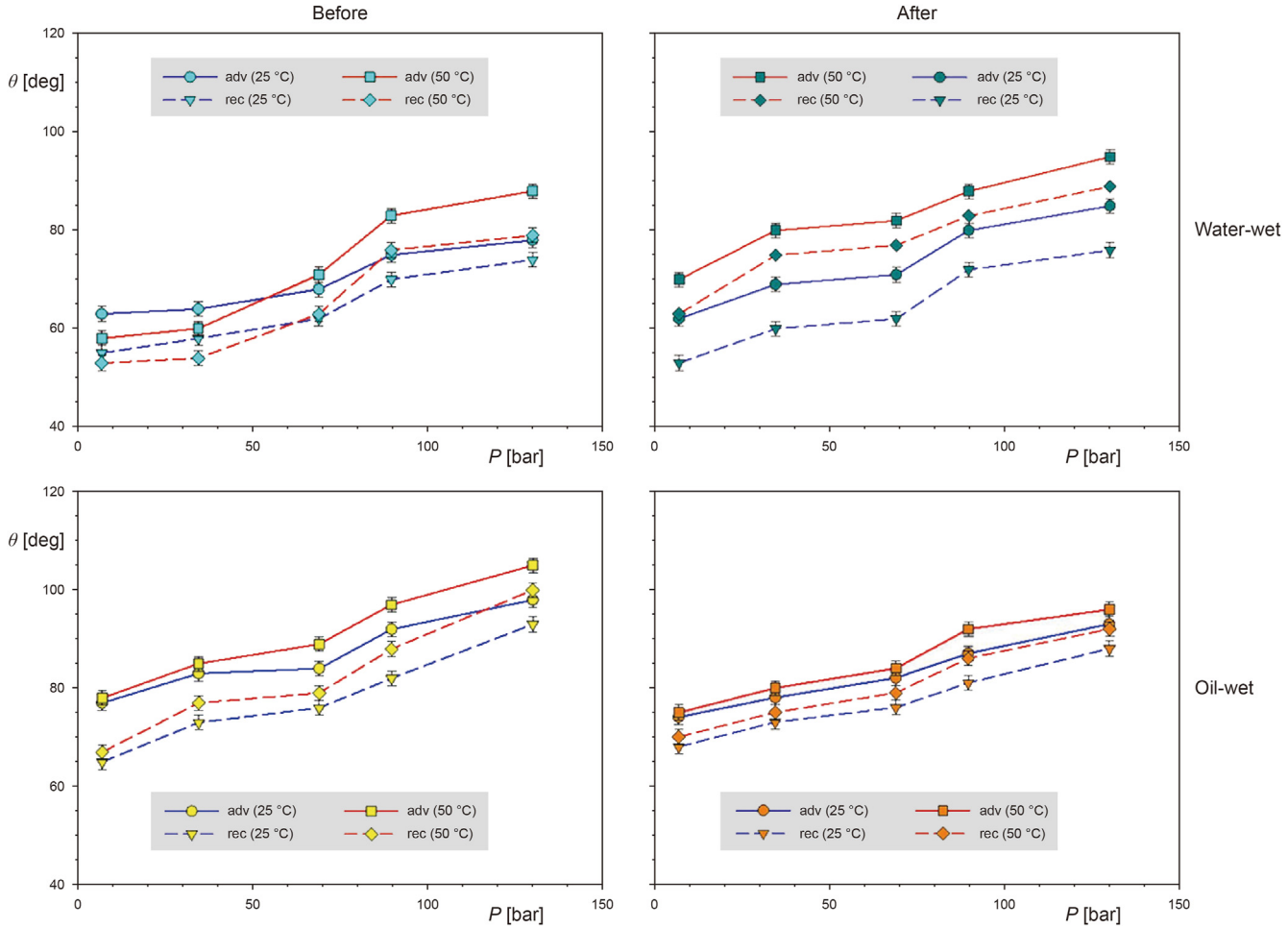

Fig. 18. Changes in advancing and receding contact angles on water-wet and oil-wet quartz surfaces before and after microbial incubation at 25 °C and 50 °C (Adapted with permission from Ali et al., 2023. Copyright, 2023; Elsevier).

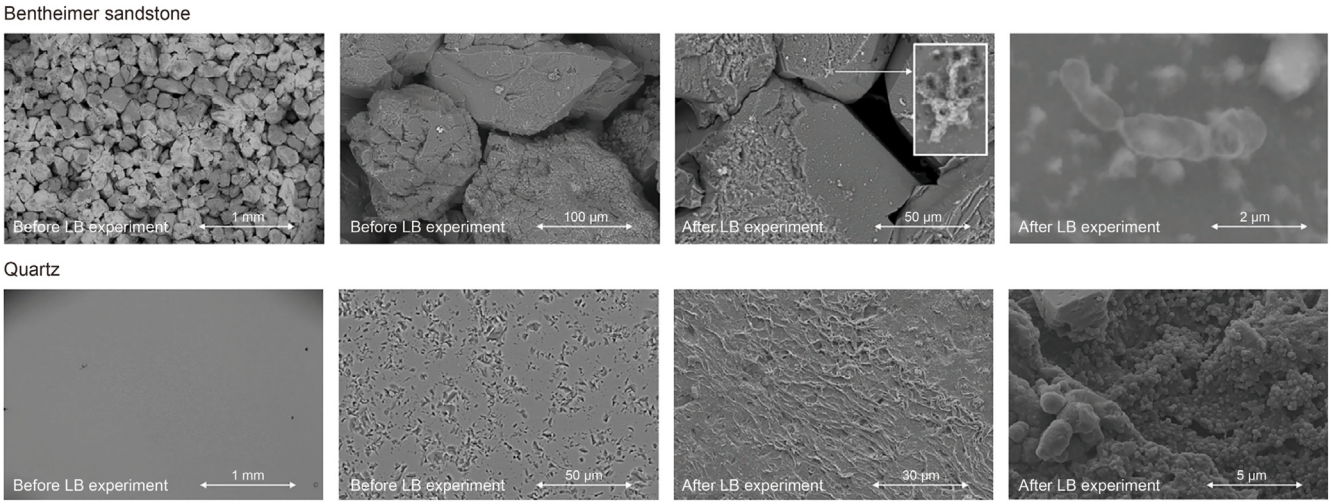

Fig. 19. SEM images of rough sandstone and smooth quartz samples before and after experiment (Adapted under the terms of the license CC BY 4.0 from Boon et al., 2024).

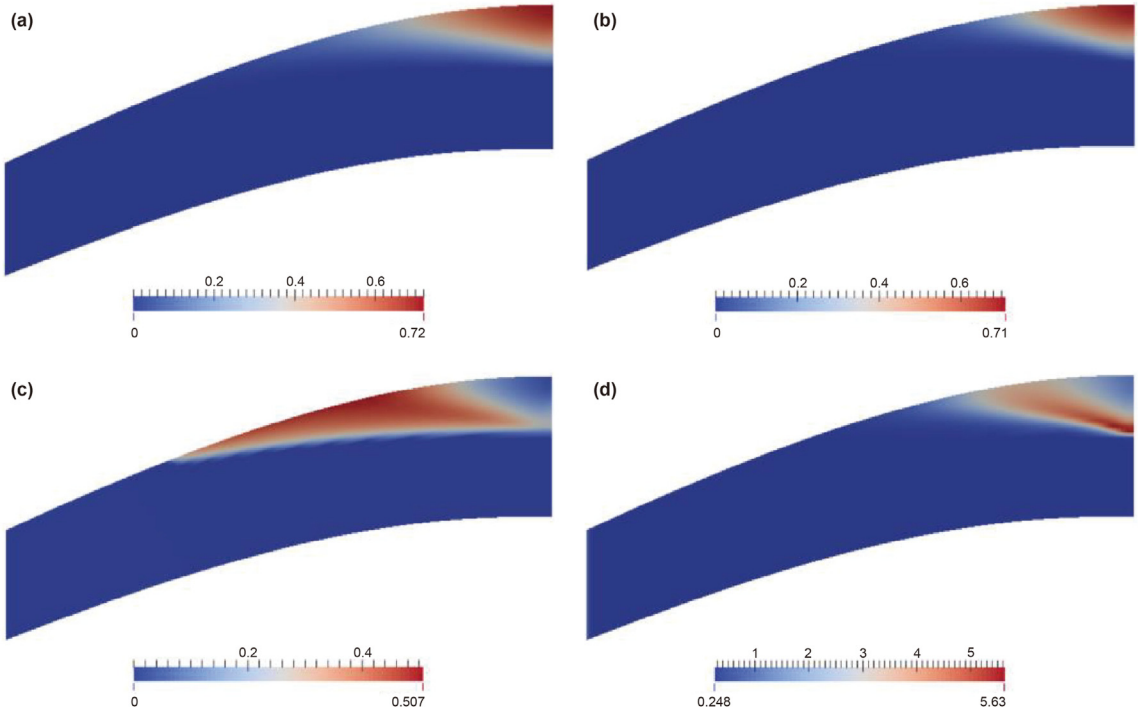

Fig. 20. (**a**) H_2 concentration without methanogenesis; (**b**) H_2 concentration with methanogenesis; (**c**) CH_4 concentration with methanogenesis; (**d**) Dimensionless microbial concentration (Adapted under the terms of the license CC BY 4.0 from Hagemann et al., 2016).

engineering operations, leading to additional H_2 consumption. For example, in the USS project experiment, CO_2 originated from potassium carbonate in the drilling mud, resulting in nearly complete H_2 consumption despite the initial gas composition being 10% H_2 + 0.3% CO_2 (Bauer, 2017). However, this effect is relatively minor at the reservoir scale because the filtration of drilling mud is primarily concentrated near the wellbore.

5.1.2.3. Sulfate availability. Sulfate serves as an electron acceptor in the metabolism of SRB, and its availability directly influences the activity of these microbes and H_2 consumption. Shojaee et al. (2024b) reported that with an initial sulfate concentration of approximately 3000 ppm in formation water, the H_2S concentration could reach 400–550 ppm in reservoirs composed of pure quartz or dolomite. This finding highlights that even minimal amounts of sulfate can result in dangerously high levels of H_2S in the gas phase. Similarly, the significant impact of sulfate reduction was demonstrated in a study by Rosman et al. (2023), which showed that 3.4 Bscf of H_2S was produced after injecting a total of 81 Bscf of H_2. Hemme and van Berk (2018) noted that once the original sulfate in the formation water is depleted, replenishment occurs very slowly through diffusion from the cap and underlying rock layers, as well as from the dissolution of minerals like anhydrite gypsum or barite (Haddad et al., 2022). Additionally, barite present in drilling mud can also contribute to sulfate replenishment, similar to how drilling mud replenishes CO_2 (Bauer, 2017). However, this effect is limited.

During the on-site UHS process, only minimal H_2S was observed

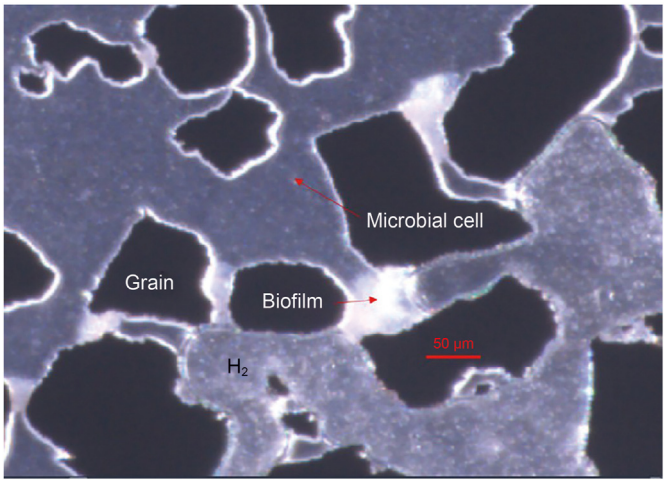

Fig. 21. Microscopic observation of microbial cells, biofilms, and H_2 gas within pores (Adapted under the terms of the license CC BY 4.0 from Liu et al., 2023b).

in the gas phase, and in some cases, no H_2S was detected at all (Table 7). This phenomenon could potentially be linked to the low sulfate concentration in the on-site formation water. Additionally, H_2S produced in the gas phase might serve to offset pH changes of formation water (Dopffel et al., 2023). For instance, Shojaee et al. (2024b) reported that in a pure calcite system, the dissolution of calcite induced by microbial metabolism caused a rapid increase in pH levels to approximately 10. This prompted the H_2S in the gas phase to dissolve back into the formation water, thereby neutralizing the rise in pH. It is plausible that this dissolved H_2S could undergo further conversion into precipitates, as detailed in Section 5.1.1.2. Consequently, the presence and behavior of H_2S in the gas phase exhibit considerable complexity.

5.2. H_2 flow

The flowability of H_2 is crucial for recovery efficiency in UHS (Wang et al., 2024b). The GWRM interactions can lead to alterations in wettability, microbial aggregation, changes in mineral composition, and water generation, among others. Each of these factors can potentially affect the flow of H_2. The key mechanisms in these areas are outlined as follows.

5.2.1. Wettability alteration

Liu et al. (2023b) observed that the wettability of a silica surface shifted from initially being water-wet, with a contact angle of 41°, to neutral-wet, exhibiting an average contact angle of 96°, within a 20-h period under the influence of SRB metabolism. In contrast, Boon et al. (2024) reported an opposite trend, where interaction with SRB led to a significant reduction in the apparent contact angle. These divergent trends in wettability alteration may stem from the utilization of different SRB strains in the experiments, which produce varying types of extracellular polymeric substances (EPS), such as polysaccharides, proteins, nucleic acids, and lipids, within the biofilms (Flemming and Wingender, 2010). Thus, the consistency of the EPS appears to be a crucial factor influencing wettability, as emphasized by Boon et al. (2024). Furthermore, microbial metabolism can alter the composition of solutions, which may be another reason for shifts in wettability. For instance, Aftab et al. (2023) noted that the activity of SRB generated considerable amounts of acidic substances with functional groups like hydroxyl, amine, and carboxyl, which enhance hydrophobicity by serving as binding sites for divalent cations. Conversely, Al-Yaseri et al. (2024) found a substantial reduction in available carboxylic acid groups due to SRB activity, further affecting shifts of wettability.

The initial wettability and the surface roughness of the rock significantly influence changes in wettability. Ali et al. (2023) observed that a clean quartz surface, which is inherently strongly water-wet, became more hydrophobic following microbial interaction, whereas a quartz surface treated with a layer of stearic acid (strongly oil-wet) became more hydrophilic post microbial exposure (Fig. 18). This phenomenon can be attributed to the silanol groups (−Si−OH) on water-wet quartz, which form hydrogen bonds with water molecules, endowing clean quartz with strong hydrophilic properties. When these surfaces are enveloped by EPS that combines both hydrophobic and hydrophilic groups, fewer hydrophilic groups remain exposed, thus diminishing the surface's hydrophilicity. The mechanism that increases the hydrophilicity of oil-wet surfaces operates in the opposite manner. Concerning surface roughness, smooth rock surfaces are more susceptible to shifts in wettability, whereas the wettability of rough rock surfaces generally remains unchanged (Boon et al., 2024). This resistance to change on rough surfaces can be explained by the tendency of biofilms to develop within the valleys of the rock surface, leaving the protruding surfaces (Fig. 19), which primarily contact the H_2 gas bubble, unaffected, and thus the contact angle remains stable.

5.2.2. Microbial aggregation

Hagemann et al. (2016) observed that microbial growth peaked at the interface where injected H_2 gas displaced the original gas, resulting in maximal concentrations of methanogens. Consequently, the H_2 concentration at the front tends to form a narrower distribution (Fig. 20). Conversely, Hogeweg et al. (2022b) reported the highest concentrations of methanogens nearer to the well, a finding that aligns with the early-stage microbial distributions reported by Minougou (2022). According to Minougou, one year post gas injection, microbial proliferation caused a notable reduction in porosity near the well, from initial 20% to approximately 18.75%. This reduction occurred because the substrate-rich environment near the well attracted microbes. Over time, the area with the highest microbial concentration progressively shifted outward by tens of meters. This shift was driven by high pressures that dispersed the microbes situated near the well. These differences in outcomes could significantly be related to methodological differences in the selection of temporal scope and physical models in numerical simulations (e.g., 2D vs. 3D, horizontal vs. vertical reservoir profiles).

Eddaoui et al. (2021) noted that while microbial growth inevitably causes pore clogging, leading to reduced porosity and permeability, these effects are not entirely negative. The accumulation of methanogens redirects H_2 flow away from undesirable vertical ascension, prompting it instead to move horizontally deeper into the formation, thereby forming nearly ideal gas bubbles. Capillary actions enhance this process, helping the bubbles become more uniformly distributed in all directions, albeit smaller and more compressed. However, Liu et al. (2023b) pointed out that bubble formation disrupts the continuity of the gas phase and increases the resistance to gas flow, this is disadvantageous for gas extraction. Additionally, although microbial growth can lead to biofilm formation (Fig. 21), affecting H_2 flow, this phenomenon is subject to change (Liu et al., 2023b). The shear stress caused by the flow of injected gas may dislodge some biofilms from the pore network, and subsequent microbial growth does not result in new biofilm formation. This change likely results from microbes transitioning from a biofilm state to a planktonic mode in H_2-rich environments, potentially reducing the negative impacts associated with pore clogging.

5.2.3. Mineral change

The GWRM interactions in UHS can lead to the precipitation and dissolution of minerals, potentially impacting rock porosity, permeability, and gas flow capacity. However, the precipitation or dissolution of minerals are not constant processes; instead, they are dynamically transformative, continuously shifting in response to environmental conditions. For instance, the acidic gas injection may reduce the pH, causing calcite dissolution. Subsequently, a pH elevation triggered by microbial extensive consumption of H^+ could facilitate the precipitation of calcite (Wu et al., 2023a). When all dissolved inorganic carbon in the formation water is depleted, calcite starts dissolving again to replenish the carbon sources, as observed by Haddad et al. (2022). Additionally, they also noted the dissolution of barite in their experiments, which serves to enhance the sulfate content in the formation water, benefiting the growth of SRB. However, the dissolution of neither calcite nor barite resulted in an increase in the porosity of the solid matrix; rather, there was a decrease in porosity, primarily due to the deposition of clay and the precipitation of iron sulfide, both of which were triggered by microbial metabolism. Similar phenomena have been reported in other experimental studies utilizing rock samples and formation waters from aquifers in France (Mura et al., 2024).

Hemme and van Berk (2018) reported that anhydrous gypsum could also be used to supplement sulfate. However, as this gypsum dissolves, excessive calcium ions might be released into the brine, potentially leading to the precipitation of calcite. The eventual precipitation or dissolution of calcite largely depends on the activity of methanogens. In their study, interactions resulted in the dissolution of minerals such as calcite, illite, and quartz, while minerals like K-feldspar, kaolinite, and dolomite precipitated. These interactions led to a decrease in the porosity of reservoir rocks from an initial 10% to between 9.79% and 9.95% over 30 years. In contrast, a study by Veshareh et al. (2022) demonstrated that interactions resulting in brucite and portlandite precipitation significantly reduced porosity, with a decrease of as much as 2.5% within just ten years, even while noticeable calcite dissolution occurred. These results were obtained at relatively low CO_2 concentrations. During UBM, both H_2 and CO_2 are relatively abundant, and microbial activity, particularly among methanogens, is heightened. This increased activity may lead to more pronounced changes in porosity and impacts on gas flow. However, there are no relevant reports on this phenomenon thus far.

It is evident that the precipitation and dissolution processes of various minerals, driven by GWRM interactions, are highly complex. Consequently, the changes in porosity and their impacts on gas flow cannot be simplistically assessed. Instead, a comprehensive analysis needs to be conducted in conjunction with the specific conditions of the actual reservoir.

5.2.4. Water generation

Water, produced as a byproduct of microbial metabolism (Table 1), has been reported in several studies to exhibit increased levels. Hemme and van Berk (2018) noted a slight increase in water content, from initial 1 to 1.007 kg over 30 years in a batch-type H_2 storage system containing 96% H_2 and 4% CO_2. In contrast, Wu et al. (2023a) reported a more significant rise to 1.05 kg within approximately one year in UBM processes, with the injected gas composition being 80% H_2 and 20% CO_2. These increases in water content invariably enhance the saturation of the water phase. However, the impact on gas flow and extraction largely depends on the specific conditions of each storage system. Nikolaev et al. (2021) observed that almost all the injected gas was converted into CH_4, and a considerable amount of water was produced near the injection well. However, the flowing water did not reach the vicinity of the production well. Additionally, due to the high mobility ratio between the gas and water phases, the gas phase's ability to displace water is markedly low, thus preventing water blocking. In a further study by Safari et al. (2024), it was noted that the advancing water front, with a saturation of 0.7, led to a water breakthrough after nearly 10 years of operation. Similarly, Wang et al. (2024a) also observed water breakthrough, noting that high flow rates exacerbate this phenomenon.

In brief, outside of UBM processes, the amount of water generated may be minimal, and its negative impact on gas flow could be insignificant. Even with substantial water generation, the adverse effects could be mitigated by strategies such as optimizing well spacing early on and controlling the production rate (Nikolaev et al., 2021; Wang et al., 2024a).

5.3. Storage safety

Microbial interactions can directly or indirectly impact well integrity, caprock integrity, and fault sealing, thereby influencing the safety of H_2 storage. Given the limited amount of research in this area, potential risks are briefly reviewed by drawing insights from the fields of oil and gas development, as well as underground storage of CO_2 and natural gas.

5.3.1. Well integrity

As previously noted, microbial activity can lead to substantial consumption of specific ions (e.g., H^+ and HCO_3^-) in formation water, which is accompanied by significant pH fluctuations. These dynamic changes may cause extensive dissolution of sensitive minerals, such as calcite, barite, kaolinite, and illite, in the near wellbore area. This can compromise the stability and integrity of the formation close to the wellbore and potentially lead to wellbore failure (Zeng et al., 2023).

Microbial metabolism can also alter the interfacial conditions of metal surfaces, thereby inducing electrochemical processes such as corrosion, which compromise the integrity of underground metal equipment. SRB are considered particularly damaging. They induce damage both chemically, through the production of H_2S, and electrochemically, by the withdrawal (Ugarte and Salehi, 2022). For instance, H_2S can react with carbon steel to produce Fe_xS_y, which

Table 8
Properties of various shale core samples before and after cultivation experiments (Data from Kolawole et al., 2021b).

Properties	Eagle Ford shales		Marcellus shales		Niobrara shales	
	Before	After	Before	After	Before	After
Mean UCS, MPa[a]	110	114	86	98	69	95
Mean UCS, MPa[b]	88	138	120	155	66	110
Mean Poisson's ratio[a]	0.2610	0.2131	0.1822	0.1511	0.3204	0.2449
Mean Poisson's ratio[b]	0.2448	0.2348	0.1900	0.1477	0.2567	0.2217
Mean FT, MPa·m$^{0.5}$ [c]	4.06	5.20	4.88	5.93	3.14	4.86
Permeability, μD	1.76000	0.00451	0.06930	0.01380	1.47000	0.02240
Porosity, %	9.46	6.48	6.22	4.41	5.41	2.50

Notes: FT-Fracture toughness; UCS-Unconfined compressive strength. [a] Scratch test result; [b] Uniaxial compression test result; [c] Scratch-derived result.

Table 9
Summary of microbial positive (P) and negative (N) impacts on UHS in porous media.

Microbially-induced phenomena	UBM	Other UHS scenarios
H_2 consumption	P: Desired phenomena	N: Energy loss
CH_4 generation	P: Desired phenomena	N: Energy loss
H_2S generation	N: Toxic and corrosive gas	N: Toxic and corrosive gas
Acetate generation	N: Extension of conversion time and energy loss	N: Energy loss
Water generation	P: Promotion of methanogen growth N: Hindrance of gas withdrawal	N: Hindrance of gas withdrawal
pH change	P: Enhanced methanogen activity improves UBM efficiency. N: Self-limiting processes reduce UBM efficiency.	P: Self-limiting processes enhance UHS performance. N: Increased microbial activity leads to greater energy loss.
Temperature change	P: Enhanced methanogen activity improves UBM efficiency. N: Self-limiting processes reduce UBM efficiency.	P: Self-limiting processes enhance UHS performance. N: Increased microbial activity leads to greater energy loss.
Microbial aggregation	P: More uniform gas distribution N: Pore clogging	P: More uniform gas distribution N: Pore clogging
Wettability alteration	P & N: The impact on gas flow, caprock integrity, and fault sealing depends on the specific alterations.	P & N: The impact on gas flow, caprock integrity, and fault sealing depends on the specific alterations.
Mineral precipitation and dissolution	P & N: The impact on UBM efficiency, gas flow, well integrity, caprock integrity, and fault sealing depends on the specific alterations.	P & N: The impact on H_2 loss, gas flow, well integrity, caprock integrity, and fault sealing depends on the specific alterations.
Metal corrosion	N: Well integrity failure	N: Well integrity failure

Notes: Other UHS scenarios include the underground storage of pure H_2, underground storage of H_2-natural gas mixtures, and underground storage of H_2-rich town gas or syngas.

when exposed to oxygen, undergoes oxidation to create elemental sulfur (S_0), a substance that significantly accelerates corrosion (Fernandez et al., 2024). Moreover, modern theories also suggest that the growth of SRB results in the formation of biofilms on the metal surface, promoting the development of an anaerobic environment conducive to the proliferation of other microbes. The collective metabolism of these microbes synergistically accelerates the corrosion rate and induces hydrogen embrittlement in steel (Fernandez et al., 2024).

Additionally, microbial metabolism can adversely affect the integrity of the cement sheath. A common metabolite, H_2S, can cause corrosion of the cement sheath through processes such as decalcification. Furthermore, if the injected gas contains CO_2, it can cause carbonation of the cement sheath. However, as methanogens consume CO_2, the extent of carbonation penetration into the cement surface may be somewhat reduced (Rooney and Li, 2023; Rooney et al., 2024).

5.3.2. Caprock integrity

Microbial metabolism can lead to changes in caprock properties, impacting its integrity in both beneficial and adverse ways. In a study by Kolawole et al. (2021b), shale core samples cultivated with *Sporosarcina pasteurii* solution exhibited favorable changes (Table 8), such as increased localized and bulk mechanical integrity, decreased permeability and porosity, and the occlusion of microfractures. However, the opposite situation may also occur (Kolawole et al., 2021a; Ngoma and Kolawole, 2024), potentially leading to sealing failures and subsequent leakage (Ugarte and

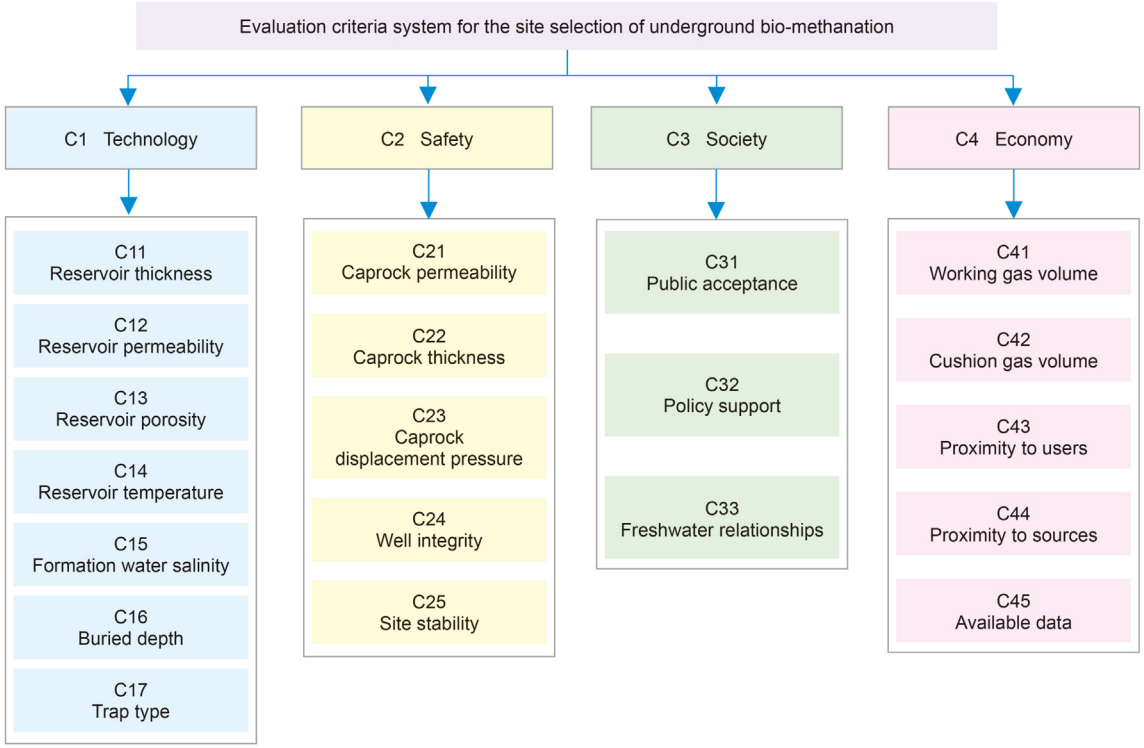

Fig. 22. Preliminary evaluation criteria system for the site selection of UBM (Adapted with permission from Wu et al., 2024. Copyright, 2024; Elsevier).

Salehi, 2022; Zeng et al., 2023). Additionally, for H_2 to penetrate the caprock, it must overcome capillary pressure. A reduction in capillary pressure induced by microbial activity may increase the risk of H_2 leakage. It is crucial to recognize that interfacial tension and the wetting contact angle are key determinants of capillary pressure. Since microbial metabolism might decrease the wetting contact angle, thereby potentially increasing capillary pressure as discussed in Section 5.2.1, the capillary pressure change caused by microbial activities can also be beneficial. This is contingent on various factors, such as the type of active microbes and the mineral composition of the caprock.

5.3.3. Fault sealing

Microbial interactions impact fault sealing in ways similar to their effects on caprock integrity, such as through changes in mechanical and interfacial properties (Zeng et al., 2023). However, faults lack cohesion and therefore possess lower mechanical strength compared to caprock. During H_2 injection and withdrawal cycles, the altered stresses increase the likelihood of shear stress on faults exceeding their shear strength, thereby promoting shear slip along the main faults and the formation of microfractures (Zoback et al., 2012). Correspondingly, using bio-cementation methods to enhance the mechanical properties and stability of faults also presents a greater challenge (Ngoma and Kolawole, 2024). Moreover, microbial metabolism produces water, which can act as a lubricant, thereby reducing friction and shear strength (Yao et al., 2020). This reduction is detrimental to fault sealing. Furthermore, microbial interactions can alter the in-situ geochemical environment as discussed in Section 5.1.1, affecting rock surface potential and energy, potentially resulting in subcritical crack growth around faults (Zeng et al., 2023). Compared to transient fault slip, subcritical crack growth takes considerably longer to manifest, as surface energy changes are governed by kinetics.

5.4. Summary of microbial impacts

As previously discussed, microbial interactions can lead to a series of phenomena, including H_2 consumption, byproduct generation, changes in the underground environment, and mineral precipitation and dissolution, among others. These phenomena can significantly influence the efficiency and safety of UHS, with both positive and negative impacts summarized in Table 9. Notably, the generation of H_2S, acetate production, and metal corrosion consistently have adverse effects. In contrast, other phenomena can have either beneficial or detrimental impacts, contingent upon the specific UHS scenarios and the particular alterations occurring within the system.

6. Implementation recommendations for UHS

Selecting suitable UHS sites, adopting effective operational modes, and conducting rigorous on-site monitoring are crucial for maximizing the positive impacts while minimizing negative ones. The following recommendations are provided.

6.1. Site selection

To minimize H_2 loss due to microbial activity and mitigate related risks, it is advisable to select reservoirs with a minimal potential for microbial presence. If significant populations of H_2-consuming microbes are encountered, employing biocides may be an effective management strategy (Raczkowski et al., 2004; Bhadariya et al., 2024). It is also essential that the formation water has low levels of sulfate or dissolved carbon to reduce the supply of substrates. Additionally, the mineralogy of the reservoir rocks should primarily consist of minerals with low sulfate and bicarbonate content. Ideally, the reservoir rock should predominantly be clean sandstone (Shojaee et al., 2024a). For the use of depleted gas reservoirs in H_2 storage, choosing fields with low concentrations of residual CO_2 is recommended (Hemme and van Berk, 2018).

In the context of UBM, preferred conditions can differ notably, such as the desirability of higher concentrations of methanogens and dissolved carbon. Additionally, the temperature of the reservoir and the salinity levels of the formation water are critical factors to consider (Thaysen et al., 2023; Wu et al., 2024). High temperatures and salinity levels are generally detrimental to methanogen proliferation. Coupling geothermal energy production could be beneficial to moderate these conditions, thereby enhancing methanogen activity (Hogeweg et al., 2022a; Wu et al., 2023c). Furthermore, reservoirs with greater rock porosity and higher surface areas are favorable for methanogen colonization. However, it is crucial to ensure that the individual pore volumes are larger than the nominal size of the methanogens to facilitate effective colonization (Khajooie et al., 2024). Based on these considerations, a preliminary evaluation criteria system for the site selection of UBM was proposed (Wu et al., 2024). This system encompasses not only technical criteria but also integrates safety and socio-economic criteria, as detailed in Fig. 22.

6.2. Engineering operation

To enhance the recovery of the target gas, it is crucial to optimize both the flow rate and the composition of the injected gas. This approach is considered the preferred method, as highlighted by Nikolaev et al. (2021). Furthermore, selecting an appropriate cushion gas plays a critical role. CO_2 should be avoided as a cushion gas, with CH_4 or N_2 often being more suitable choices (Minougou, 2022; Muhammed et al., 2024). If significant generation of H_2S in the gas phase is inevitable, strategies such as perforating the upper part of the reservoir might be useful to mitigate its extraction (Rosman et al., 2023). Additionally, microbial activities can alter wettability, thereby impeding gas flow. To counter this adverse effect, the injection of surfactants could be considered.

In the context of UBM, it is crucial to ensure that H_2 is directed toward methanogenesis rather than competing microbial pathways, which could lead to the production of acetate and its relatively slow subsequent utilization. Instead of injecting a large volume of substrate gas in a single batch (batch operation), it is more effective to limit the injection volume of substrate gas to small quantities and inject these repeatedly at predetermined intervals (fed-batch operation), or dilute the substrate gas with a carrier gas such as natural gas and N_2 (Konegger et al., 2023). Nikolaev et al. (2021) recommended a gas composition of 40% H_2, 10% CO_2, and 50% N_2, advising pre-injection of CO_2 to mitigate early H_2 breakthrough. In scenarios where the reservoir lacks indigenous highly active methanogens, it may also be feasible to inject ground-cultured high-activity methanogens along with the necessary nutrients. This strategy is akin to methods employed in microbial enhanced coalbed methane production and microbial enhanced oil recovery (Ritter et al., 2015; Niu et al., 2020).

6.3. On-site monitoring

On-site monitoring plays a pivotal role in mitigating the adverse impacts of microbial metabolism or enhancing the conversion efficiency of H_2 and CO_2 into CH_4. For monitoring methanogenesis, indicators such as the fractions of H_2 and CO_2, along with pressure, are less reliable because their changes might be obscured by acetogenesis. Instead, variations in the CH_4 content of the produced gas are more indicative. In the case of monitoring acetogenesis,

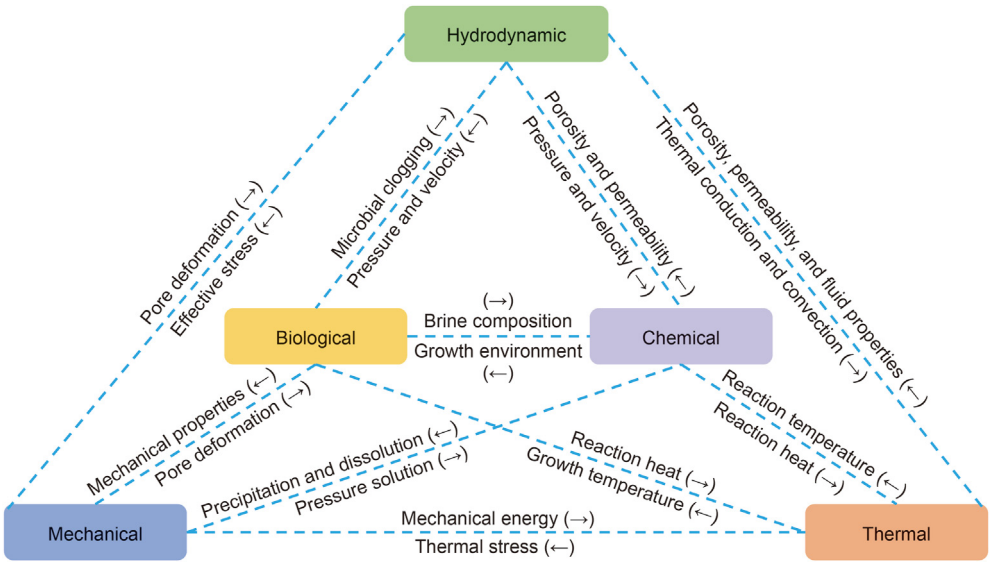

Fig. 23. Primary multi-field coupling processes in UHS (arrows indicate directions).

dynamic shifts in acetate levels in the formation water serve as the most reliable indicators. For monitoring sulfate reduction, the presence of H_2S in the produced gas typically acts as a direct marker. However, it's crucial to recognize that in some instances, the measurement of H_2S in the gas phase may not be accurate due to its potential redissolution and subsequent precipitation. Additionally, since the principal H_2-consuming microbial metabolic reactions are strongly exothermic, monitoring the temperature of the reservoir also becomes a viable and informative approach.

For more precise monitoring of microbial activity, stable isotope analysis of H_2, CO_2, CH_4 gases, and dissolved sulfate is crucial. This technique leverages the fact that microbes exhibit isotopic selectivity, causing shifts in the ratios of heavy to light isotopes (e.g., $^{13}C/^{12}C$, $^{2}H/^{1}H$, $^{18}O/^{16}O$, and $^{34}S/^{32}S$) during biological processes (Dopffel et al., 2024). For instance, isotopic analyses of carbon have been utilized effectively during previous field tests (Vítězová et al., 2023; Hellerschmied et al., 2024).

7. Conclusions and outlook

7.1. Conclusions

UHS represents a large-scale energy storage technology with substantial potential to mitigate the instability of energy supply. However, the presence of abundant H_2-consuming microbes in porous media, such as methanogens, acetogens, and SRB, can impact the efficiency and safety of UHS systems.

Complex GWRM interactions can result in the consumption of H_2 and the production of CH_4, H_2S, acetate, and other substances. It is important to note that in the emerging field of UBM, a new type of UHS method, H_2 consumption by methanogens is desirable. Conversely, in other UHS scenarios, H_2 consumption is generally considered undesirable. This consumption is heavily influenced by underground environmental conditions such as pH levels, salinity, temperature, and the availability of substrates like CO_2, H_2, and sulfate. Consequently, the rate and extent of H_2 consumption observed in laboratory experiments and field tests can vary significantly. For instance, rapid on-site conversion was observed at the Tvrdonice gas storage in the Czech Republic, where the 50% H_2 and 12.5% CO_2 components of the injected 392 Sm^3 of mixed gas were completely consumed within approximately forty days.

Microbial interactions can also induce complex changes in wettability. Due to SRB metabolism, wettability can shift from water-wet, with a contact angle of 41°, to neutral-wet, with an average contact angle of 96° within a 20-h period. The opposite trend has also been observed. Additionally, microbial aggregation, changes in mineral composition, and water generation can occur. These factors can impact H_2 flow both positively and negatively, depending on geological conditions, engineering operations, and native microbial species. Furthermore, outcomes of microbial interactions, such as steel corrosion and significant dissolution of sensitive minerals, can compromise well integrity, caprock integrity, and fault sealing, thereby posing risks to the safe storage of H_2.

Therefore, careful site selection, optimization of operating modes and parameters prior to implementing UHS, and rigorous monitoring during UHS are crucial for minimizing the adverse effects of microbial interactions or effectively harnessing the catalytic function of methanogens to synthesize carbon-neutral CH_4 in UBM technology.

7.2. Future research directions

Despite an extensive array of laboratory experiments, numerical simulations, and some field trials, numerous aspects still demand more comprehensive investigation. The details are outlined below.

In laboratory experiments, it is crucial to integrate various methods to comprehensively investigate the complex GWRM interactions. These methods encompass physico-chemical analyses of aqueous and gas phases, solid-phase X-Ray tomography and diffraction, nucleic acid extraction and RNA retro-transcription, polymerase chain reaction and sequencing, among others (Haddad et al., 2022). The combination of these techniques is pivotal for elucidating the metabolic pathways of diverse microbes, understanding the mechanisms of competitive H_2 consumption, and examining their impacts on underground environments. Additionally, dynamic visualization experiments are indispensable. Techniques such as microfluidic models or large-scale physical simulation apparatuses can shed light on the temporal and spatial dynamics that closely mimic those in actual porous media.

In numerical modelling, research has predominantly focused on either bio-geochemistry or bio-hydrodynamics. Future simulations need to adopt a more holistic approach by fully integrating

interactions across multiple domains, including thermal, hydrodynamic, mechanical, chemical, and biological processes (Fig. 23). Moreover, current microbial kinetic models and their parameters, primarily derived from laboratory data, lack the accuracy needed for reliable field predictions. Therefore, for subsequent field tests, it is recommended to implement comprehensive dynamic monitoring and detailed analysis of key parameters, such as gas composition, microbial community structure, and formation water composition. This approach will aid in the development of more precise kinetic models and yield more accurate kinetic parameters.

Investigating the impact of different engineering operations on H_2 consumption during field tests is also crucial. Factors to consider include the type of cushion gas used, the ratio of injected gas, the total pressure of the injected gas, injection-production rates, operational modes (e.g., batch versus cycle operation), among others. These areas have not yet been comprehensively examined in current field tests. Additionally, the feasibility of storing pure H_2 in porous media and injecting ground-cultured high-activity methanogens into cooled-down, high-temperature reservoirs to promote UBM, deserves in-depth study. Moreover, examining the feasibility of conducting UBM in existing CO_2 geological storage sites, as previous studies have indicated this potential (Vilcáez, 2015; Tyne et al., 2021).

Integrating emerging technologies such as big data and artificial intelligence into UHS processes is recommended to enhance the prediction of microbial impacts (Katterbauer et al., 2023, 2024). Additionally, greater attention should be directed towards socio-economic aspects. This includes analyzing the carbon footprint of UHS and examining the feasibility of using non-pure CO_2 and H_2-containing industrial waste gases for UBM to mitigate environmental impacts while enhancing economic benefits. Policy research is also essential. It should encompass formulating a standardized system for the entire UHSindustry chain, investigating tax incentives for UHScompanies, and exploring how the carbon trading market can support UHSprojects, among other considerations.

Data availability

Data will be made available on request.

CRediT authorship contribution statement

Lin Wu: Writing – review & editing, Writing – original draft, Formal analysis, Conceptualization. **Zheng-Meng Hou:** Writing – review & editing, Supervision, Project administration, Funding acquisition. **Zhi-Feng Luo:** Writing – review & editing, Visualization. **Yan-Li Fang:** Methodology, Investigation, Data curation. **Liang-Chao Huang:** Investigation, Formal analysis. **Xu-Ning Wu:** Writing – review & editing, Methodology, Formal analysis. **Qian-Jun Chen:** Visualization, Formal analysis. **Qi-Chen Wang:** Investigation.

Declaration of competing interest

The authors declare that they have no known competing financial interests or personal relationships that could have appeared to influence the work reported in this paper.

Acknowledgments

This work was supported by the European Union's “Horizon Europe programme” – LOC3G (Grant No. 101129729) and the Henan Center for Outstanding Overseas Scientists (Grant No. GZS2024001).

References

Addassi, M., Omar, A., Ghorayeb, K., et al., 2021. Comparison of various reactive transport simulators for geological carbon sequestration. Int. J. Greenh. Gas Control 110, 103419. https://doi.org/10.1016/j.ijggc.2021.103419.

Aftab, A., Al-Yaseri, A., Nzila, A., et al., 2023. Quartz–H_2–brine bacterium wettability under realistic geo-conditions: towards geological hydrogen storage. Energy Fuels 37 (7), 5623–5631. https://doi.org/10.1021/acs.energyfuels.3c00163.

Aftab, A., Al-Yaseri, A., Nzila, A., et al., 2024. Microbial impact on basalt-water-hydrogen system: insights into wettability, capillary pressure, and interfacial tension for subsurface hydrogen storage. Greenhouse Gases Sci. Technol. 14 (3), 546–560. https://doi.org/10.1002/ghg.2277.

Al-Yaseri, A., Sakthivel, S., Yekeen, N., et al., 2024. The influence of microbial activities on the capillary pressure during H_2 injection: implications for underground H_2 storage. Energy Fuels 38 (1), 499–505. https://doi.org/10.1021/acs.energyfuels.3c03640.

Ali, H., Hamdi, Z., Talabi, O., et al., 2022. Comprehensive approach for modeling underground hydrogen storage in depleted gas reservoirs. In: SPE Asia Pacific Oil & Gas Conference and Exhibition. https://doi.org/10.2118/210638-MS.

Ali, M., Arif, M., Sedev, R., et al., 2023. Underground hydrogen storage: the microbiotic influence on rock wettability. J. Energy Storage 72, 108405. https://doi.org/10.1016/j.est.2023.108405.

Amirante, R., Cassone, E., Distaso, E., et al., 2017. Overview on recent developments in energy storage: mechanical, electrochemical and hydrogen technologies. Energy Convers. Manage. 132, 372–387. https://doi.org/10.1016/j.enconman.2016.11.046.

Aslannezhad, M., Ali, M., Kalantariasl, A., et al., 2023. A review of hydrogen/rock/brine interaction: implications for hydrogen geo-storage. Prog. Energy Combust. Sci. 95, 101066. https://doi.org/10.1016/j.pecs.2022.101066.

Bassani, I., Bellini, R., Vizzarro, A., et al., 2023. Biogeochemical characterization of four depleted gas reservoirs for conversion into underground hydrogen storage. Environ. Microbiol. 25 (12), 3683–3702. https://doi.org/10.1111/1462-2920.16538.

Bauer, S., 2017. Underground sun storage final report. Vienna. https://www.underground-sun-storage.at.

Bauer, S., 2023. Underground sun conversion final report. Vienna. https://www.underground-sun-conversion.at/.

Bellini, R., Bassani, I., Vizzarro, A., et al., 2022. Biological aspects, advancements and techno-economical evaluation of biological methanation for the recycling and valorization of CO_2. Energies 15 (11), 4064. https://doi.org/10.3390/en15114064.

Bellini, R., Vasile, N.S., Bassani, I., et al., 2024. Investigating the activity of indigenous microbial communities from Italian depleted gas reservoirs and their possible impact on underground hydrogen storage. Front. Microbiol. 15, 1392410. https://doi.org/10.3389/fmicb.2024.1392410.

Bhadariya, V., Kaur, J., Sapale, P., et al., 2024. Hydrogen storage in porous media: understanding and mitigating microbial risks for a sustainable future. Int. J. Hydrogen Energy 67, 681–693. https://doi.org/10.1016/j.ijhydene.2024.04.178.

Blanco, H., Codina, V., Laurent, A., et al., 2020. Life cycle assessment integration into energy system models: an application for power-to-methane in the EU. Appl. Energy 259, 114160. https://doi.org/10.1016/j.apenergy.2019.114160.

Boon, M., Buntic, I., Ahmed, K., et al., 2024. Microbial induced wettability alteration with implications for underground hydrogen storage. Sci. Rep. 14 (1), 8248. https://doi.org/10.1038/s41598-024-58951-6.

Bryant, M., 1972. Commentary on the Hungate technique for culture of anaerobic bacteria. Am. J. Clin. Nutr. 25 (12), 1324–1328. https://doi.org/10.1093/ajcn/25.12.1324.

Bültemeier, H., 2023. Bio-UGS - biological conversion of carbon dioxide and hydrogen to methane in porous underground gas storage facilities. https://co2-utilization.net/fileadmin/Abschlusskonferenz/Praesentationen_zum_Upload/12_230928_Abschlusskonferenz_CO2WIN_BioUGS_final_en_print_fuer_Upload.pdf.

Buriánková, I., Molíková, A., Vítězová, M., et al., 2022. Microbial communities in underground gas reservoirs offer promising biotechnological potential. Fermentation 8 (6), 251. https://doi.org/10.3390/fermentation8060251.

Buzek, F., Onderka, V., Vančura, P., et al., 1994. Carbon isotope study of methane production in a town gas storage reservoir. Fuel 73 (5), 747–752. https://doi.org/10.1016/0016-2361(94)90019-1.

Chen, L., Msigwa, G., Yang, M., et al., 2022. Strategies to achieve a carbon neutral society: a review. Environ. Chem. Lett. 20 (4), 2277–2310. https://doi.org/10.1007/s10311-022-01435-8.

Cavallaro, A., Martinez, M.G., Ostera, H., et al., 2005. Oilfield reservoir souring during waterflooding: a case study with low sulphate concentration in formation and injection waters. In: SPE International Conference on Oilfield Chemistry. https://doi.org/10.2118/92959-MS.

Chen, Q., Hou, Z., Wu, X., et al., 2023. A two-step site selection concept for underground pumped hydroelectric energy storage and potential estimation of coal mines in Henan Province. Energies 16 (12), 4811. https://doi.org/10.3390/en16124811.

COMSOL, M., 2021. Introduction to COMSOL multiphysics. https://cdn.comsol.com/doc/6.0.0.405/IntroductionToCOMSOLMultiphysics.pdf.

Cui, Q., He, L., Han, G., et al., 2020. Review on climate and water resource implications of reducing renewable power curtailment in China: a nexus perspective. Appl. Energy 267, 115114. https://doi.org/10.1016/j.apenergy.2020.115114.

Denholm, P., Mai, T., 2019. Timescales of energy storage needed for reducing

renewable energy curtailment. Renew. Energy 130, 388–399. https://doi.org/10.1016/j.renene.2018.06.079.
Dohrmann, A.B., Kruger, M., 2023. Microbial H_2 consumption by a formation fluid from a natural gas field at high-pressure conditions relevant for underground H_2 storage. Environ. Sci. Technol. 57 (2), 1092–1102. https://doi.org/10.1021/acs.est.2c07303.
Dopffel, N., An-Stepec, B.A., Bombach, P., et al., 2024. Microbial life in salt caverns and their influence on H_2 storage – current knowledge and open questions. Int. J. Hydrogen Energy 58, 1478–1485. https://doi.org/10.1016/j.ijhydene.2024.01.334.
Dopffel, N., Jansen, S., Gerritse, J., 2021. Microbial side effects of underground hydrogen storage – knowledge gaps, risks and opportunities for successful implementation. Int. J. Hydrogen Energy 46 (12), 8594–8606. https://doi.org/10.1016/j.ijhydene.2020.12.058.
Dopffel, N., Mayers, K., Kedir, A., et al., 2023. Microbial hydrogen consumption leads to a significant pH increase under high-saline-conditions: implications for hydrogen storage in salt caverns. Sci. Rep. 13 (1), 10564. https://doi.org/10.1038/s41598-023-37630-y.
Du, Z., Dai, Z., Yang, Z., et al., 2024. Exploring hydrogen geologic storage in China for future energy: opportunities and challenges. Renewable Sustainable Energy Rev. 196, 114366. https://doi.org/10.1016/j.rser.2024.114366.
Du, Z., Liu, C., Zhai, J., et al., 2021. A review of hydrogen purification technologies for fuel cell vehicles. Catalysts 11 (3), 393. https://doi.org/10.3390/catal11030393.
Dupraz, S., Stephant, S., Perez, A., et al., 2018. Patagonia Wind–using methanogenesis to store hydrogen on large scales. In: 22st World Hydrogen Energy Conference-WHEC 2018. https://brgm.hal.science/hal-01742093/.
Ebigbo, A., Golfier, F., Quintard, M., 2013. A coupled, pore-scale model for methanogenic microbial activity in underground hydrogen storage. Adv. Water Resour. 61, 74–85. https://doi.org/10.1016/j.advwatres.2013.09.004.
Eddaoui, N., Panfilov, M., Ganzer, L., et al., 2021. Impact of pore clogging by bacteria on underground hydrogen storage. Transp. Porous Media 139 (1), 89–108. https://doi.org/10.1007/s11242-021-01647-6.
Elgendy, A.M.S., Pizzolato, A., Maniglio, M., et al., 2023. Reactive transport modelling of H_2 storage in depleted gas fields: an approach to implement biogeochemical reactions in a compositional reservoir simulator. In: SPE EuropEC-Europe Energy Conference. https://doi.org/10.2118/214434-MS.
Fernandez, D.M., Emadi, H., Hussain, A., et al., 2024. A holistic review on wellbore integrity challenges associated with underground hydrogen storage. Int. J. Hydrogen Energy 57, 240–262. https://doi.org/10.1016/j.ijhydene.2023.12.230.
Flemisch, B., Darcis, M., Erbertseder, K., et al., 2011. DuMux: DUNE for multi-{phase, component, scale, physics,…} flow and transport in porous media. Adv. Water Resour. 34 (9), 1102–1112. https://doi.org/10.1016/j.advwatres.2011.03.007.
Flemming, H.-C., Wingender, J., 2010. The biofilm matrix. Nat. Rev. Microbiol. 8 (9), 623–633. https://doi.org/10.1038/nrmicro2415.
Gao, Q., Liu, J., Elsworth, D., 2024. Phenomenal study of microbial impact on hydrogen storage in aquifers: a coupled multiphysics modelling. Int. J. Hydrogen Energy 79, 883–900. https://doi.org/10.1016/j.ijhydene.2024.07.004.
Glenk, G., Reichelstein, S., 2019. Economics of converting renewable power to hydrogen. Nat. Energy 4 (3), 216–222. https://doi.org/10.1038/s41560-019-0326-1.
Haddad, P.G., Ranchou-Peyruse, M., Guignard, M., et al., 2022. Geological storage of hydrogen in deep aquifers –an experimental multidisciplinary study. Energy Environ. Sci. 15 (8), 3400–3415. https://doi.org/10.1039/d2ee00765g.
Hagemann, B., 2018. Numerical and Analytical Modeling of Gas Mixing and Bio-Reactive Transport during Underground Hydrogen Storage. Clausthal University of Technology. Doctoral Thesis. https://dokumente.ub.tu-clausthal.de/receive/clausthal_mods_00000546.
Hagemann, B., Rasoulzadeh, M., Panfilov, M., et al., 2016. Hydrogenization of underground storage of natural gas. Comput. Geosci. 20 (3), 595–606. https://doi.org/10.1007/s10596-015-9515-6.
Hamdi, Z., Rosman, A., Partoon, B., et al., 2024. Salinity effects on H_2S generation in subsurface hydrogen storage. In: GOTECH, Dubai, UAE. https://doi.org/10.2118/219391-MS.
Heinemann, N., Alcalde, J., Miocic, J.M., et al., 2021. Enabling large-scale hydrogen storage in porous media – the scientific challenges. Energy Environ. Sci. 14 (2), 853–864. https://doi.org/10.1039/d0ee03536j.
Hellerschmied, C., Schritter, J., Waldmann, N., et al., 2024. Hydrogen storage and geo-methanation in a depleted underground hydrocarbon reservoir. Nat. Energy 9 (3), 333–344. https://doi.org/10.1038/s41560-024-01458-1.
Hemme, C., van Berk, W., 2018. Hydrogeochemical modeling to identify potential risks of underground hydrogen storage in depleted gas fields. Appl. Sci. 8 (11), 2282. https://doi.org/10.3390/app8112282.
Hogeweg, S., Hagemann, B., Bobrov, V., et al., 2024. Development and calibration of a bio-geo-reactive transport model for UHS. Front. Energy Res. 12, 1385273. https://doi.org/10.3389/fenrg.2024.1385273.
Hogeweg, S., Hagemann, B., Ganzer, L., 2022a. Simulation of freshwater injection to enable underground bio-methanation in high-saline gas storage formations. EAGE GET. https://doi.org/10.3997/2214-4609.202221055.
Hogeweg, S., Strobel, G., Hagemann, B., 2022b. Benchmark study for the simulation of underground hydrogen storage operations. Comput. Geosci. 26 (6), 1367–1378. https://doi.org/10.1007/s10596-022-10163-5.
Hou, Z., Huang, L., Xie, Y., et al., 2023a. Economic analysis of methanating CO_2 and hydrogen-rich industrial waste gas in depleted natural gas reservoirs. Energies 16 (9). https://doi.org/10.3390/en16093633.
Hou, Z., Luo, J., Xie, Y., et al., 2023b. Carbon circular utilization and partially geological sequestration: potentialities, challenges, and trends. Energies 16 (1). https://doi.org/10.3390/en16010324.
Hou, Z., Wu, L., Zhang, L., et al., 2023c. CO_2-based underground biochemical synthesis of natural gas coupled with geothermal energy production: technology system, challenges, and prospects. Nat. Gas. Ind. 43 (11). https://doi.org/10.3787/j.issn.1000-0976.2023.11.017.
Hou, Z., Wu, X., Luo, J., et al., 2024. Major challenges of deep geothermal systems and an innovative development mode of REGS integrated with energy storage. Coal Geol. Explor. 52 (1), 1–13. https://doi.org/10.12363/issn.1001-1986.23.12.0848.
Hou, Z., Xiong, Y., Luo, J., et al., 2023d. International experience of carbon neutrality and prospects of key technologies: lessons for China. Pet. Sci. 20 (2), 893–909. https://doi.org/10.1016/j.petsci.2023.02.018.
IEA, 2024. CO_2 emissions in 2023. https://www.iea.org/reports/co2-emissions-in-2023.
Jeong, M.S., Lee, J.H., Lee, K.S., 2019. Critical review on the numerical modeling of in-situ microbial enhanced oil recovery processes. Biochem. Eng. J. 150, 107294. https://doi.org/10.1016/j.bej.2019.107294.
Jia, G., Lei, M., Li, M., et al., 2023. Hydrogen embrittlement in hydrogen-blended natural gas transportation systems: a review. Int. J. Hydrogen Energy 48 (82), 32137–32157. https://doi.org/10.1016/j.ijhydene.2023.04.266.
Jin, Q., 2023. Building microbial kinetic models for environmental application: a theoretical perspective. Appl. Geochem. 158, 105782. https://doi.org/10.1016/j.apgeochem.2023.105782.
Katterbauer, K., Al Shehri, A., Qasim, A., et al., 2023. A data-driven deep learning framework for microbial reaction prediction for hydrogen underground storage. In: SPE Reservoir Simulation Conference. https://doi.org/10.2118/212187-MS.
Katterbauer, K., Qasim, A., Al Shehri, A., et al., 2024. Predicting the microbial effects on hydrogen storage quality-A McKee reservoir study. In: Offshore Technology Conference Asia. https://doi.org/10.4043/34733-MS.
Khajooie, S., Gaus, G., Dohrmann, A.B., et al., 2024. Methanogenic conversion of hydrogen to methane in reservoir rocks: an experimental study of microbial activity in water-filled pore space. Int. J. Hydrogen Energy 50, 272–290. https://doi.org/10.1016/j.ijhydene.2023.07.065.
Kolawole, O., Ispas, I., Kumar, M., et al., 2021a. Biogeomechanical alteration of near-wellbore properties: implications for hydrocarbon recovery. J. Nat. Gas Sci. Eng. 94, 104055. https://doi.org/10.1016/j.jngse.2021.104055.
Kolawole, O., Ispas, I., Kumar, M., et al., 2021b. How can biogeomechanical alterations in shales impact caprock integrity and CO_2 storage? Fuel 291, 120149. https://doi.org/10.1016/j.fuel.2021.120149.
Kolditz, O., Bauer, S., Bilke, L., et al., 2012. OpenGeoSys: an open-source initiative for numerical simulation of thermo-hydro-mechanical/chemical (THM/C) processes in porous media. Environ. Earth Sci. 67, 589–599. https://doi.org/10.1007/s12665-012-1546-x.
Konegger, H., Loibner, A., Waldmann, N., et al., 2023. Underground sun conversion–flexible storage final report. Vienna and Bern. https://www.underground-sun-conversion.at/en/flexstore.html.
Leonzio, G., 2016. Process analysis of biological Sabatier reaction for bio-methane production. Chem. Eng. J. 290, 490–498. https://doi.org/10.1016/j.cej.2016.01.068.
Leroi, F., Fall, P.A., Pilet, M.F., et al., 2012. Influence of temperature, pH and NaCl concentration on the maximal growth rate of Brochothrix thermosphacta and a bioprotective bacteria Lactococcus piscium CNCM I-4031. Food Microbiol. 31 (2), 222–228. https://doi.org/10.1016/j.fm.2012.02.014.
Lie, K.-A., 2019. An Introduction to Reservoir Simulation Using MATLAB/GNU Octave: User Guide for the MATLAB Reservoir Simulation Toolbox (MRST). Cambridge University Press. https://www.cambridge.org/9781108492430.
Lie, K.-A., Møyner, O., 2021. Advanced Modelling with the MATLAB Reservoir Simulation Toolbox. Cambridge University Press. https://doi.org/10.1017/9781009019781.
Liu, H., Were, P., Li, Q., et al., 2017. Worldwide status of CCUS technologies and their development and challenges in China. Geofluids 2017 (1), 6126505. https://doi.org/10.1155/2017/6126505.
Liu, H., Yang, C., Liu, J., et al., 2023a. An overview of underground energy storage in porous media and development in China. Gas Sci. Eng., 205079 https://doi.org/10.1016/j.jgsce.2023.205079.
Liu, N., Kovscek, A.R., Fernø, M.A., et al., 2023b. Pore-scale study of microbial hydrogen consumption and wettability alteration during underground hydrogen storage. Front. Energy Res. 11. https://doi.org/10.3389/fenrg.2023.1124621.
Lu, P., Zhang, G., Apps, J., et al., 2022. Comparison of thermodynamic data files for PHREEQC. Earth Sci. Rev. 225, 103888. https://doi.org/10.1016/j.earscirev.2021.103888.
Maniglio, M., Rivolta, G., Elgendy, A., et al., 2023. Evaluating the impact of biochemical reactions on H2 storage in depleted gas fields. In: SPE Annual Technical Conference and Exhibition.. https://doi.org/10.2118/215142-MS.
Minougou, J.D., Gholami, R., Poirier, S., 2024. A one-dimensional diffusive transport model to evaluate H_2S generation in salt caverns hydrogen storage sites. Gas Sci. Eng. 126. https://doi.org/10.1016/j.jgsce.2024.205336.
Minougou, W.J.D., 2022. Numerical Study of Geological Hydrogen Conversion. Montanuniversitaet Leoben. Master's Thesis. https://pure.unileoben.ac.at/en/publications/numerical-study-of-geological-hydrogen-conversion.
Molíková, A., Vítězová, M., Vítěz, T., et al., 2022. Underground gas storage as a promising natural methane bioreactor and reservoir? J. Energy Storage 47, 103631. https://doi.org/10.1016/j.est.2021.103631.

Muhammed, N.S., Haq, B., Al Shehri, D., et al., 2022. A review on underground hydrogen storage: insight into geological sites, influencing factors and future outlook. Energy Rep. 8, 461–499. https://doi.org/10.1016/j.egyr.2021.12.002.
Muhammed, N.S., Haq, M.B., Al Shehri, D., et al., 2024. Comparative study on hydrogen losses via microbial byproduct in the presence of methane and nitrogen cushion gas. Int. J. Hydrogen Energy 81, 237–248. https://doi.org/10.1016/j.ijhydene.2024.07.272.
Muloiwa, M., Nyende-Byakika, S., Dinka, M., 2020. Comparison of unstructured kinetic bacterial growth models. S. Afr. J. Chem. Eng. 33, 141–150. https://doi.org/10.1016/j.sajce.2020.07.006.
Mura, J., Ranchou-Peyruse, M., Guignard, M., et al., 2024. Comparative study of three H_2 geological storages in deep aquifers simulated in high-pressure reactors. Int. J. Hydrogen Energy 63, 330–345. https://doi.org/10.1016/j.ijhydene.2024.02.322.
Ngoma, M.C., Kolawole, O., 2024. Porosity and bedding controls on bio-induced carbonate precipitation and mechanical properties of shale and dolomitic rocks: EICP vs MICP. Biogeotechnics, 100102. https://doi.org/10.1016/j.bgtech.2024.100102.
Nikolaev, D.S., Moeininia, N., Ott, H., et al., 2021. Investigation of underground biomethanation using bio-reactive transport modeling. In: SPE Russian Petroleum Technology Conference. https://doi.org/10.2118/206617-MS.
Niu, J., Liu, Q., Lv, J., et al., 2020. Review on microbial enhanced oil recovery: mechanisms, modeling and field trials. J. Pet. Sci. Eng. 192, 107350. https://doi.org/10.1016/j.petrol.2020.107350.
Okoroafor, E.R., Sampaio, L., Gasanzade, F., et al., 2023. Intercomparison of numerical simulation models for hydrogen storage in porous media using different codes. Energy Convers. Manage. 292, 117409. https://doi.org/10.1016/j.enconman.2023.117409.
Panfilov, M., 2010. Underground storage of hydrogen: in situ self-organisation and methane generation. Transp. Porous Media 85 (3), 841–865. https://doi.org/10.1007/s11242-010-9595-7.
Panfilov, M., 2016. Underground and pipeline hydrogen storage, Compendium of Hydrogen. Energy 91–115. https://doi.org/10.1016/B978-1-78242-362-1.00004-3.
Panfilov, M., Reitenbach, V., Ganzer, L., 2016. Self-organization and shock waves in underground methanation reactors and hydrogen storages. Environ. Earth Sci. 75 (4), 313. https://doi.org/10.1007/s12665-015-5048-5.
Paraschiv, S., Paraschiv, L.S., 2020. Trends of carbon dioxide (CO_2) emissions from fossil fuels combustion (coal, gas and oil) in the EU member states from 1960 to 2018. Energy Rep. 6, 237–242. https://doi.org/10.1016/j.egyr.2020.11.116.
Parkhurst, D.L., Appelo, C., 2013. Description of input and examples for PHREEQC version 3—a computer program for speciation, batch-reaction, one-dimensional transport, and inverse geochemical calculations. https://pubs.usgs.gov/tm/06/a43/.
Parkhurst, D.L., Kipp, K.L., Charlton, S.R., 2010. PHAST Version 2—a program for simulating groundwater flow, solute transport, and multicomponent geochemical reactions. https://pubs.usgs.gov/tm/06A35/.
Peleg, M., 2021. A new look at models of the combined effect of temperature, pH, water activity, or other factors on microbial growth rate. Food Eng. Rev. 14 (1), 31–44. https://doi.org/10.1007/s12393-021-09292-x.
Pérez, A., Pérez, E., Dupraz, S., et al., 2016. Patagonia wind-hydrogen project: underground storage and methanation. In: 21st World Hydrogen Energy Conference 2016. https://brgm.hal.science/hal-01317467/.
Peszynska, M., Trykozko, A., Iltis, G., et al., 2016. Biofilm growth in porous media: experiments, computational modeling at the porescale, and upscaling. Adv. Water Resour. 95, 288–301. https://doi.org/10.1016/j.advwatres.2015.07.008.
Pfeiffer, W.T., Graupner, B., Bauer, S., 2016. The coupled non-isothermal, multiphase-multicomponent flow and reactive transport simulator OpenGeoSys–ECLIPSE for porous media gas storage. Environ. Earth Sci. 75 (20), 1347. https://doi.org/10.1007/s12665-016-6168-2.
Quarton, C.J., Samsatli, S., 2018. Power-to-gas for injection into the gas grid: what can we learn from real-life projects, economic assessments and systems modelling? Renewable Sustainable Energy Rev. 98, 302–316. https://doi.org/10.1016/j.rser.2018.09.007.
Raczkowski, J., Turkiewicz, A., Kapusta, P., 2004. Elimination of biogenic hydrogen sulfide in underground gas storage. A case study. In: SPE Annual Technical Conference and Exhibition. https://doi.org/10.2118/89906-MS.
RAG, 2024. Underground sun storage 2030. https://www.uss-2030.at/. (Accessed 1 July 2024).
Rahman, M.M., Oni, A.O., Gemechu, E., et al., 2020. Assessment of energy storage technologies: a review. Energy Convers. Manage. 223, 113295. https://doi.org/10.1016/j.enconman.2020.113295.
Ramió-Pujol, S., Ganigué, R., Bañera, L., et al., 2015. Incubation at 25 °C prevents acid crash and enhances alcohol production in Clostridium carboxidivorans P7. Bioresour. Technol. 192, 296–303. https://doi.org/10.1016/j.biortech.2015.05.077.
Ranchou-Peyruse, M., Guignard, M., Chiquet, P., et al., 2024. Assessment of the in situ biomethanation potential of a deep aquifer used for natural gas storage. FEMS Microbiol. Ecol. 100 (6), fiae066. https://doi.org/10.1093/femsec/fiae066.
Ritter, D., Vinson, D., Barnhart, E., et al., 2015. Enhanced microbial coalbed methane generation: a review of research, commercial activity, and remaining challenges. Int. J. Coal Geol. 146, 28–41. https://doi.org/10.1016/j.coal.2015.04.013.
Rivolta, G., Maniglio, M., Elgendy, A., et al., 2024. Evaluating the impact of biochemical reactions on H_2 storage in depleted gas fields. SPE J 29 (8), 4494–4509. https://doi.org/10.2118/215142-PA.
Rooney, C., Li, Q., 2023. Biogeochemical reactions in a diffusion-limited zone around wellbore cement relevant to underground hydrogen storage. In: Proceedings of the 11th Unconventional Resources Technology Conference. https://doi.org/10.15530/urtec-2023-3867104.
Rooney, C., Tappero, R., Nicholas, S., et al., 2024. Wellbore cement alteration and roles of CO_2 and shale during underground hydrogen storage. Appl. Geochem., 106088 https://doi.org/10.1016/j.apgeochem.2024.106088.
Rosman, A., Hamdi, Z., Ali, M., et al., 2023. Mitigating global warming with underground hydrogen storage: impacts of H_2S generation. In: SPE Offshore Europe Conference & Exhibition. https://doi.org/10.2118/215551-MS.
Rosso, L., Lobry, J., Bajard, S., et al., 1995. Convenient model to describe the combined effects of temperature and pH on microbial growth. Appl. Environ. Microbiol. 61 (2), 610–616. https://doi.org/10.1128/aem.61.2.610-616.1995.
Saeed, M., Jadhawar, P., 2024. Modelling underground hydrogen storage: a state-of-the-art review of fundamental approaches and findings. Gas Sci. Eng., 205196 https://doi.org/10.1016/j.jgsce.2023.205196.
Safari, Z., Fatehi, R., Azin, R., 2024. Developing a numerical model for microbial methanation in a depleted hydrocarbon reservoir. Renew. Energy 227, 120426. https://doi.org/10.1016/j.renene.2024.120426.
Schleussner, C.-F., Rogelj, J., Schaeffer, M., et al., 2016. Science and policy characteristics of the Paris Agreement temperature goal. Nat. Clim. Change 6 (9), 827–835. https://doi.org/10.1038/nclimate3096.
Schwab, L., Popp, D., Nowack, G., et al., 2022. Structural analysis of microbiomes from salt caverns used for underground gas storage. Int. J. Hydrogen Energy 47 (47), 20684–20694. https://doi.org/10.1016/j.ijhydene.2022.04.170.
Schwab, L., Prinsen, L., Nowack, G., et al., 2023. Sulfate reduction and homoacetogenesis at various hypersaline conditions: implications for H_2 underground gas storage. Front. Energy Res. 11, 1125619. https://doi.org/10.3389/fenrg.2023.1125619.
Shen, B., Hove, A., Hu, J., et al., 2024. Coping with power crises under decarbonization: the case of China. Renewable Sustainable Energy Rev. 193, 114294. https://doi.org/10.1016/j.rser.2024.114294.
Shojaee, A., Ghanbari, S., Wang, G., et al., 2024a. Integrated modelling of biogeochemical aspects in underground hydrogen storage: implications for reservoir selection and performance. In: SPE Europec featured at EAGE Conference and Exhibition. https://doi.org/10.2118/220056-MS.
Shojaee, A., Ghanbari, S., Wang, G., et al., 2024b. Interplay between microbial activity and geochemical reactions during underground hydrogen storage in a seawater-rich formation. Int. J. Hydrogen Energy 50, 1529–1541. https://doi.org/10.1016/j.ijhydene.2023.10.061.
Šmigáň, P., Greksak, M., Kozánková, J., et al., 1990. Methanogenic bacteria as a key factor involved in changes of town gas stored in an underground reservoir. FEMS Microbiol. Ecol. 6 (3), 221–224. https://doi.org/10.1111/j.1574-6968.1990.tb03944.x.
Song, R., Wu, M., Liu, J., et al., 2024. Pore scale modeling on microbial hydrogen consumption and mass transfer of multicomponent gas flow in underground hydrogen storage of depleted reservoir. Energy, 132534. https://doi.org/10.1016/j.energy.2024.132534.
Stangeland, K., Kalai, D., Li, H., et al., 2017. CO_2 methanation: the effect of catalysts and reaction conditions. Energy Proc. 105, 2022–2027. https://doi.org/10.1016/j.egypro.2017.03.577.
Steefel, C.I., Appelo, C.A.J., Arora, B., et al., 2015. Reactive transport codes for subsurface environmental simulation. Comput. Geosci. 19, 445–478. https://doi.org/10.1007/s10596-014-9443-x.
Stephant, S., Dupraz, S., Joulian, C., et al., 2018. Conversion of H_2 and CO_2 into CH_4 by methanogens as a potential way of energy storage. In: Conference of the European Biogas Association. https://energnet.eu/wp-content/uploads/2021/02/stephant_et_al_2019_poster_ues_workshop.pdf.
Strobel, G., Hagemann, B., Huppertz, T.M., et al., 2020. Underground bio-methanation: concept and potential. Renewable Sustainable Energy Rev. 123, 109747. https://doi.org/10.1016/j.rser.2020.109747.
Strobel, G., Hagemann, B., Luddeke, C.T., et al., 2023a. Coupled model for microbial growth and phase mass transfer in pressurized batch reactors in the context of underground hydrogen storage. Front. Microbiol. 14, 1150102. https://doi.org/10.3389/fmicb.2023.1150102.
Strobel, G., Zawallich, J., Hagemann, B., et al., 2023b. Experimental and numerical investigation of microbial growth in two-phase saturated porous media at the pore-scale. Sustain. Energy Fuels 7 (16), 3939–3948. https://doi.org/10.1039/d3se00037k.
Taron, J., Elsworth, D., Min, K.-B., 2009. Numerical simulation of thermal-hydrologic-mechanical-chemical processes in deformable, fractured porous media. Int. J. Rock Mech. Min. Sci. 46 (5), 842–854. https://doi.org/10.1016/j.ijrmms.2009.01.008.
Thaysen, E.M., Armitage, T., Slabon, L., et al., 2023. Microbial risk assessment for underground hydrogen storage in porous rocks. Fuel 352, 128852. https://doi.org/10.1016/j.fuel.2023.128852.
Thaysen, E.M., McMahon, S., Strobel, G.J., et al., 2021. Estimating microbial growth and hydrogen consumption in hydrogen storage in porous media. Renewable Sustainable Energy Rev. 151, 111481. https://doi.org/10.1016/j.rser.2021.111481.
Tremosa, J., Jakobsen, R., Le Gallo, Y., 2023. Assessing and modeling hydrogen reactivity in underground hydrogen storage: a review and models simulating the Lobodice town gas storage. Front. Energy Res. 11, 1145978. https://doi.org/10.3389/fenrg.2023.1145978.
Tyne, R., Barry, P., Lawson, M., et al., 2021. Rapid microbial methanogenesis during CO_2 storage in hydrocarbon reservoirs. Nature 600 (7890), 670–674. https://

doi.org/10.1038/s41586-021-04153-3.
Ugarte, E.R., Salehi, S., 2022. A review on well integrity issues for underground hydrogen storage. J. Energy Res. Technol. 144 (4), 042001. https://doi.org/10.1115/1.4052626.
Vasile, N.S., Bellini, R., Bassani, I., et al., 2024a. Innovative high pressure/high temperature, multi-sensing bioreactors system for microbial risk assessment in underground hydrogen storage. Int. J. Hydrogen Energy 51, 41–50. https://doi.org/10.1016/j.ijhydene.2023.10.245.
Vasile, N.S., Suriano, A., Bellini, R., et al., 2024b. Biogeochemical modelling of HP-HT bioreactor systems for enhanced microbial risk assessment in underground hydrogen storage. In: SPE Europec Featured at EAGE Conference and Exhibition. https://doi.org/10.2118/220064-MS.
Veshareh, M.J., Thaysen, E.M., Nick, H.M., 2022. Feasibility of hydrogen storage in depleted hydrocarbon chalk reservoirs: assessment of biochemical and chemical effects. Appl. Energy 323, 119575. https://doi.org/10.1016/j.apenergy.2022.119575.
Vilcáez, J., 2015. Numerical modeling and simulation of microbial methanogenesis in geological CO_2 storage sites. J. Pet. Sci. Eng. 135, 583–595. https://doi.org/10.1016/j.petrol.2015.10.015.
Vítězová, M., Onderka, V., Urbanová, I., et al., 2023. In situ field experiment shows the potential of methanogenic archaea for biomethane production from underground gas storage in natural rock environment. Environ. Technol. Innovation 32, 103253. https://doi.org/10.1016/j.eti.2023.103253.
Wang, F., Harindintwali, J.D., Yuan, Z., et al., 2021. Technologies and perspectives for achieving carbon neutrality. Innovation 2 (4), 100180. https://doi.org/10.1016/j.xinn.2021.100180.
Wang, G., Pickup, G., Sorbie, K., et al., 2024a. Bioreaction coupled flow simulations: impacts of methanogenesis on seasonal underground hydrogen storage. Int. J. Hydrogen Energy 55, 921–931. https://doi.org/10.1016/j.ijhydene.2023.11.035.
Wang, J., Wu, R., Wei, M., et al., 2023. A comprehensive review of site selection, experiment and numerical simulation for underground hydrogen storage. Gas Sci. Eng., 205105 https://doi.org/10.1016/j.jgsce.2023.205105.
Wang, J., Wu, R., Zhao, K., et al., 2024b. Numerical simulation of underground hydrogen storage converted from a depleted low-permeability oil reservoir. Int. J. Hydrogen Energy 69, 1069–1083. https://doi.org/10.1016/j.ijhydene.2024.05.102.
Wiel, K.v.d., Bloomfield, H.C., Lee, R.W., et al., 2019. The influence of weather regimes on European renewable energy production and demand. Environ. Res. Lett. 14 (9), 094010. https://doi.org/10.1088/1748-9326/ab38d3.
Wijtzes, T., Rombouts, F., Kant-Muermans, M., et al., 2001. Development and validation of a combined temperature, water activity, pH model for bacterial growth rate of Lactobacillus curvatus. Int. J. Food Microbiol. 63 (1–2), 57–64. https://doi.org/10.1016/S0168-1605(00)00401-3.
Wood, B.D., Ginn, T.R., Dawson, C.N., 1995. Effects of microbial metabolic lag in contaminant transport and biodegradation modeling. Water Resour. Res. 31 (3), 553–563. https://doi.org/10.1029/94WR02533.
Wu, L., Hou, Z., Luo, Z., et al., 2024. Site selection for underground bio-methanation of hydrogen and carbon dioxide using an integrated multi-criteria decision-making (MCDM) approach. Energy 306, 132437. https://doi.org/10.1016/j.energy.2024.132437.
Wu, L., Hou, Z., Luo, Z., et al., 2023a. Efficiency assessment of underground biomethanation with hydrogen and carbon dioxide in depleted gas reservoirs: a biogeochemical simulation. Energy 283. https://doi.org/10.1016/j.energy.2023.128539.
Wu, L., Hou, Z., Luo, Z., et al., 2023b. Numerical simulations of supercritical carbon dioxide fracturing: a review. J. Rock Mech. Geotech. Eng. 15 (7), 1895–1910. https://doi.org/10.1016/j.jrmge.2022.08.008.
Wu, L., Hou, Z., Xie, Y., et al., 2023c. Carbon capture, circular utilization, and sequestration (CCCUS): a multifunctional technology coupling underground biomethanation with geothermal energy production. J. Cleaner Prod. 426. https://doi.org/10.1016/j.jclepro.2023.139225.
Xie, Y., Wu, X., Hou, Z., et al., 2023. Gleaning insights from German energy transition and large-scale underground energy storage for China's carbon neutrality. Int. J. Min. Sci. Technol. 33 (5), 529–553. https://doi.org/10.1016/j.ijmst.2023.04.001.
Xiong, Y., Hou, Z., Xie, H., et al., 2023. Microbial-mediated CO_2 methanation and renewable natural gas storage in depleted petroleum reservoirs: a review of biogeochemical mechanism and perspective. Gondwana Res. 122, 184–198. https://doi.org/10.1016/j.gr.2022.04.017.
Xu, T., 2008. TOUGHREACT user's guide: a simulation program for non-isothermal multiphase reactive geochemical transport in variably saturated geologic media. V1. 2.1. https://escholarship.org/content/qt9r80098d/qt9r80098d.pdf.
Yao, Q., Tang, C., Xia, Z., et al., 2020. Mechanisms of failure in coal samples from underground water reservoir. Eng. Geol. 267, 105494. https://doi.org/10.1016/j.enggeo.2020.105494.
Zeng, L., Sarmadivaleh, M., Saeedi, A., et al., 2023. Storage integrity during underground hydrogen storage in depleted gas reservoirs. Earth Sci. Rev. 247, 104625. https://doi.org/10.1016/j.earscirev.2023.104625.
Zhang, X., Knapp, R., McInerney, M., 1992. A mathematical model for microbially enhanced oil recovery process. In: SPE/DOE Enhanced Oil Recovery Symposium. https://doi.org/10.2118/24202-MS.
Zhang, Z., Zhang, C., Yang, Y., et al., 2022. A review of sulfate-reducing bacteria: metabolism, influencing factors and application in wastewater treatment. J. Cleaner Prod. 376, 134109. https://doi.org/10.1016/j.jclepro.2022.134109.
Zivar, D., Kumar, S., Foroozesh, J., 2021. Underground hydrogen storage: a comprehensive review. Int. J. Hydrogen Energy 46 (45), 23436–23462. https://doi.org/10.1016/j.ijhydene.2020.08.138.
Zoback, M.D., Kohli, A., Das, I., et al., 2012. The importance of slow slip on faults during hydraulic fracturing stimulation of shale gas reservoirs. In: SPE Unconventional Resources Conference/Gas Technology Symposium. https://doi.org/10.2118/155476-MS.
Zwietering, M.H., Wijtzes, T., De Wit, J.C., et al., 1992. A decision support system for prediction of the microbial spoilage in foods. J. Food Prot. 55 (12), 973–979. https://doi.org/10.4315/0362-028X-55.12.973.